# COMPUTATIONAL STUDIES OF SPIN INTERACTIONS IN ORGANIC RADICALS AND EXPERIMENTAL DESIGN OF NEW MOLECULE-BASED MAGNETIC MATERIALS

A Thesis
Submitted for the Degree of
DOCTOR OF PHILOSOPHY

by

B. Lakshmi Vara Prasad

School of Chemistry
University of Hyderabad
Hyderabad - 500 046
India
April 1997

*to*
**amma, nanna**
**sree and radhi**

# CONTENTS

# DECLARATION

**I** hereby declare that the matter embodied in this thesis is the **result** of investigations carried out by me in the School of Chemistry, University of Hyderabad, Hyderabad under the supervision of Dr. T. P. Radhakrishnan.

In keeping with the general practice of reporting scientific observations, due acknowledgments have been made wherever the work described is based on the findings of other investigators.
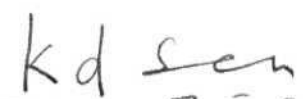
B. Lakshmi Vara Prasad

# CERTIFICATE

This is to certify that the work described in this thesis entitled **Computational Studies of Spin Interactions in Organic Radicals and Experimental Design of New Molecule-Based Magnetic Materials** has been carried out by *Mr. B. Lakshmi Vara Prasad* under my supervision and the same has not been submitted elsewhere for any degree.

Dr. T. P. Radhakrishnan
(Thesis Supervisor)

DEAN  7.5.97
School of Chemistry

# ACKNOWLEDGEMENTS

# ABBREVIATIONS

| | |
|---|---|
| **AM1** | Austin Model 1 |
| CT | charge transfer |
| **CI** | configuration interaction |
| **DDQ**$^{-}$ | 2,3-dichloro-5,6-dicyano-1,4-benzoquinonide |
| DPPH | 2,2-diphenyl-1-picryl hydrazyl |
| esr | electron spin resonance |
| **GIC** | graphite intercalation compounds |
| HCTMCP-. | hexacyanotrimethylene cyclopropenium |
| HOPG | highly oriented pyrolitic graphite |
| **NMP**$^{+}$ | N-methylphenazonium |
| **p-NPNN** | p-nitrophenylnitronyl nitroxide |
| RHF | restricted Hartree Fock |
| TPC+ | tris(pyrrolidine) cyclopropenium |
| UHF | unrestricted Hartree Fock |

# SYNOPSIS

Quest for molecular materials exhibiting a great variety of interesting and useful properties is one of the major areas of research today. Such properties include electrical conduction, magnetism and nonlinear optical effects. Magnetic molecular materials have been projected as having great significance in the field of molecular electronics, memory devices and telecommunication. Molecules are predominantly diamagnetic with a closed shell electronic configuration. However, many transition metal complexes and organic free/ion radicals have unpaired electrons. The spin interactions in the solid state of these systems are mostly antiferromagnetic. From a technological point of view as well as to obtain a fundamental understanding of the magnetic phenomena, it is important to design such molecular materials with ferromagnetic couplings and ultimately bulk ferromagnetism.

This thesis presents our studies on the problem of molecular magnetism, along two different approaches : i) investigation of the nature of spin coupling in conjugated and non-conjugated organic di and multiradicals using semiempirical computational methods, and ii) experimental design of new approaches to achieve cooperative magnetic interactions in molecular materials. The thesis is divided into five Chapters. We describe below salient features of the contents of each Chapter.

# CHAPTER 1. INTRODUCTION

Section 1, presents an introduction to the phenomenon of magnetism. An overview of the relevance of molecular magnetism in the backdrop of the general field of magnetism is presented in Section 2. The varieties of magnetic order relevant to the present work are also discussed. Various models proposed for achieving ferromagnetic or ferrimagnetic interactions in organic and organometallic systems are summarized in Section 3. Approaches to the design of purely organic ferromagnets are reviewed in detail in the next Section. The final section in this chapter describes the motivation for the present work and the layout of this thesis.

# CHAPTER 2. COMPUTATIONAL STUDIES OF SPIN COUPLING IN ORGANIC CONJUGATED AND NONCONJUGATED RADICALS

In connection with the topological models proposed for the design of polymeric organic ferromagnets, several empirical rules have been put forth to predict the ground state spin of organic di and multiradicals. In the introductory Section of this Chapter, we review these rules. We have addressed the problem of spin coupling in organic radicals using semiempircial quantum chemical calculations. The computational methods we have employed are summarised in Section 2.

Organic diradicals constitute the basic units in the topological models. The basic features of these diradicals are the ground state spin and the singlet-triplet energy gap. The zero field splitting (ZFS) parameters D and E are the signatures of triplet diradicals. Earlier computational work has mainly addressed the problem of predicting the ground state spin and the singlet-triplet energy gap. The ZFS parameters, on the other hand, have been rather difficult to compute in good agreement with experimental values. Semiempirical AM1 calculations (including limited CI) have been shown to provide fairly accurate predictions of the ground state spin in organic radical systems. In Section 3, using computations on a large set of organic diradicals, we demonstrate that open shell RHF AM1/CI procedure provides a good theoretical estimate of their zero field splitting parameters. These calculated ZFS parameters are found to be in much better agreement with experimental data than the earlier computational predictions. The ground state spin determination of tetramethyleneethane (TME) has been a notable case of conflict between theory and experiment. While experimentally it was shown that TME has a triplet ground state with a likely nonplanar geometry, theoretical calculations at various levels have consistently predicted a singlet ground state at planar as well as nonplanar geometries. However, recent high level *ab initio/Cl* calculations have shown that TME has a weakly stabilised triplet ground state at a twist angle of about $50°$. In Section 4, we provide our detailed semiempirical computational study of TME which showed that CI calculations involving all the six *n* MO's in the active space lead to a clear preference of a triplet state at twisted geometries. We have also examined the ZFS parameters of TME.

Our detailed analysis of the singlet-triplet energy gap in organic conjugated diradicals within the framework of a spin polarisation picture is presented in Section 5. We developed a simple algorithm to compute a spin coupling parameter in organic diradicals,. and show that it is strongly correlated to the singlet-triplet energy gap in these systems and provides a means of predicting the latter.

Theoretical studies aimed at understanding the nature of spin coupling in non-conjugated organic radicals (with radical sites separated by saturated, $sp^3$ carbon atoms) are relatively sparse compared with the studies on their conjugated counterparts. Several recent developments including a model of a "ferrocarbon" proposed by Ovchinnikov suggests that spin interaction in non-conjugated organic radicals could be of fundamental interest. In Section 6, we describe our computational investigation of the ground state spin of model non-conjugated organic radicals. We present a systematic analysis of the spin coupling in terms of the relative orientation of spin orbitals in these systems. An appraisal of the ferrocarbon model as well as suggestions for viable experimental systems are also discussed.

## CHAPTER 3. EXPERIMENTAL INVESTIGATION OF TWO APPROACHES TO MOLECULAR FERROMAGNETISM BASED ON THE SPIN POLARISATION PICTURE

In this chapter we propose two new approaches to ferromagnetism, both based on the notion of spin polarisation discussed in Section 1. Here the term spin polarisation is used in the sense that a and b spin show spatial preference over the molecular or polymer framework. In the first approach, charge transfer interactions in stacked organic complexes are envisaged, wherein the spin polarisation of diamagnetic spacer molecules/molecular ions are expected to lead to ferromagnetic alignment of spins on free or ion radicals. In the second approach based on a coordination polymer, spin polarisation in the bridging ligand species having π-conjugation, is expected to lead to ferromagnetic coupling of the metal ion spins.

Models for organic ferromagnets based on crystalline charge transfer complexes (as opposed to polymers) are of fundamental interest, since they offer insight into structural features that influence observed magnetic properties. We propose in Section 2, a new model combining basic aspects of charge transfer interaction and spin polarization. A mixed stack of ion radicals and diamagnetic molecular counterion spacers is considered. If the ion radicals stack such that they interact strongly with the same spin orbital of the spin polarised spacer, then the system would have overall ferromagnetic spin alignment along the stack. We have considered in this study, charge transfer complexes of dichlorodicyano-p-benzoquinonide $(DDQ^{-\cdot})$ and hexacyanotrimethylenecyclopropanide $(HCTMCP^{-\cdot})$ with tris(pyrrolidino)cyclopropenium $(TPC^{+})$ and N-methylphenazenium $(NMP^{+})$ cations as diamgnetic spacers. Three of these new compounds were prepared by metathesis reactions and characterized. Since good quality

crystals could not be grown, structural information on the complexes could not be obtained. Magnetic properties of these materials were investigated by variable temperature electron spin resonance studies. While TPC-DDQ and TPC-HCTMCP showed Curie-Weiss antiferromagnetic behaviour, NMP-DDQ showed a more complex behaviour with antiferromagnetic, ferromagnetic and simple paramagnetic behaviours at different temperature regimes. Qualitative models to explain these observations are presented.

The main drawback of the polycarbene/polyradical systems based on the topological models for organic ferromagnets, is their chemical reactivity which often leads to low spin concentrations. If paramagnetic transition metal ions are used instead of carbon based radical systems, this problem could be circumvented. In a coordination polymer, if metal ion spin orbitals are in conjugation with the $n$ - orbitals of the bridging ligand that has a suitable topological framework, then a system similar to the organic topological models could be visualized. In Section 3, we describe the synthesis, characterization and magnetic susceptibility measurements on three novel copper(II) complexes containing 4,5-dicyanoimidazole (DCI). Crystal structure analysis of the first complex prepared as a model system for the monomer unit revealed that the dicyanoimidazole does not coordinate to Cu(II). Since the counterion of the copper salt, namely the nitrate group was strongly coordinated to the metal ion in the complex, we prepared the next two systems, one from $CuSO_4$ and the second. one from $Cu(NO_3)_2$ with an acidic buffer In these two cases the ir spectral analysis indicated that the initial counterions are absent and that the DCI" is formed, perhaps

covalently linked to Cu(II). Crystal structural analysis of the complex prepared from $CuSO_4$ confirmed this. Magnetic properties of these complexes were studied using SQUID magnetometry. In all cases, only antiferromagnetic interactions were observed. The possible reasons for the observed magnetic properties in light of their structural analysis will be discussed.

## CHAPTER 4. NOVEL MAGNETIC MATERIALS BASED ON ORGANIC RADICALS IN HOST LATTICES

This chapter presents the results of our experimental investigations on establishing novel methodologies to achieve cooperative magnetic interactions between organic spin systems. It is well known that no long range order is possible in a purely one-dimensional system at finite temperatures. The bulk of the investigations in the area of purely organic magnetic materials have been based on one-dimensional models. We envisaged that if organic free/ion radicals could be included in a suitable host lattice that mediates the exchange coupling of the spins, interesting cooperative magnetic interactions may be realized. This would also allow flexibility in choosing the appropriate dimensionality.

One of the best known two-dimensional host lattice is graphite. An important property of graphite is that a wide variety of guests (alkali metals, alkaline earth metals, rare earth metals, halogens, transition metal halides

**etc.)** can be inserted between the graphene layers, thus forming the well known graphite intercalation compounds **(GIC's)**. We considered the preparation of GIC's having organic radicals as intercalants. It was expected that the spins of the radicals would interact through the mediation of the conduction electrons of graphite, leading to novel magnetic materials. The approach we followed is described in Section 2, and involves the intercalation of a suitable electron donor like an alkali metal into graphite, followed by a strong organic acceptor; the electrons donated to the graphite gallery in the initial step would be subsequently partially or **fully** transferred to the organic acceptor. The net result is the production of the alkali metal - organic acceptor ion radical salt as an inetercalant in graphite. We developed a simple two step procedure to prepare these ternary intercalation compounds using highly oriented pyrolitic graphite. They were characterized by weight uptake, infra red spectral and powder diffraction studies. The magnetic properties of these materials were probed with the help of variable temperature esr and SQUID **magnetometry**. Our studies showed that tetracyanoquinodimethane (TCNQ) does not inercalate, perhaps owing to its size. However intercalation experiments were **successful** with the smaller tetracyanoethylene (TCNE) molecule producing ternary systems with the first and second stage **potassium-GIC's,** CgK and $C_{24}K$ respectively. Detailed powder diffraction studies following the *001* peaks indicated that the final products formed with CgK are inhomogeneous mixtures of CgK and $KC_n(TCNE)_x$. However, the esr studies revealed that the spin properties of these compounds were very different from the parent CgK, including a Curie - Weiss ferromagnetic coupling in restricted

temperature regions in one of the stoichiometries. On the other hand $C_{24}K$ forms a homogeneous ternary intercalation compound with TCNE. Magnetic susceptebility studies showed a Curie - Weiss behaviour down to 140K with a positive Weiss constant of 29K. Strong antiferromagnetic interactions take over at lower temperatures in all the cases. The interesting ferromagnetic behaviour observed in restricted temperature regimes is novel and warrants further research.

We were interested in investigating the nature of spin interactions of organic radicals between the extreme limits of isolated molecules in solution and the bulk crystalline state. For this purpose we chose polystyrene as a suitable amorphous host which is unlikely to intervene in the spin interactions. We focused our attention on diphenylpicrylhydrazyl (DPPH) a stable free radical, included in polystyrene film. High concentrations of DPPH are required to initiate exchange interactions among radicals in the film; however, conventional film growth techniques did not allow homogeneous inclusion of more than 15 - 20% of DPPH in polystyrene. We developed a simple procedure to make good quality polystyrene films containing appreciable amounts (up to 50%) of DPPH, by casting these films on water surface. These radical doped films were studied using esr spectroscopy. Strong dependence of line widths on the concentration of **the** radical was noticed. Further, esr signal intensity versus temperature plots indicated fairly strong antiferromagnetic interactions between the spins as opposed to nearly Curie paramagnetic behaviour observed in the crystalline state of DPPH. We discuss possible orientational ordering of the radicals in

the film as a result of the preparation procedure and the likely origin of magnetic exchange interactions in the host lattice.

# CHAPTER 5. OVERVIEW OF THE PRESENT WORK AND FUTURE PROSPECTS

This chapter provides a summary of the studies presented in this thesis, with possible avenues for future studies.    The results of the semiempirical computational studies on organic conjugated and non-conjugated radicals are summarised.  An overview and the relevance of the novel charge transfer complexes, metal coordination compounds and ternary graphite intercalation compounds we have developed  in our attempt to design new approaches to molecule-based magnetic materials, is presented. Directions for future work in this area including experimental verification of the mode of spin couping in nonconjugtaed multiradicals is provided. Suggestions, both in terms of more extensive experimental and theoretical modelling studies on the novel ternary intercalation compounds we have developed in the present work, are also mentioned.

# CHAPTER 1

## INTRODUCTION

## 1.1 BACKGROUND

Ever since they were discovered, and exploited by the ancient Greeks and Chinese for the advancement of trade, science and technology and for innumerable other purposes, *'magnets'* have become an indispensable part of human life. Their significant role in the development of science and technology as well as in the evolution of society cannot be overemphasised. The development of condensed matter physics as well as quantum mechanics and the investigation of electronic structure of molecules in chemistry have been intimately tied up with fundamental research in magnetism. Magnets and magnetic materials are present everywhere around us; be it in routine gadgets such as accoustic devices, data storage media, generators and motors, or playing crucial roles in the development of present day telecommunications and information technology.

Of late there has been a great deal of interest in fabricating magnets based on completely new type of materials, for example, molecular or polymeric organic/organometallic/coordination compounds. Possibility of developing molecular magnets as memory storage devices has greatly enhanced the scope of constructing super fast computers. Also the smart materials envisaged for the future, which respond to external stimuli such as light, heat or electric and magnetic fields will require fast switches, sensors and transducers. Molecular magnetic materials are expected to play a crucial role in these areas, hence the great interest in molecular magnetic

systems.   Even though magnetism is of immense practical utility, it continues to remain as one of the fundamental properties which is not completely understood.  All the magnets that are being used today contain metals.  So the construction of a molecular magnetic material would not only open new vistas in the field of technology but also would provide important insight into the very phenomenon of magnetism.

## 1.2 MAGNETISM - THE PHENOMENON AND MATERIALS [1]

At the simplest level, magnetic behaviour is characterised by the response of a material (attraction or repulsion) towards a magnetic field. Magnetism is the cumulative effect based primarily on the interaction or coupling of angular momenta of unpaired electrons in the various molecules/atoms that constitute the entire solid.   Nuclear spin can also contribute to a material's magnetic property, though usually to a smaller extent than the contribution of unpaired electrons.

The electronic spin can take two orientations, spin up ($\uparrow$), say, spin aligned with an applied magnetic field or spin down ($\downarrow$),  say, spin aligned opposing the magnetic field. Each orbital can take two electrons one with spin up and the other with spin down and the spins cancel each other in a system with completely filled orbitals.   A molecule/atom with all the orbitals completely filled is called a 'closed shell' system and is diamagnetic.  A radical (open shell) is an atom, ion or molecule with an odd

number of electrons or having an even number, n of electrons occupying > $n/2$ orbitals. Thus a radical has at least one orbital with an unpaired electron and hence has a net spin. If such spins are far apart and do not interact (*ie.* do not align cooperatively) they form a paramagnet. When these spins come sufficiently close or interact through some mechanism, the exchange coupling manifests itself and influences their mutual alignment. If this alignment is such that the spins are forced to be antiparallel, it leads to antiferromagnetic behaviour. Ferromagnetic behaviour occurs when all the spins in a solid align in the same direction, resulting in a strong net magnetic moment. Ferrimagnetism results when there are different spin moments (essentially different number of spins) on neighbouring sites which align antiferromagnetically leading to incomplete cancellation of the magnetic moments and a net magnetic moment in the solid.

Apart from the basic types of magnetic order described above there are several other magnetic behaviours possible[2]. For example metamagnetism is the transformation from an antiferromagnetic state to a ferromagnetic state by application of an external magnetic field. A canted or weak ferromagnet can form when spins that are coupled ferromagnetically are only partially aligned. In contrast to a paramagnet, a spin glass occurs when spins point in similar directions but only over a short distance. The spin directions in a paramagnet vary with time; in a spin glass, they are fixed or vary very slowly. When several spins, aligned in a ferromagnetic fashion, act together like small paramagnets, such a behaviour is called superparamagnetism. Superparamagnetism has its

antecedents in ideal ferromagnetism and paramagnetism although any magnetically ordered substance when finely divided into sub-micron sized particles can show superparamagnetism.

As mentioned above, magnets are characterised by their response to an applied magnetic filed H. When a magnetic material is exposed to an external magnetic field H, a net magnetic moment per unit volume known as magnetization, M is induced in the material. M, even for small applied fields, is negative for diamagnetic materials, small and positive for paramagnets and antiferromagnets, and large and positive for ferro- and ferrimagnets. The magnetic properties of a material are not only characterised by the magnitude and sign of M, but also by the way in which M varies with H represented by $\chi$.

$$\chi = dM/dH \cong M/H$$

$\chi$ is called the magnetic susceptibility. In the case of ideal noninteracting spins in a paramagnetic solid, $\chi$ is temperature dependent and follows the Curie equation,

$$\chi = C/T$$

The Curie constant is defined by the equation,

$$C = Ng^2\mu_B^2\ J(J+1)/3k_B$$

where J, the total angular quantum number, can be replaced by S, the spin angular quantum number, in systems such as organic molecules where orbital contribution can be neglected. N is the Avagadro number, g is the Landé factor, $\mu_B$ is Bohr magneton and $k_B$ is the Boltzmann constant.

When the spins experience an effective exchange field due to the interactions with the neighbouring spins, the measured susceptibility and its temperature variation deviate from that predicted for independent spins by Curie law. In these cases if the temperatures are high enough so that the spins are not in any ordered state, a mean field treatment shows that the susceptibility can be fit to the Curie-Weiss law,

$$\chi = C/(T - \Theta)$$

where $\Theta$ is greater than zero if the interactions are ferromagnetic and less than zero if the interactions are antiferromagnetic.

Depending on the materials the magnetization M shows characteristic H dependence. Typical curves of M *vs* H called magnetization curves are shown in Fig. 1.1. Note that the behaviour shown in curve (c), for typical ferro- or ferrimagnet (below an ordering temperature, called the Curie temperature, $T_C$) is quite different from that of the linear M-H curves for dia-(curve (a)), para- and antiferromagnetic (curve (b)) substances.

**Figure 1.1:** *Typical M vs H curves for (a) dia- (b) para- and antiferro and (c) ferro- and ferrimagnets (the last three, below their ordering temperatures)*
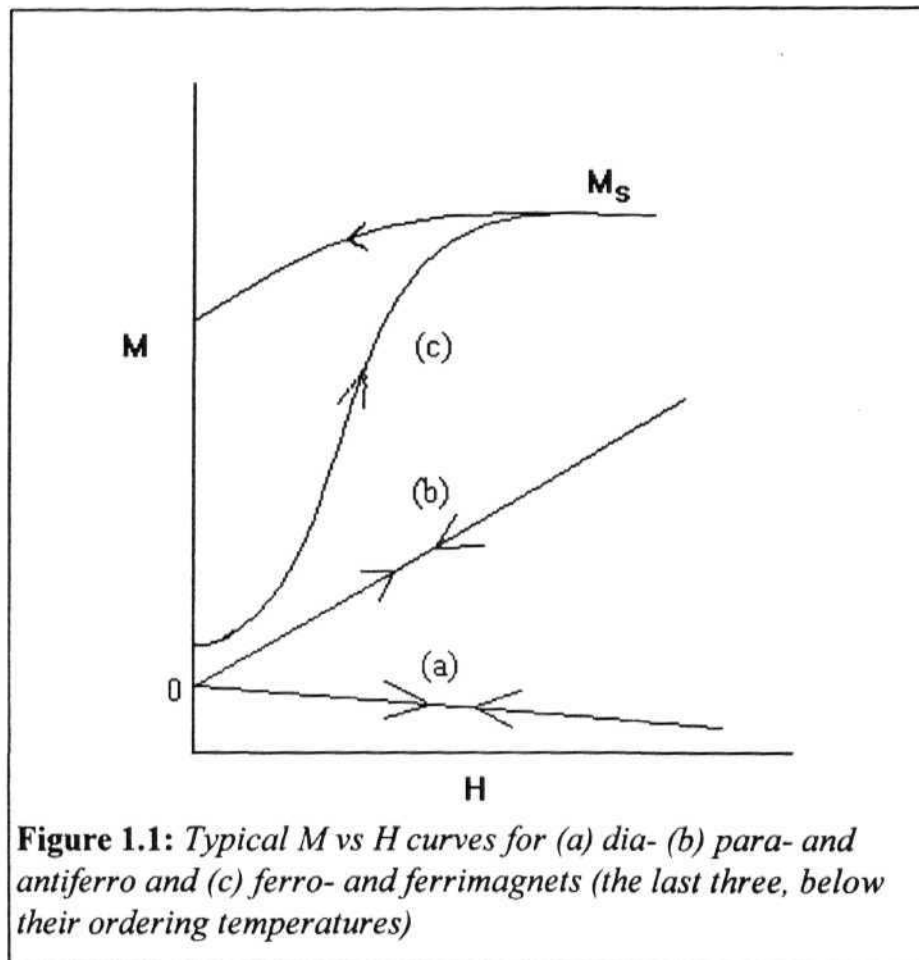
The curves of ferro- and ferrimagnets are nonlinear and M approaches a limiting value called the saturation magnetization $M_s$, normally at high magnetic fields. After attaining saturation ($+M_s$), a decrease in H to zero does not reduce M to zero. The value of M at zero external field is called
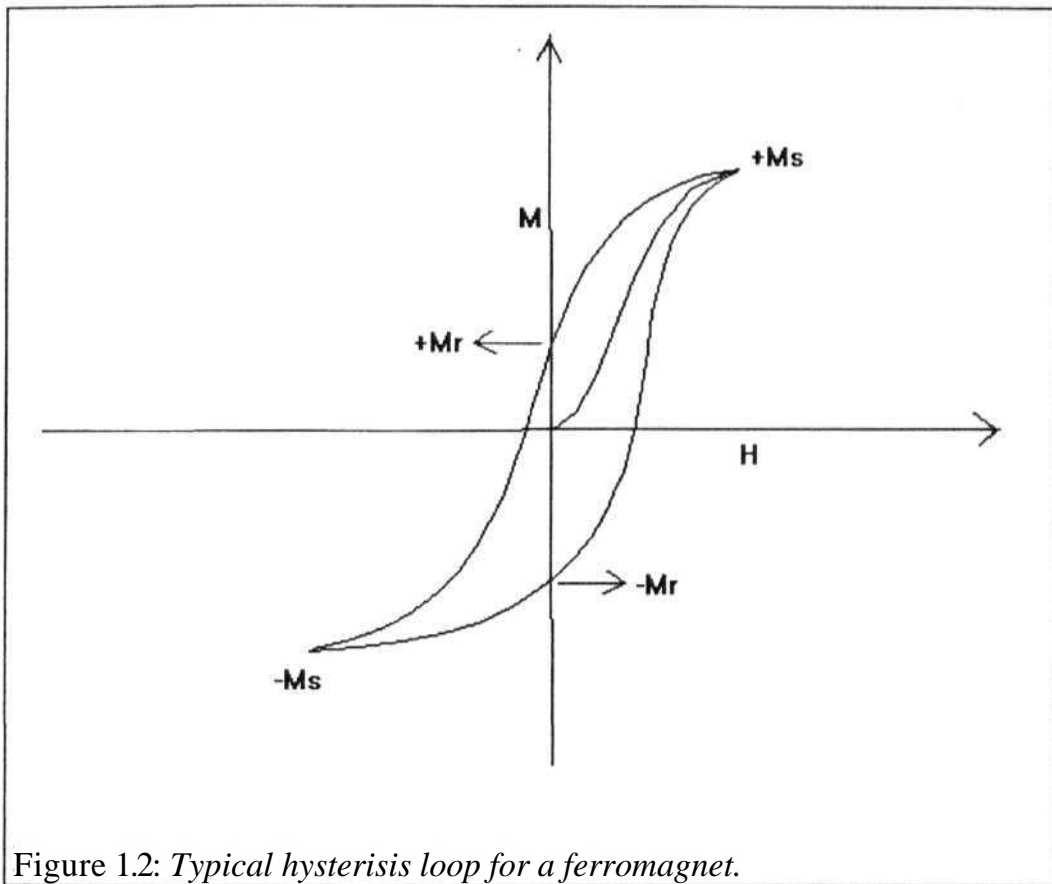
Figure 1.2: *Typical hysterisis loop for a ferromagnet.*

remnant magnetization ($M_r$). Reversing the direction of external magnetic field will cause the spins within the magnet to reverse and the magnetization becomes zero at the coercive field, $H_c$. At a large enough applied magnetic field in the reverse direction, the magnetization peaks again, but in the opposite direction ($-M_s$). If the field is now reduced to zero and again

applied in the original direction, the magnetization will follow the curve -
$M_r$, $+M_s$ and so on. The magnetization loop thus traced is called the
hysterisis loop and is shown in Fig. 1.2.

The above behaviour can be explained as follows. When a
ferromagnet is cooled in the absence of an external magnetic field,
competing exchange and dipolar forces lead to the formation of domains at
the phase transition temperature, $T_C$ known as the Curie temperature. The
overall magnetization of the material will be still zero because the net
magnetic moments of these domains will point in different directions and
cancel each other, as shown schematically if Fig. 1.3. Application of an
external magnetic field causes one domain to grow at the expense



[a]                                                    [b]

**Figure 1.3:** *Domain structure in a ferromagnet (a) before applying
external magnetic field; (b) after applying external field to reach
saturation ($M_s$).*
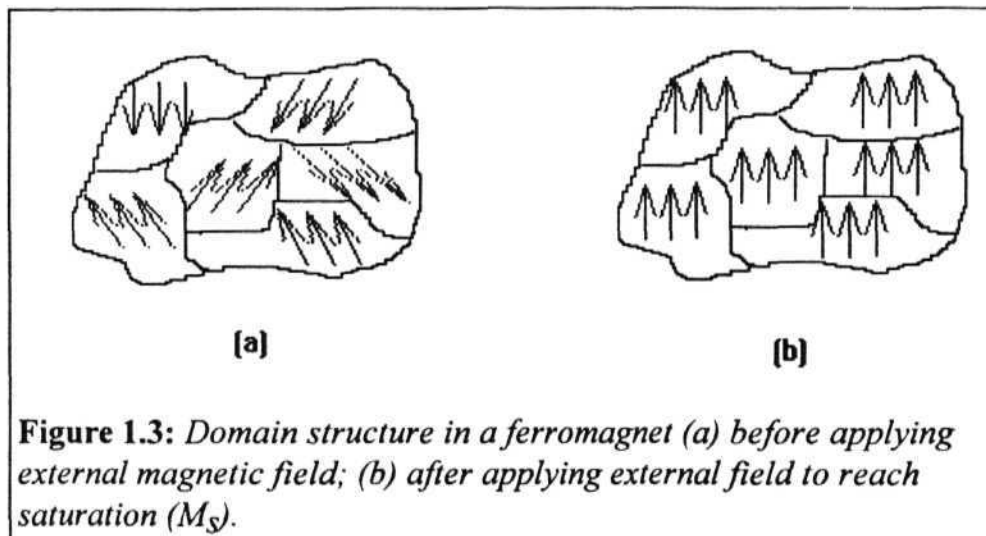
of the others and when it engulfs all the others, $M_S$ is attained. The hallmark of ferromagnets is the magnetisation ($M_r$) that remains even when the applied field is removed.

Traditional magnetic materials include, apart from the ferromagnetic metals iron, cobalt and nickel, the steels alloyed with tungsten and chromium[1,3]. Some of the magnetic alloys that have been developed recently contain a number of alloying elements that include cobalt, nickel, aluminium, copper and silicon. For example Alnico, which is actually a family of alloys, contains substantial amounts of all the three ferromagnetic metals, Fe, Co and Ni along with smaller amounts of Al, Cu and sometimes other elements. These are the most widely used permanent magnetic materials. Several ferrimagnetic materials were also developed based on cubic ferrites. These materials represented by the general formula $MFe_2O_4$, have the spinel and inverse spinel structures. M represents any one of the several metallic elements and adjustment of the composition of M leads to ferrite compounds having a wide range of magnetic properties. There are many hexagonal ferrimagnetic oxides, including the commercially popular barium ferrite and strontium ferrite, which are widely used as hard magnetic materials. Rare earth elements like Nd and Gd are extensively used in modern high energy density magnetic materials.

## 1.3 MOLECULAR MAGNETIC MATERIALS[4]

Molecular materials are of great interest in the field of materials science and technology today. There has been a concerted effort to develop the so-called area of "molecular electronics" and "molecule scale electronics". The former addresses electronic applications of molecules and polymeric solids whereas the latter refers to the concept of individual molecules acting as electronic devices. Molecular material based semiconductors, conductors and superconductors have been developed. Molecular transistors, rectifiers and switches have been fabricated. Tremendous activity has been going on in the field of conducting polymers. Molecular materials have become an integral part of modern materials research in the field of nonlinear optics. The faster and stronger response of molecular systems to electromagnetic fields, as opposed to conventional inorganic materials, shows great promise. A variety of optical devices, electroluminiscent systems etc. could be developed using molecular building blocks. Liquid crystals have revolutionized display technology. Nanostructured materials based on molecular systems are opening up new vistas of research and technology.

Molecular magnetic materials have occupied no less prominent a position in recent materials chemistry scenario. They suggest possibilities of fabricating novel magnetic, electromagnetic and magnetooptic devices. Polymer magnets may offer novel mechanical properties for magnetic

materials. Molecular magnetic material developement will be based on novel concepts and chemistry.

Miller and Epstein[4a] have broadly identified three mechanisms through which ferro- or antiferromagnetic spin coupling could be achieved (Table 1.1) in a bulk molecular solid.

**Table 1.1.** *Spin coupling mechanisms for molecular systems.*

| Mechanism | Spin Interaction | Spin Coupling |
|-----------|-----------------|---------------|
| Spin coupling resulting from orthogonal orbitals | Intramolecular (extendable to intermolecular also) | Ferromagnetic |
| Spin coupling from Configuration Interaction (CI) | Intra- or intermolecular | Ferromagnetic or Antiferromagnetic |
| Dipole - dipole (through- space) interaction | Intra- or intermolecular | Ferromagnetic or Antiferromagnetic |

It should be noted here that, for molecule-based systems **with their** complex compositions and structures, it is often very difficult to decide which mechanism is operational. It is possible that more than one mechanism plays a crucial role of determining the mode of spin coupling in

many cases. It is also often observed that the suggested mechanisms may not stand the test of time and new mechanisms may evolve with increased understanding of the structures and properties of more materials.

In most cases an accurate description of the magnetic properties of nonconducting molecular systems can be given by the interaction Hamiltonian,

$$H = -2J \sum_{i,j} [aS_i^z S_j^z + b(S_i^x S_j^x + S_i^y S_j^y)]$$

where the sum extends over nearest neighboring spins and J is the exchange constant. If magnetic interaction is isotropic *ie* a = b = 1 we obtain the isotropic Heisenberg model. In the case of Ising model, where a = 1 and b = 0, the anisotropy constrains the magnetic moments to precess around a given direction, in this case z axis. Suppose the anisotropy forces the moments to lie within a given plane, say *xy* plane, then a = 0 and b = 1 and we have the XY model.

Below we provide several important examples of molecular magnetic materials and briefly indicate the suggested mechanisms of spin interactions. Because of the greater focus on organic materials in this thesis, the models and materials related to organic systems are collected separately in the next section (Section 1.4).

### 1.3.1 METAL CHAIN SYSTEMS

A large number of metal linear chain compounds have been prepared and structurally analyzed and their magnetic properties have been investigated in great detail. This led to a very good understanding of the magneto-structural correlations of these metal chain compounds. The groups of Kahn, Hatfield, Willett and others[5] have developed several kinds of exotic systems like linear chains, alternating linear chains, chains with zig-zag structures and chains with ladder like structures involving a variety of ligands. Although the main emphasis has been on copper (II) complexes, since being a spin 1/2 system it has only one magnetic orbital per site, systems involving other ions such as chromium(III), manganese(II) and iron(II) are also known.

Day and coworkers[6] have studied extensively 2-D layered systems with a general formula $A_2[CrCl_4]$, where 'A' can be either rubidium ion or alkyl ammonium ions. These systems form layered structures in which each $Cr^{II}$ is surrounded by four bridging chloride ions. This structural arrangement puts the four unpaired electrons on the metal ion in orthogonal orbitals, thus leading to ferromagnetic materials with $T_c$'s above 50 K. The $T_c$ however, is independent of the cation. An important property of these materials is that they are relatively transparent.

Another interesting system in this class are the materials similar to the ferric ferrocyanide pigment, Prussian blue, with substituted metal ions

forming 3-D network structures that are ferromagnetic or antiferromagnetic[7]. A prototypical example is $CsNi[Cr(CN)_6].2H_2O$, where the metal ions are $Ni^{II}$ and $Cr^{III}$. Here adjacent spins reside in orthogonal orbitals and the $T_C$ for this material is 90 K. In some other cases like in $Cs_2Mn^{II}(V^{II}(CN)_6)$, the orbitals in which the spins reside are not orthogonal and the material is a ferrimagnet with a $T_c$ of 125 K. Recently a similar system with more complex composition involving vacancies in the Prussian blue structure *viz* $V(Cr(CN)_6)_{0.86}.2.8H_2O$, was found to be a ferrimagnet above room temperature.

This general idea of designing a material with adjacent metal ion spins in orthogonal orbitals was pursued by the group of Kahn and several others. In many of the cases only high spin molecules with no appreciable bulk magnetic property were obtained[8]. Okawa *et al*[9] have succeeded in preparing materials having the general formula $[Bu_4N][MCr(ox)_3]$ (ox = oxalato; M = Fe, Co,Ni,Mn and Cu) that have been reported to exhibit ferromagnetic transition and hysterisis loop.

Iwamura and coworkers[10] have identified pyrimidine as a potential ferromagnetic coupling unit between metal ion spins. They have reported a ferromagnetic transition in the complex $pm[VO(hfa)_2]_2$, at 0.14 K. (hfa = hexafluoroacetylacetonato, pm = pyrimidine). The mechanism operating here may be similar to the topological models presented later. Extension of this model to polymer metal complexes with ferromagnetic bridging ligands may produce high $T_c$ materials.

## 1.3.2 FERRIMAGNETIC CHAINS

The strict orthogonality of the molecular orbitals, necessary for a ferromagnetic interaction between the spins, is quite difficult to extend beyond the scale of molecular units. A small structural distortion may destroy this orthogonality and stabilize an antiferromagnetic state. Hence, the ferrimagnetic approach where adjacent spins of different magnitudes couple antiferromagnetically so as to partially cancel out one another, leading to an effective magnetic moment, has been adopted by many groups to prepare magnetic materials.

Kahn *et al*[8] have pursued this approach systematically to prepare a



**Figure 1.4 :** *Spin alignment proposed in MnCu(PbaOH)(H₂O)₃.*
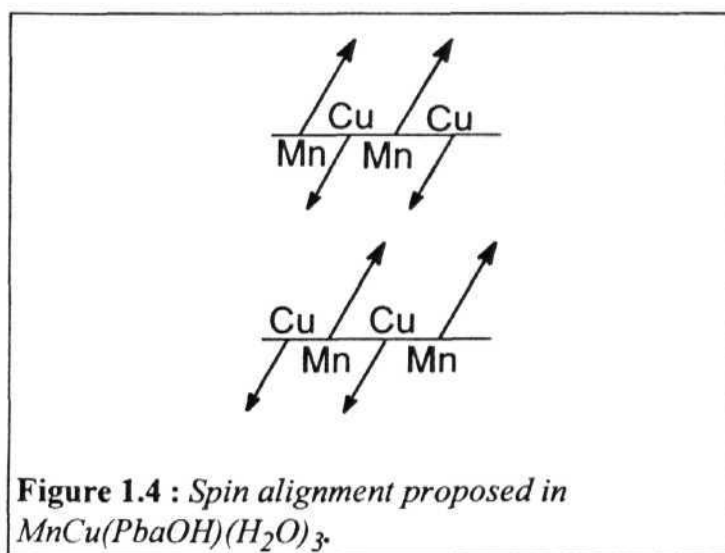
class of very interesting compounds. The first in this series was [MnCu(PbaOH)(H$_2$O)$_3$][11] (PbaOH= 2-hydroxy-l,3-propylene bisoxamato). This compound has shown some typical features of a ferromagnetic transition below 4.6 K. The spin alignment in this system is shown schematically in Fig. 1.4. Another interesting feature observed in this compound was that when partially dehydrated, this compound [MnCu(PbaOH)2.H$_2$O] showed a $T_c$ rise to 30 K[12]. It has been suggested that in the dehydrated system polymerisation is possibly taking place leading to higher $T_c$'s[13].

## 1.3.3 METAL ORGANIC FREE RADICAL COMPOUNDS

The ferrimagnetic approach described above for some bimetallic chains, was extended to organometallic compounds, with assemblies
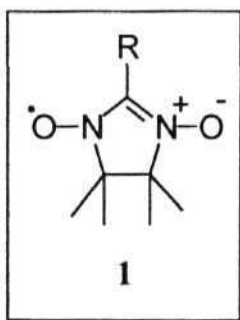


consisting of transition metal ions covalently linked to organic free radicals/ion radicals as ligands. Gatteschi, Rey and coworkers have reported a series of Mn(II) complexes with nitronyl nitroxide free radicals **[1].** They prepared [Mn(hfa)$_2$(NITipr)] (hfa = hexafluoroacetylacetonato, NITipr = isopropyl nitronylnitroxide), which shows a ferromagnetic transition at 7.6 K[14]. A series of related compounds by changing the 'R' group and by substituting the nitronyl nitroxide with imino nitroxyls and the metal ion with Cu, Zn, Rh and Y and some rare earth elements like Eu and Gd were prepared and studied[15].

However most of the above materials form 1-D spin structures with weak interchain interactions. In order to form 2-D and 3-D networks which may be essential to realize higher transition temperatures, Iwamura, Inoue and coworkers have considered employing π-conjugated polynitroxides which have more than two ligating sites in the ligand[16]. They used
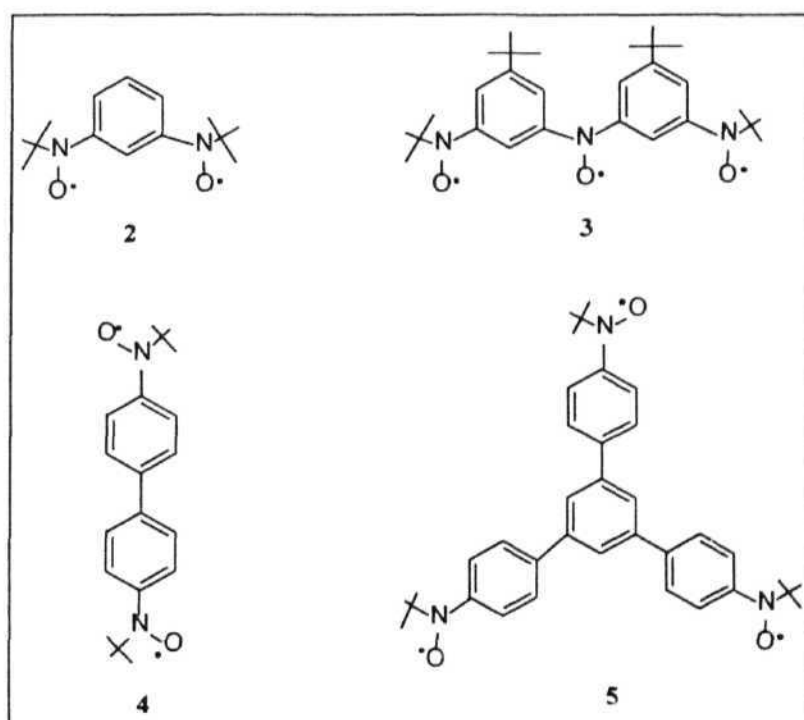


polynitroxide radicals [2 - 5] to prepare a series of compounds with Mn(hfa)$_2$. For example a 2:3 complex of 4 and Mn(hfa)2 showed a $T_c$ of 9.5 K, the 2:3 complex of 5 and Mn(hfa)$_2$ formed a beautiful honeycomb

structure showing a ferromagnetic transition at 3.4 $K^{17}$ etc.   Another interesting example is the 2:3 complex of 3 with $Mn(hfa)_2$. The structural analysis of this compound revealed the formation of a parallel cross - shaped 3-D polymeric network with the highest $T_c$ reported for this series of compounds, 46 $K^{18}$.

## 1.3.4 ORGANOMETALLIC CHARGE TRANSFER SYSTEMS

So far the most successful and extensively studied family of molecular magnetic systems are the metallocene - organic ion radical



M = Fe, Mn                    TCNE                    TCNQ

**Figure 1.5:** *Some donors and acceptors in the metallocene CT complexes.*
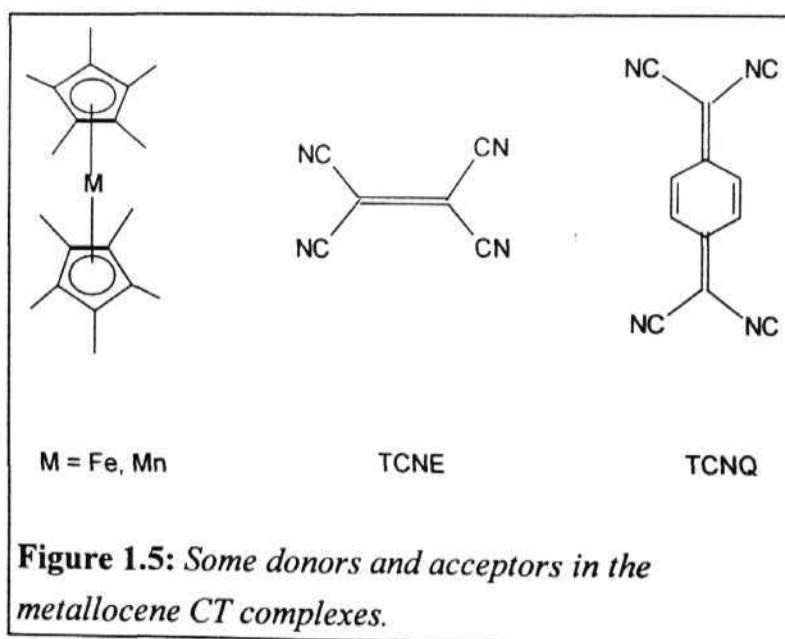
donor-acceptor complexes reported by Miller, Epstien and their coworkers[7]. The first molecule in this series $[Fe^{III}Cp_2^*]^+[TCNQ]^{-\cdot}$ [Fig. 1.5] was shown to exhibit a metamagnetic[19] behaviour. Subsequently in an attempt to elucidate the structure and magnetic property relationship they have prepared a large number of compounds by modifying the acceptors, changing the substituents on $C_5Me_5$ ring and substituting the metal ions. Based on the supposition that a smaller radical anion would have a greater concentration of spin density which could lead to increased spin-spin interactions, they selected $TCNE^{-\cdot}$ as the radical anion in place of $TCNQ^{-\cdot}$, which resulted in the first molecule-based magnet $[Fe^{III}Cp_2^*]^{+\cdot}[TCNE^{-\cdot}]$, with a $T_c$ of 4.8 K[20]. They have also made the first room temperature molecule-based ferromagnet by reacting TCNE with $V(C_6H_6)_2$ in $CH_2Cl_2$. The resulting polymeric compound is extremely air sensitive and has an empirical composition $[V(TCNE)_x] \cdot yCH_2Cl_2$ ($x \approx 2$, $y \approx 0.5$) and variations in this composition are observed depending on the preparation conditions. The critical temperature of this compound was estimated to be around 400 K, exceeding 350 K, its thermal decomposition temperature[21].

## 1.4 PURELY ORGANIC MAGNETIC MATERIALS

Compared to the inorganic and organometallic systems we discussed in the previous sections, purely organic systems have proved more difficult in the fabrication of molecular magnetic materials. However, since the spins in such systems reside in the s and p orbitals, investigation of their

magnetic properties is expected to provide valuable insights into the basic phenomenon of magnetism. Since the spin-orbit coupling is negligible in these materials they are expected to lead to soft ferromagnets, which may prove to be very important in information technology . The versatility of organic synthesis should enable fine tuning of the solid state magnetic characteristics by performing subtle structural modifications. Solubility in common organic solvents is a general characteristic of most organic compounds that confers on them easy processability. Biocompatibility is another characteristic of several organic compounds that suggests the possibility of  their usefulness for drug addressing and as selective contrasting agents in magnetic resonance imaging. Therefore, organic magnets should be ideal candidates to obtain magnetically active thin films and colloidal dispersions with ferrofluid properties. Apart from the various advantages that other molecule-based magnetic materials are also likely to possess, these materials, especially polymer based ones, could be transparent and therefore useful as magneto-optical switches.

Various theoretical models were suggested and experimentally tested to look for ferromagnetic interactions in organic materials[22]. They can be classified as follows.

a) Negative spin density product model
b) Configuration interaction model
c) Topological models

We discuss details of these models below. Before that it is essential to note that there are some other approaches, actively pursued by many groups, which are not specifically based on any of the theoretical models proposed. Particular mention should be made of the many stable free radical solids being made wherein the localized spins on the -N-O· group are found to couple ferromagnetically in the solid state; a combination of the above mechanisms and others may be operating here[23]. The observation of unusual magnetic properties in some of the pyrolised hydrocarbons is another interesting aspect of organic ferromagnetism, where the basic mechanism of spin coupling is hardly understood. It should be stressed at the outset that there are many similarities in the mechanisms proposed for molecular magnetic materials containing metal ions and those based on pure organic systems. There were attempts to explain the observed magnetic interactions in metallic and organometallic systems with some of the models which are described below. A significant aspect of these models is that they are predominantly based on 1-dimensional systems. However, it is well known that long range order cannot be obtained in a purely one-dimensional system at finite temperatures[24]. We explain this point further in Section 4.1. Hence it should be emphasised that these models envisage the attainment of ferromagnetism in quasi 1-dimensional systems i.e., those with appreciable 2-D and/or 3-D interactions.

## 1.4.1 NEGATIVE SPIN DENSITY PRODUCT MODEL

The early spurt of activity in the field of organic ferromagnetism could be attributed to the theoretical models proposed by McConnell[25]. We describe the first model as the negative spin density product model. He proposed that radicals with "........large positive and negative spin densities.........[that stack like] pancake[s] - so that atoms of positive spin density are exchange coupled.... to atoms of negative spin density in neighbouring molecules......gives rise to a ferromagnetic interaction". This point may be elaborated as follows. Consider a pair of conjugated molecules, A and A' which are neutral or ionic radicals having both positive and negative spin densities on their atoms. The overall exchange interaction between A and A' is given by the spin Hamiltonian

$$H = -JS_A S_{A'} = -\sum_{i,j} J_{ij}^{AA'} S_i^A S_j^{A'} = -[\sum_{i,j} J_{ij}^{AA'} \rho_i^A \rho_j^{A'}] S_A S_{A'}$$

where $S_A$ and $S_{A'}$ are the spins on molecules A and A', $S_i^A$, $S_j^{A'}$ are the spins at atomic sites i and j of A and A' respectively and $\rho_i^A$ and $\rho_j^{A'}$ are the π-electron spin densities at atomic sites i and j of A and A' respectively. McConnell's argument is that, since the largest exchange integrals $(J_{ij}\text{'s})$ are usually negative; if the product $\rho_i^A \rho_j^{A'}$ is made negative by design (i. e., by making regions of positive and negative spin densities on A and A' interact closely ) the effective exchange

$$ J' = \sum_{i,j} J_{ij}{}^{AA'} \rho_i{}^{A} \rho_j{}^{A'} $$

will be positive *ie,* ferromagnetic.

It should be highlighted here that, this is a mechanism proposed only for realizing ferromagnetic interactions between adjacent **radicals** and for bulk **ferromagnetism,** extended (preferably 3-D or at least 2-D) interactions of this nature are necessary.



pseudo ortho        pseudo meta        pseudo para

**Figure 1.6:** *The dicarbenes studied by Izuoka et al[26] to test the negative spin denisity model.*
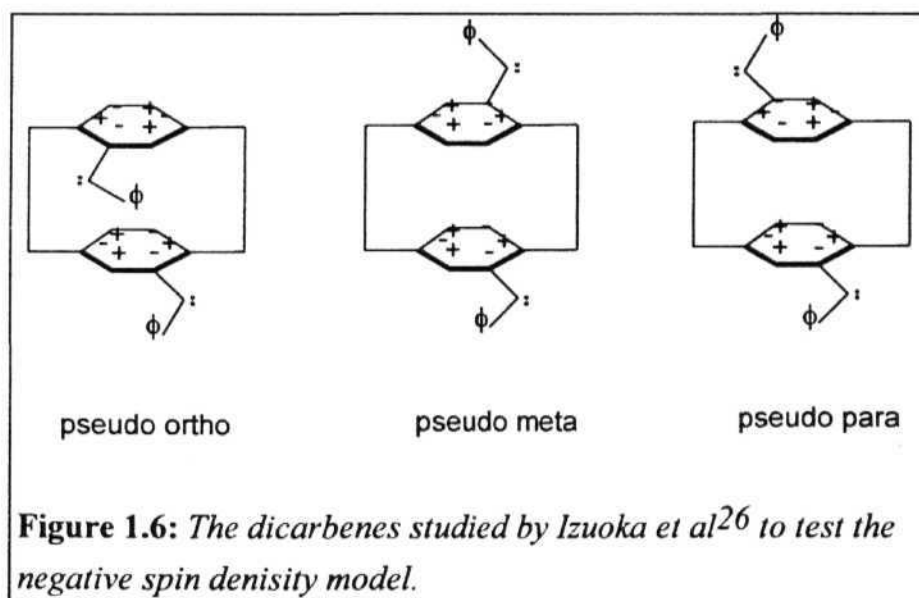
Izuoka *et al*[26] have successfully tested the veracity of this mechanism by designing a set of dicarbenes incorporated in a rigid [2.2] cyclophane skeleton [Fig. 1.6].  They have proved with the help of esr data on these systems that the pseudo ortho and pseudo para isomers have quintet ground states and the pseudo meta isomer has a singlet ground state and as seen from the spin density distributions on the carbene fragments depicted in Fig. 1.6, these observations are consistent with McConnell's picture.  Achievement of bulk ferromagnetic behaviour in materials tailor made for this model is yet to be reported.  Nevertheless, the observed ferromagnetic interactions in solid triphenyl verdazyl[27] and the mixed crystals of galvinoxyl radical[28] and its closed shell precursor have been attributed to similar mechanisms.  Wudl *et al*[29] with the help of a 'designed' lattice have shown that the negative spin density product model can in principle be used to fabricate molecular solids with desired magnetic properties.  Even the ferromagnetic intermolecular interactions observed in the first purely organic molecular ferromagnet ($T_c$= 0.65 K), the y-phase of p-NPNN [6], has been explained by invoking this model[30], in the light of its crystal structures and the detailed picture of spin densities within this free radical.  Following the observation of ferromagnetism in p-NPNN, several derivatives of the stable organic free radicals bisnitroxy, a- nitronyl nitroxide, galvinoxyl, verdazyl and TEMPO have been reported, with some of them showing interesting magnetic properties[23].
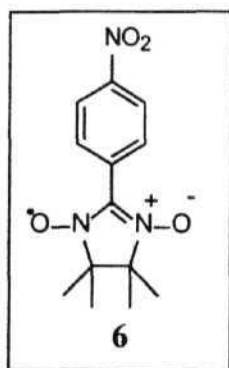


6

## 1.4.2 CONFIGURATION INTERACTION (CI) MODELS

The possibility of attaining ferromagnetic coupling of spins in organic ion radical systems by invoking Mulliken type CT models was also suggested by McConnell[31]. According to this model, if one considers a solid containing a mixed stack of donor $(D^+)$ and acceptor (A") organic radical ions ....$D^+A^-D^+A^-D^+A^-$........., a back charge transfer (from A" to D) would lead to a singlet or triplet excited state respectively, for the dimer, depending on whether the neutral D and A have singlet (S=0) ground state or one of them has a triplet ground state [Fig. 1.7]. If the neutral state is a singlet [Fig. 1.8(a)] as is often the case, configuration interaction stabilizes the singlet ground state. However, if the donor or acceptor is designed so



**Figure 1.7 :** *Charge transfer models for ferromagnetic coupling of spins.*
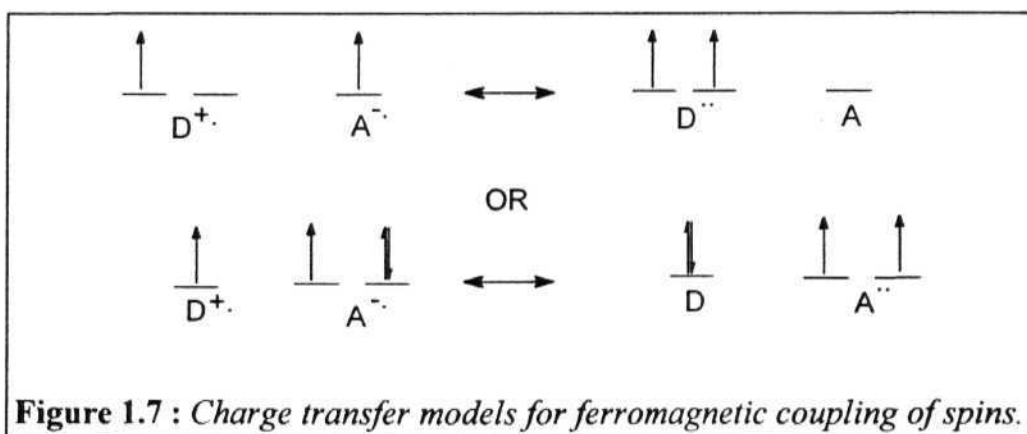
that it has a degenerate HOMO, the excited state is a triplet and CI would lead to the stabilization of the triplet ground state [Fig. 1.8(b)] and extension

of such interaction throughout the stack should lead to a ferromagnetic material.
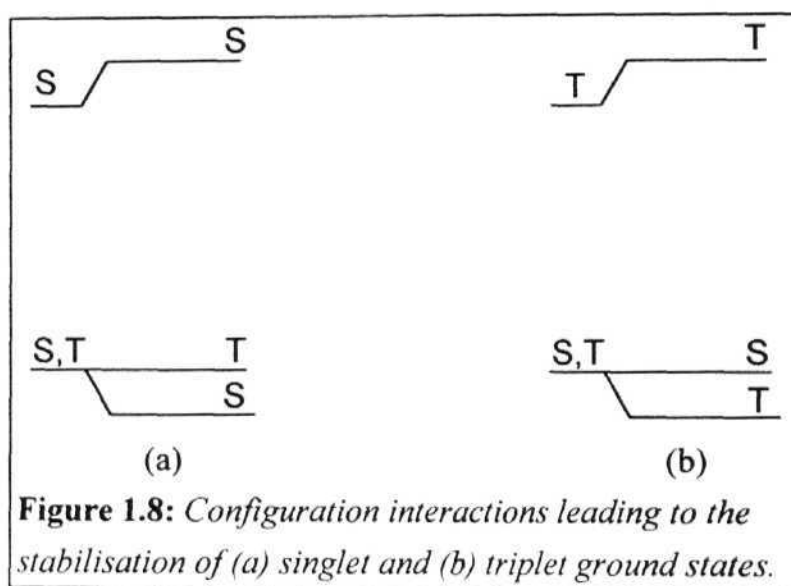


**Figure 1.8:** *Configuration interactions leading to the stabilisation of (a) singlet and (b) triplet ground states.*

Several variations of this model were suggested by Breslow[32], Wudl[33] and Torrance[34] and their coworkers. A good overview of these modified versions can be found in the review by Radhakrishnan[22]. Soos and coworkers[35] attempted to extend the superexchange (magnetic interaction of spins on two metal ions through connecting ligand orbitals) mechanism to organic stacked complexes. According to this model, in a stack, ....R˙SR˙S..., where R' is a radical or ion radical and S is a spacer molecule having an appropriate degenerate MO, a triplet excited state may be obtained, if the radical spins are transferred to these degenerate orbitals during the virtual excitation. Two factors are very important for this

mechanism to work; i) the relevant molecular orbital degeneracy in S is to be maintained in the solid complex and ii) the orientation of R"s which sandwich any S should be such that the perturbations on the degenerate MOs are equal. They have prepared a series of complexes based on symmetric diamagnetic anion and cation spacers and studied their magnetic properties. Ferromagnetic coupling was not obtained in any of these materials owing to a variety of reasons[36].

Observation of ferromagnetic interactions in many metallocene - TCNE charge transfer complexes has been attributed to the configuration interaction mechanism. Subsequently the validity of this mechanism has been questioned[37] using model calculations involving other low lying excited states. The soft ferromagnetism[38] observed in the charge transfer complex of tetrakis(dimethylamino)ethylene (TDAE) and $C_{60}$ has also been explained with this mechanism.

## 1.4.3 TOPOLOGICAL MODELS

These models are based on the mechanism originally proposed by Mataga[39] for polymeric hydrocarbons with carbene or carbyne units (an example is shown in [Fig. 1.9(a)). He suggested that the carbene or carbynic spins would show ferromagnetic alignment due to the specific topological placement of the molecular orbitals [Fig. 1.9(b)]. The energy band diagram of the polycarbene [Fig. 1.9(c)] would consist of the narrow band (N), formed from the non bonding $\pi$-MOs and $\sigma$ type lone pair orbitals

at the bridge site and would be populated by ferromagntically aligned spins. Iwamura *et al*[40] have prepared these systems with m upto 5 and it indeed showed an undecet ground state.



**Figure. 1.9:** *(a)poly-m-phenyldicarbene; (b) spin polarisation in (a); and (c) energy band diagram*[39].
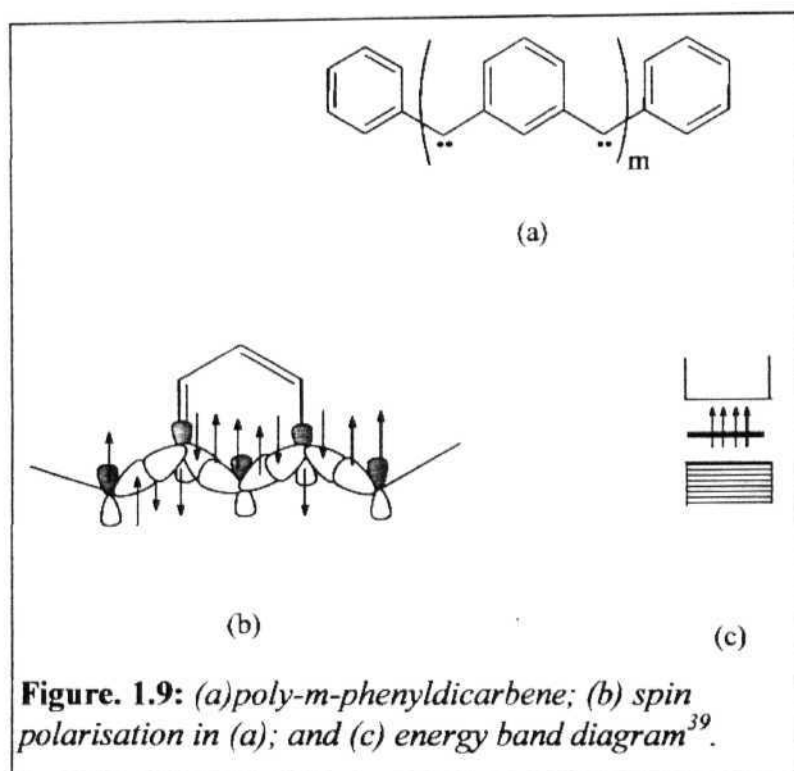
*Odd alternant polymers*

Based on the theorem of Lieb *et al*[41], Ovchinnikov[42] proved that the ground state spin, S of an alternant hydrocarbon is given by $|N^*-N|/2$, where $N^*$ and $N$ give the number of starred and unstarred atoms. Several

other rules proposed to predict the ground state spin of non-Kekulé systems are discussed later in Section 2.1. Ovchinnikov, based on his theoretical studies,



X = O, S

7                    8
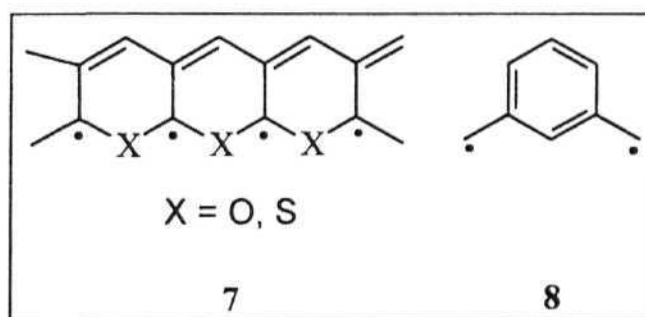
suggested several hydrocarbons and heterocycles, which at infinite size could become ferromagnetic. A typical example is 7. Note that Mataga's polycarbenes are also conceptually similar. The simple prototypical system trimethylenemethane has been shown to have a triplet ground state experimentally[43], giving validity to these models. Another system that has been used extensively as ferromagnetic spin coupling unit is m-phenylenediyl, 8.

Several groups worldwide are involved in the quest for polymeric systems that could show bulk ferromagnetic behaviour. Some typical systems experimentally reported are 9 and 10. Raj ca *et al*[44] have shown that, the triarylmethyl multiradical 9 has S = 7/2. Veciana and his group[45], in an attempt to stabilize the highly reactive polyradicals, have focussed their attention on other high-spin macromolecules based on the

perchlorinated multiradicals.  In fact the triradical 10 was obtained in two highly stable and isolable stereoisomeric forms, with $D_3$ and $C_2$ symmetries, both having highly robust quartet ground state structures. Iwamura *et al*[46] have extended their polycarbenes mentioned earlier and
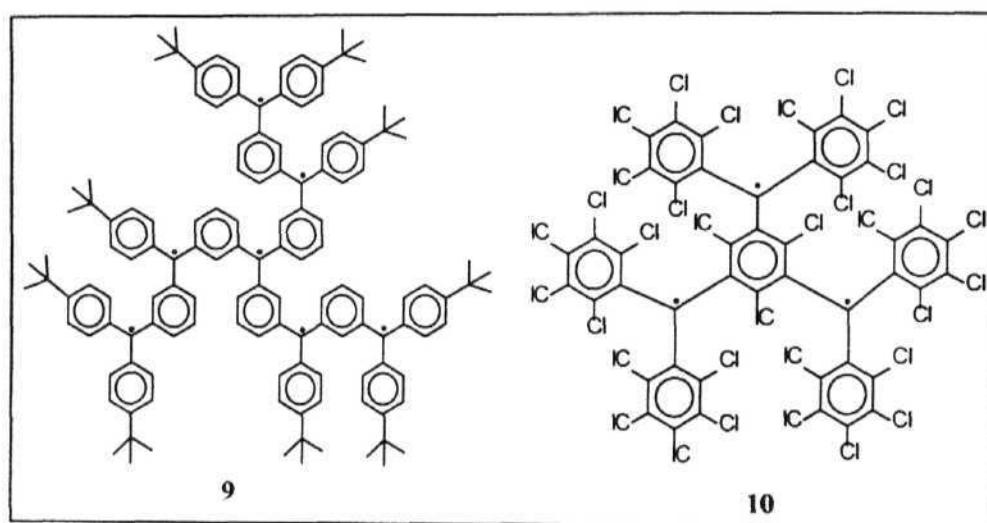


prepared a two-dimensional structure shown below [**11**]; the $m = 9$ molecule was the highest multiradical synthesised and it showed, as expected, an $S = 9$ ground state.  This is perhaps the highest spin organic molecule reported to date.

**11**
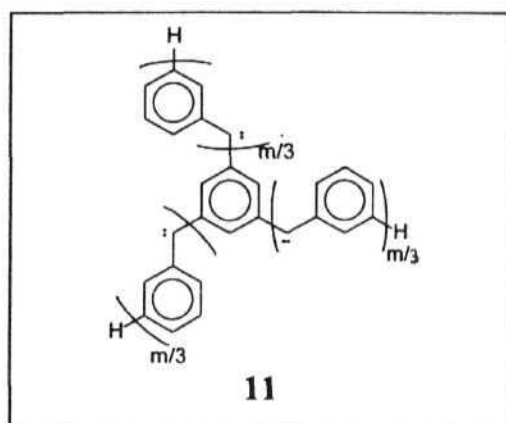
*Nonalternant non-Kekulé systems*

There has been some discussion regarding the potential high spin ground states of some nonalternant non-Kekulé **multiradicals**. Semiempirical and *ab initio* studies have shown that **12, 13, 14** and 15 and



12        13        14        15
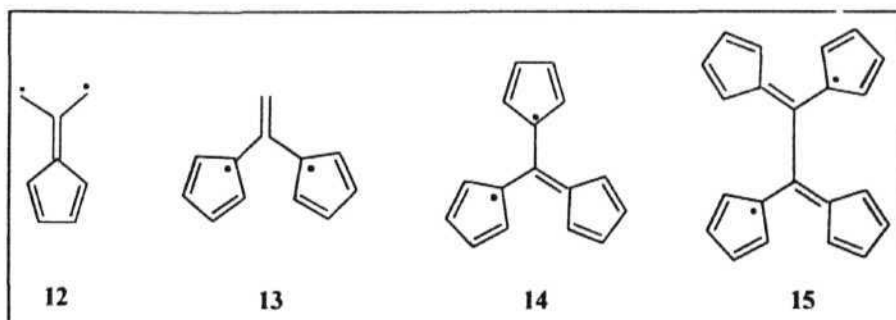
their derivatives would have high spin ground states. High degeneracies in systems like 14 and 15 arising from the connectivities have also been discussed.[47]

*Polaronic ferromagnetism*

A polaron, is an ion radical self trapped in a local lattice distortion and is formed by doping a conjugated conducting polymer with an electron or a hole. Polyacetylene, polyparaphenylene etc. are some of the well known conducting polymers. Fukutome[48] suggested that if block copolymers of conducting oligomers and ferromagnetic spin coupling segments could be prepared and the conducting units doped, the polarons produced would be ferromagnetically coupled. Polyacetylene fragments with a cationic polaron [Fig. 1.10(a)] connected by an oligomer unit [Fig. 1.10(b)] with odd chain length which serves as the ferromagnetic coupling unit, could be used to test this mechanism.



(a)                                                                    (b)

**Figure 1.10 :** *Schematic figure of (a) polaron in a conducting polymer and (b) a ferromagnetic coupling unit.*
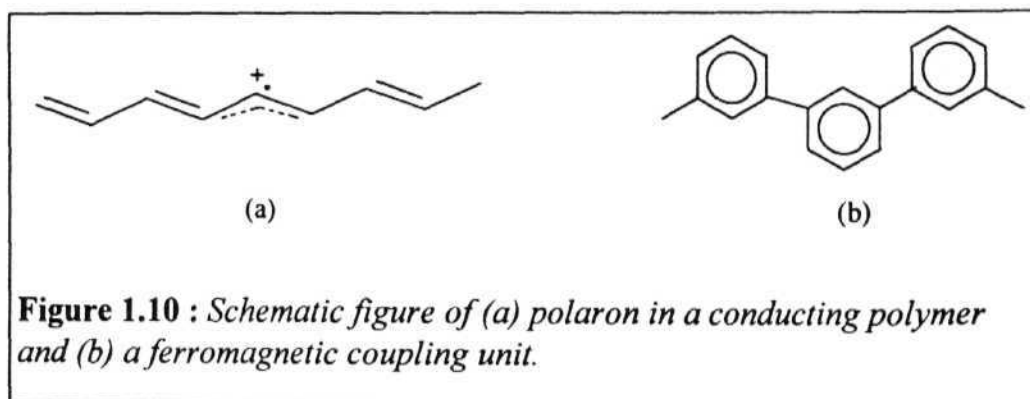
Recently Dougherty *et al*[49] reported a series of compounds synthesized to test this model. They doped several copolymers like 16 and 17 with $I_2$ or $AsF_5$ and studied their magnetic properties. Most of them showed magnetization best described by $S = 1/2$ while a few showed $S > 2$. The spin concentrations were very low and all the systems showed antiferromagnetic coupling of these spins at low temperatures (below 50 K).
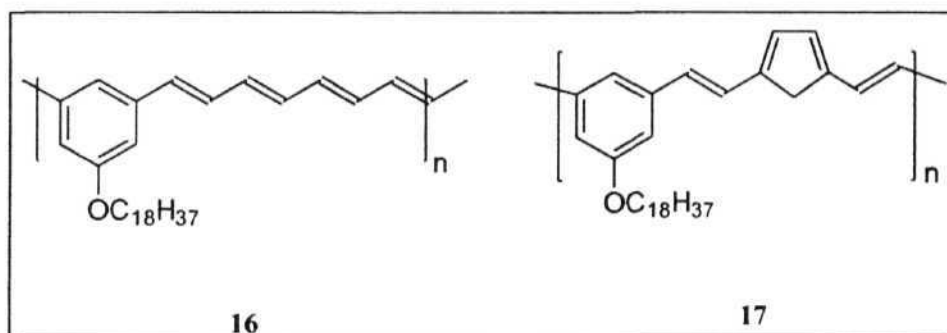


The major drawback of these polyradicals is their chemical reactivity and their instability at ambient temperatures. Veciana *et al* have attempted to circumvent this problem with their perchlorinated triarylmethyl oligomers [10]. Polymers based on these systems have been reported[50]; however, the saturation magnetization corresponds to only about 1% of the spin concentration. Because of the polymeric nature, these materials are often poorly characterised structurally.

*Spin couplings in nonconjugated systems*

Most of the models proposed for ferromagnetic interactions in organic materials involved planar $\pi$-conjugated system. This is due to the fact that the spin coupling through $\pi$-bonds in these systems is stronger than that possible through the $\sigma$ - bonds in their non-conjugated counterparts. Further, nonconjugated multiradicls are relatively unstable species. However, recently there have been some interesting studies based on the systems with saturated carbon atoms.

It has been shown that tanol suberate, 18, which has a sheet like crystal structure, exhibits a Curie-Weiss behaviour at higher temperature regions with a positive Weiss constant (0 = 0.7 K) and a metamagnetic behaviour below 0.38 K[51]. Neutron scattering studies revealed that the spins located on the -NO groups couple ferromagnetically within layers and antiferromagnetically between the layers[52]. The mechanism operative in this case was suggested to be the dipole-dipole (through space) exchange mentioned in Section 1.3. Recently Rassat *et al*[53] prepared the tetramethyl diazaadamantanedioxyl, which they call as, Dupeyre-dioxyl, 19, and it was found to order to a ferromagnetic state below 1.48 K. This molecule also shows a triplet ground state suggesting that, in addition to the through space intermolecular interactions, there is some intramolecular ferromagnetic coupling as well[54].

The reports[55] of ferromagnetic materials by pyrolysis of hydrocarbons and other organic compounds are extremely interesting. Ovchinnikov[56] has proposed a new model, based on a hypothetical phase between graphite and diamond christened by him as 'ferrocarbon'. He has claimed (based on some model calculations) that this phase, wherein the quasi graphite layers of alternately connected $sp^2$ and $sp^3$ hybridised carbon atoms are in turn linked at $sp^3$ carbons to form a 3-D lattice, would have a
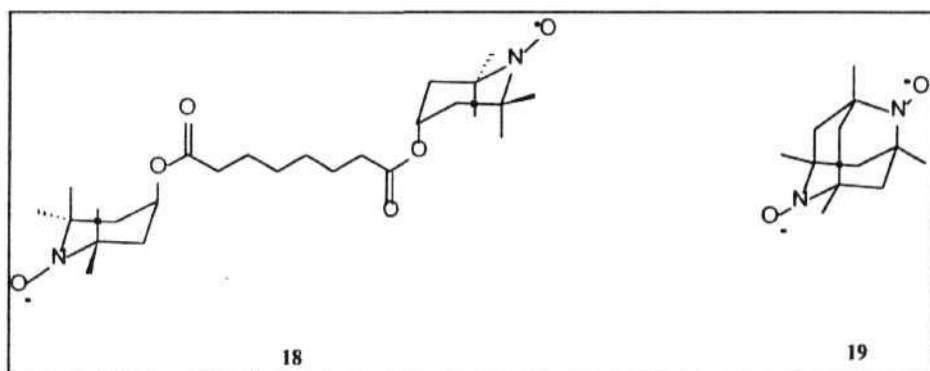


ferromagnetic alignment of the spins at the $sp^2$ radical sites. There has not been any experimental verification of this model so far.

## 1.4.4 MISCELLANEOUS ASPECTS

Another direction in which the search for organic ferromagnetism has progressed relates to the investigations of the influence of additional electrons in spin coupled chains of polyradicals. Rajca *et al*[51] have found

that in diradical anions of triarylmethyl triradicals, when the charge (electron pair) is localized at the terminal sites, ferromagnetic coupling of the spin chain is unaffected by the additional electron. However, when the charge is localized at the centre, anti ferromagnetic coupling between the remaining unpaired electrons is observed. However, Itoh *et al*, found that an excess of electrons in the *n* - conjugated organic high-spin systems, does not cause any drastic effect on the spin polarization.

Veciana *et al*[59] and Sugawara and his group[60] have found that hydrogen bonds are not only able to control the crystal packing of open-shell molecules, but also to propagate ferromagnetic interactions through them. It was shown that the variation of the number and position of OH substituents on the phenyl ring of a- phenyl nitronyl nitroxide radicals yields different hydrogen bonded self assemblies, with some of them forming 3-D networks with bulk ferromagnetic transitions, albeit at very low temperatures.

## 1.5 OUR INVESTIGATIONS OF THE MOLECULAR FERROMAGNET PROBLEM -  LAYOUT OF THE THESIS

As seen in the previous sections, research on molecular magnetic materials is an extremely active field today. There is a great deal of scope to carry out computational or theoretical studies to understand basic mechanisms of spin interactions at the intra and intermolecular level and to

design novel systems to fabricate magnetic materials. In spite of several sporadic successes, the synthesis or fabrication of a viable molecule-based magnet continues to be a great challenge. Developing new molecular magnetic materials and new approaches to such materials is a fascinating area of research. We address in this thesis both lines of investigation, through computational and experimental studies, towards the realisation of a molecule-based magnet.

Systems based on topological models mentioned in Section 1.4.3 are some of the most studied candidates for organic ferromagnetic materials. Considerable amount of theoretical and computational work has been done in this area. Most of the efforts have been directed towards gaining an understanding of the ground spin state and the energy gap between ground and excited spin states of $n$ - conjugated di- or multi- radicals. Several empirical rules have been proposed to predict the ground spin state of radicals and were tested computationally and/or experimentally. Theoretical studies on non-conjugated di- and poly- radicals, on the other hand has been very limited.

In Chapter 2, we provide our results of semiempirical quantum chemical (AM1/CI) calculations on conjugated organic non-Kekulé systems. We also present our studies on the spin coupling in nonconjugated multiradicals. To assess the efficacy of the AM1/CI procedure for problems involving organic radicals, we initially investigated the problem of predicting zero field splitting parameters, important signatures of triplet

diradicals.  Section 2.2 presents the evaluation of ZFS parameters of organic diradicals using spin densities calculated from RHF-AM1/CI method.  The ZFS parameters thus evaluated were found to be superior to results from earlier computations and correlated well with experimental data.  In Section 2.3, the elusive case of the ground state spin of tetramethyleneethane is taken up and it is proved that when sufficient CI is invoked the RHF-AM1/CI calculations can be effective in explaining controversial problems like this, which have earlier been addressed using high level *ab initio* methods.  We next discuss, in Section 2.4, the dependence of spin coupling in conjugated diradicals, on the *n* - electron network and the empirical quantification of the singlet-triplet energy gap in these systems, using a spin coupling parameter.  In view of the fact that there has so far been sparse attention paid to the problem of spin coupling in nonconjugated systems and since some interesting models like the ferrocarbon model for achieving ferromagnetic materials based on this type of spin coupling have been suggested recently, we have taken up an investigation of this problem next.  In Section 2.5 we first present results of some pilot calculations done to test the efficiency of AM1/CI method in studying this class of radicals.  The results of the systematic calculations done to determine the mode of spin coupling in saturated hydrocarbon radicals is presented in detail.  A simple analysis of these results in terms of spin orbital orientations allowed us to present an appraisal of the ferrocarbon model.  Possible extensions of these computational studies to experimental systems are also indicated.

Charge transfer complexes based on the CI models have been investigated in great detail in the search for molecular ferromagnetism. Ferromagnetic transitions in the metallocene-organic acceptor complexes were originally explained invoking these mechanisms. However validity of these models has been questioned[61]. Kahn et al[37] have stressed the importance of considering the several additional excitations in the CI, than just the lowest excited state. However, from a synthetic point of view CT complexes continue to be very appealing for the realization of organic ferromagnets since structurally they are well defined, and problems of spin destruction due to chemical reactivity which plague polymeric systems are virtually absent in the crystalline ion radical stacked systems. In Chapter 3, we present some experimental studies on some novel CT complexes. We propose a simple new model combining some basic features of spin polarisation and charge transfer to achieve ferromagnetism in stacked ion radical complexes. Model calculations (AM1/CI) which support the logic of our mechanism are presented. We have prepared the complexes of the unsymmetrical radical anion $DDQ^{-.}$ (dichlorodicyano-p-benzoquinonide) and the symmetrical anion radical $HCTMCP^{-.}$ (hexacyanotrimethylene-cyclopropanide) with $NMP^+$ (N-methylphenazonium) and $TPC^+$ (trispyrrolidinocyclopropenium) to test this model. Magnetic properties were probed by variable temperature esr experiments. While TPC-DDQ and TPC-HCTMCP turned out to be antiferromagnetic systems following the Curie-Weiss law, NMP-DDQ followed a more complex pattern with regions of antiferromagnetic, ferromagnetic and paramagnetic behaviour. Possible reasons for such behaviour are discussed.

**Figure 1.11:** *Potential ferromagntetic coupling units (a) m-phenylene, (b) pyrimidine and (c) dicyanoimidazole.*
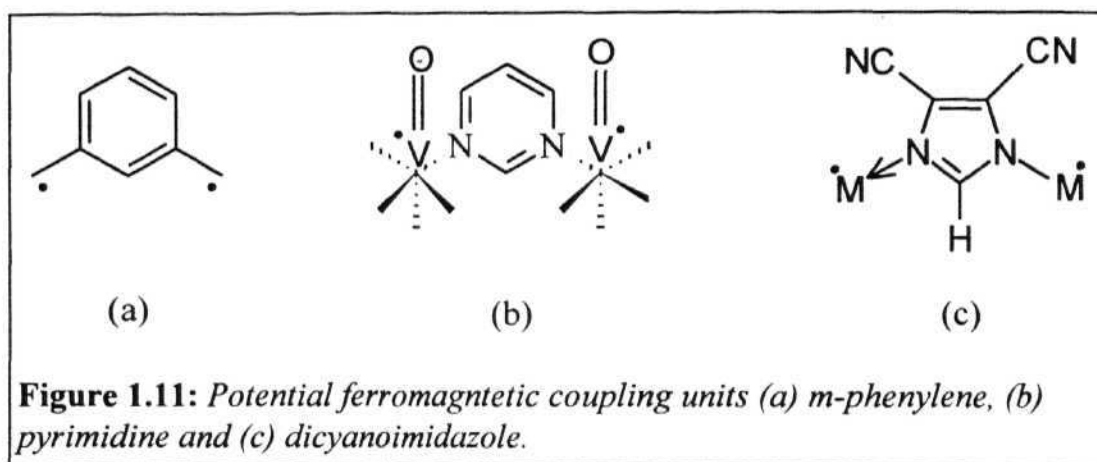
Transition metal coordination polymers have captivated the attention of material scientists due to their interesting physical properties including magnetic properties. Spin coupling between transition metal ions bridged by organic ligands such as pyrimidines [Fig.1.1 1(b)] are mentioned in Section 1.3.1. This is in principle similar to the topological models proposed for organic polycarbenes and polyradicals based on coupling units such as m-phenylenediyl [Fig.1.11(a)]. Earlier studies in our laboratory and a report by Rasmussen *et at[1]* indicated that 4,5-dicyanoimidazole anion, DCI- [Fig. 1.1 1(c)] could be a potential briding ligand between metal ions. We hoped that, it would lead to some 1-D or 2-D polymeric chain structures which may have interesting magnetic properties, if the metal ions had spins residing in orbitals that are in conjugation with the ligand $\pi$-orbitals. Section 3.3 discusses the preparation, structural characterisation and studies

of magnetic properties by susceptibility measurements on some novel copper(II) - DCl complexes.

The need for going beyond 1-D and fabricating 2-D and 3-D structures for achieving high $T_c$ bulk ferromagnetic materials is well known and several workers have focused their attention on preparing materials having appreciable 2-D and 3-D spin interactions. In purely organic materials this approach of involving a second or higher dimension spin interactions is still in its early stages. Synthetic efforts towards branched polymeric radicals have been reported. No model with an inherent two dimensionality built into the magnetic interactions of organic molecular species has been investigated in detail. One of the best known 2-D systems is graphite. An important property of graphite is its ability to form intercalation compounds, graphite intercalation compounds (GIC's) with a wide variety of Lewis acids, alkali metal ions etc. We envisaged that if organic radicals could be intercalated into graphite a novel two dimensional molecular spin system could be obtained, which can have interesting cooperative magnetic interactions mediated by the conduction electrons of the graphite host. We have discovered that TCNE can be intercalated into potassium-graphite binary GIC's. Further, the intercalation can be controlled to different extents, leading to different compositions, with some of them displaying strong Curie-Weiss ferromagnetic behaviour in restricted temperature regimes. We describe in Chapter 4, a simple and efficient procedure to prepare these ternary GIC's with molecular spin subsystems.

Their characterisation by powder diffraction and magnetic studies by esr and susceptibility measurements are described.

As an extension of this study of organic radicals in host lattices, we attempted an investigation of 1,1-diphenyl-2-picrylhydrazyl . (DPPH) embedded in polystyrene films. We describe a simple procedure of growing the DPPH-incorporated films on water surface, which makes it possible to include large amounts of the radicals in the polymer, without unwanted aggregation and clustering. Such large dopant concentrations allow us to reach situations wherein strong exchange interactions develop between the radicals trapped inside the films. Our esr experiments indicate that the radical interactions are quite different from that observed in the pure crystalline state. These studies are described in Section 4.4.

Chapter 5 presents an overview of our computational and experimental investigations in the field of organic/molecular magnetism. Prospects of developing these novel approaches to provide new classes of molecular magnetic materials is discussed.

The various computations reported in this thesis were carried out on the following machines : Micro Vax 3300, Sun Sparc 10 Work Station and Silicon Graphics Power Indigo 2 Work Station. AM1/CI calculations were performed either with MOP AC 5.0 or MOPAC 93 programme package. The *ab initio* study in Sec.2.6 was carried out using the Gaussian 94 suite of programmes.

The powder x-ray diffraction studies were performed on either a Seifert x-ray Diffractometer using Ni filtered Cu $K_\alpha$ radiation or in the case of GIC's where we have specifically looked at $(00l)$ x-ray diffraction peaks, on a Rigaku x-ray diffractometer equipped with a graphite monochromator and $MoK_\alpha$ radiation. The IR spectra were recorded on a JASCO FT/IR-5300 Spectrometer using KBr pressed pellets. UV-Vis spectra were recorded on JASCO 7800 Spectrophotometer. Elemental analysis were carried out on a Perkin-Elmer Elemental Analyser Model 240C.

Magnetic properties were investigated by esr spectroscopy and magnetic susceptibility measurements. Esr studies were carried out on a JEOL JES-FE 3X or JES TE2000 X-band Spectrometer employing $100\,kHz$ modulation. The microwave powers were kept sufficiently low (typically about 0.1 - 0.5 $mW$) so that signal saturation is avoided and modulation widths employed were usually about 10% of the linewidth to prevent line shape distortions. Variable temperature studies were carried out using a JEOL JNM-VT-3C variable temperature accessory and a West Model 3510 Temperature Controller with an overall accuracy of $\pm1°C$ or with an OXFORD Cryostat model 910 with an accuracy of $\pm0.1$ °C. Magnetic susceptibility measurments were performed with a SQUID magnetometer (QUANTUM DESIGN MPMS5). Crystal structure data was collected on an Enraf - Nonius CAD4 computer-controlled diffractometer. $CuK_\alpha$ ($\lambda$ = 1.54178 A) radiation with a graphite crystal monochromator in the incident beam was used. Standard CAD4 centering, indexing and data collection soft ware were used.

# REFERENCES

1. (a) A. H. Morrish, *The Physical Principles of Magnetism*, Wiley-Interscience, New York, 1988. (b) B. D. Cullity, *Introduction to Magnetic Materials*, Addison - Wesley, Massachussetts, 1972. (c) J. C. Anderson, *Magnetsim and Magnetic Materials*, Chapmann and Hall, London, 1968. (d) W. P. Selwood, *Magnetochemistry*, Interscience, New York, Second edition, 1956.

2. C. M. Hurd, *Contemp. Phys.*, 23, 469 (1982).

3. W. D. Callister, Jr., *Materials Science and Engineering : An Introduction*, John Wiley, New York, 1994, p. 659.

4. (a) J. S. Miller and A. J. Epstein, *Angew. Chem. Int. Edn. Engl.*, 33, 385 (1994). (b) *Magnetic Molecular Materials*, D. Gatteschi, O. Kahn, J. S. Miller and F. Palacio (eds.) NATO ASI Series **198,** Kluwer Academic, Dordrecht, 1993. (c) Proceedings of the Fourth International Conference on Molecule-Based Magnets, *Mol. Cryst. Liq. Cryst.*, **271-274,** 1995. (d) O. Kahn, *Molecular Magnetism*, VCH, New York, 1993.

5. For a good overview of this topic, see for example, *Magneto-Structural Correlations in Exchange Coupled Systems*, R. D. Willett, D. Gatteschi and O. Kahn (eds.), NATO ASI Series, D. Reidel Publishing Company, Dordrecht, 1985.

6. (a) P. Day, *Acc. Chem. Res.*, **14,** 236 (1979). (b) C. Bellito and P. Day, *J. Mater. Chem.*, 2, 265 (1992).

7. (a) V. Gadet, M. B. Doeuff, L. Force, M. Verdaguer, K. E. Malkhi, A. Deroy, J. P. Besse, C. Chappert, P. Veillet, J. P. Renard and P.

Beuvillain, *Magnetic Molecular Materials,* D. Gatteschi, O. Kahn, J. S. Miller and F. Palacio (eds.) NATO ASI Series **198, Kluwer** Academic, Dordrecht, 1993. p. 281. (b) W. D. Griebler and D. Babel, Z *Naturforsch.,* **87B,** 832 (1982). (c) J. S. Miller, A. J. Epstein and W. Reiff, *Chem. Rev.,* **88,** 201 (1988).

8. (a) O. Kahn, *Struct. Bonding,* 68, 89 (1987). (b) O. Kahn, *Angew. Chem. Int. Edn. Engl.,* 24, 834 (1985).

9. H. Tamaki, Z. J. Zhong. N. Matsumoto, S. Kida, M. Koikawa, N. Achiwa and H. Okawa. *J. Am. Chem. Soc,* **114,** 6974 (1992).

10. (a) S. Mitsubori, T. Ishida, T. Nogami, H. Iwamura, N. Takeda and M. Ishikawa, *Chem. Lett..* 685 (1994). (b) S. Mitsubori, T. Ishida, T. Nogami and H. Iwamura, *Chem. Lett.,* 285 (1994).

11. O. Kahn, Y. Pei, M. Verdaguer, J. P. Renard and J. Sletten, *J. Am. Chem. Soc.,* 110,782(1988).

12. K. Nakatani, P. Bergerat, E. Codjovi, C. Mathoniere, Y. Pei and O. Kahn, *Inorg. Chem.,* 30, 3977 (1991).

13. O. Kahn, Y. Pei and Y. Journaux in *Inorganic Materials,* D. W. Bruce and D. O' Hare (eds.), John Wiley, New York, 1994, p. 59.

14. (a) A. Caneschi, D. Gatteschi, P. Rey and R. Sessoli, *Inorg. Chem.,* 27, 1756 (1988). (b) A. Caneschi, D. Gatteschi and R. Sessoli, *Acc. Chem. Res.,* 22, 392(1989).

15. (a) A. Caneschi, D. Gatteschi and R. Sessoli, in *Magnetic Molecular Materials,* D. Gatteschi, O. Kahn, J. S. Miller and F. Palacio (eds.) NATO ASI Series **198,** Kluwer Academic, Dordrecht, 1993, p. 215. (b) C. Benelli, A. Caneschi, D. Gatteschi and L. Pardi, in *Magnetic*

*Molecular Materials,* D. Gatteschi, 0. Kahn, J. S. Miller and F. Palacio (eds.) NATO ASI Series **198,** KluwerAcademic, Dordrecht, 1993, p. 233.

16. K. Inoue, T. Hayamizu and H. Iwamura, *Chem. Lett.,*745 (1995).

17. K. Inoue and H. Iwamura, *J. Am. Chem. Soc,* **116,** 3173 (1994).

18. K. Inoue, T. Hayamizu, H. Iwamura, D. Hashizume and Y. Ohashi, *J. Am. Chem. Soc,* **118,** 1803 (1996).

19. G. A. Candela, L. Swartzendruber, J. S. Miller and M. J. Rice, *J. Am. Chem. Soc,* **101,** 2755 (1979).

20. S. Chittipeddi, K. R. Cromack, J. S. Miller and A. J. Epstein, *Phys. Rev. Lett.,* 58, 2695 (1987).

21. (a) J. M. Manriquez, G. T. Yee, R. S. McLean, A. J. Epstein and J. S. Miller, *Science,* **252,** 1415 (1991). (b) A. J. Epstein and J. S. Miller in *Conjugated Polymers and Related Materials; The Interconnection of Chemical and Electronic Structure,* W. R. Salaneck, I. Lündstrom and B. Rånby (eds.), *Proc. Nobel Symp.* No **NS81,** Oxford Univeristy Press, Oxford, 1993, p. 475.

22. (a) T. P. Radhakrishnan, *Curr. Sci.,* 62, 669 (1992). (b) T. P. Radhakrishnan in *Strongly Correlated Electron Systems in Chemistry,* S. Ramasesha and D. D. Sharma (eds.), Narosa Publishers, New Delhi, 1996, p. 167.

23. (a) G. Chouteau and C. Veyret-Jeandey, *J. Phys.,* 42, 1441 (1981). (b) K. Awaga and Y. Murayama, *Chem. Phys. Lett.,* **158,** 556 (1989). (c) K. Awaga, T. Sugano and M. Kinoshita, *J. Chem. Phys.,* **85,** 2211 (1986). (d) N. Azuma, J. Yamauchi, K. Mukai, H. Ohya-Nishiguchi and Y.

Deguchi, *Bull. Chem. Soc. Jpn.*, **46**, 2728 (1973). (e) See also articles in Ref. 3(c).

24. G. Wannier, *Solid State Theory*, Cambridge University, Cambridge, 1959, p. 104.

25. H. M. McConnell,./ *Chem. Phys.*, 39, 1910(1963).

26. (a) A. Izuoka, S. Murata, T. Sugawara and H. Iwamura, *J. Am. Chem. Soc.*, **107**, 1786 (1985). (b) A. Izuoka, S. Murata, T. Sugawara and H. Iwamura, *J. Am. Chem. Soc,* **109,** 2631 (1987).

27. N. Azuma, Y. Yamauchi, K. Mukai, H. Ohya-Nishiguchi and Y. Deguchi, *Bull. Chem. Soc Jpn.*, 46, 2728 (1973).

28. (a) K. Awaga, T. Sugano and M. Kinoshito, *J. Chem. Phys.,* 85, 2211 (1986). (b) K. Awaga, T. Sugano and M. Kinoshito, *Solid State Commun.*, 57, 453 (1986). (c) K. Awaga, T. Sugano and M. Kinoshita, *Chem. Phys. Lett.,* **128,** 587 (1986).

29. P. -M. Allemand, G. Srdanov and F. Wudl, *J. Am. Chem. Soc,* **112,** 9391 (1990).

30. K. Awaga and Y. Maruyama, *J. Chem. Phys.,* **91,** 2743 (1989).

31. H. M. McConnell, *Robert A. Welch Found. Conf. Chem. Res.,* **11,** 144 (1967).

32. (a) R. Breslow, *Pure and Appl. Chem.,* 54, 927 (1982). (b) R. Breslow, *Mol. Cryst. Liq.Cryst.,* **176,** 199 (1989).

33. E. Dormann, M. J. Nowack, K. A. Williams, R. O. Angus Jr. and F. Wudl,./. *Am Chem. Soc.*, **109,** 2594 (1987).

34. J. B. Torrance, P. S. Bagus, I. Johannsen, A. I. Nazzal and S. S. P. Parkin,./. *Appl. Phys.,* 63, 2962 (1988).

35. T. P. Radhakrishnan, Z. G. Soos, H. Endres and L. J. Azevedo, *J. Chem. Phys.,S5,* 1126 (1985).

36. T. P. Radhakrishnan, Ph. D. Thesis, Princeton University, 1987.

37. C. Kollmar and O. Kahn, *J. Am. Chem. Soc,* **113,** 7987 (1991).

38. P. -M. Allemand, K. C. Khemani. A. Koch, F. Wudl, K. Holczer, S. Donovan, G. Gruner and J. D. Thompson, *Science,* **253,** 301 (1991).

39. N. Mataga, *Theor. Chim. Acta.,* 10, 372 (1968).

40. (a) S. Murata and H. Iwamura, *J. Am. Chem. Soc.,***113,** 5547 (1991). (b) H. Iwamura and N. Koga, *Acc. Chem. Res.,* 26, 346 (1993).

41. (a) E. Lieb, T. Schultz and D. C. Mattis, *Ann. Phys.,* 16, 407 (1961).(b) E. Leib and D. C. Mattis, *J. Math. Phys.,* 3, 749 (1962).

42. A. A. Ovchinnikov, *Theor. Chim. Acta.,*47, 297 (1978).

43. P. Dowd,./. *Am. Chem. Soc,* 88, 2587 (1966).

44. (a) A. Rajca. *Chem. Rev.,* 94, 871 (1994). (b) A. Rajca, S. Utamapanya and S. Thayumanavan, *J. Am. Chem. Soc,* **114,** 1884 (1992).

45. (a) J. Veciana, C. Rovira, E. Hernadez and N. Ventosa, *Ann. de Quimica,* 73 (1993). (b) J. Veciana, C. Rovira, M. I. Crespo, O. Armet, V. M. Domingo and F. Palacio, *J. Am. Chem. Soc,* **113,** 2552 (1991).

46. (a) H. Iwamura, *Pure and Appl. Chem.,* 65, 57 (1993). (b) N. Nakamura, K. Inoue H. Iwamura, T. Fujioka and Y. Sawaki, *J. Am. Chem. Soc,* **114,** 1484(1992).

47. (a) P. Dowd, *Tetrahedron Lett.,* **32,** 445 (1991). (b) T. P. Radhakrishnan, *Tetrahedron Lett.,* **32,** 4601 (1991).

48. H. Fukutome. A. Takahashi and M. Ozaki, *Chem. Phys. Lett.,* **133,** 34 (1987).

49. M. M. Murray, P. Kaszynski, D. A. Kaisaki, W. Chang and D. A. Dougherty,./. *Am. Chem. Soc.* **116**, 8152 (1994).

50. M. Ota and S. Otani, *Chem. Lett.,* 1179 (1989); 1183 (1989).

51. G. Chouteau and C. Veyret-Jeandey, *J. Phys (Paris),* **42,** 1441 (1981).

52. P. J. Brown. A. Capiomont, B. Gillon and J. Schweizer, *J. Magn. Magn. Mater.,* **14**, 289 (1979).

53. R Chiarelli, M. A. Novack, A. Rassat and J. L. Tholence, *Nature,* **363,** 147(1993).

54. R. Chiarelli, A. Rassat and P. Rey, *Phys. Scr.,* **T49,** 706 (1993).

55. (a) K. Tanaka, M. Kobashi, H. Sanekata. A. Takata, T. Yamabe, S. Mizogami, K. Kawabata and J. Yamauchi, J. *Appl. Phys.,* **71,** 836 (1992). (b) K. Murata, H. Ushijima, H. Ueda and K. Kawaguchi, *J. Chem. Soc, Chem. Commn.,* 567 (1992).

56. (a) A. A. Ovchinnikov and 1. L. Shamovsky, *J. Mol. Str. (THEOCHEM),* **251,** 133 (1990). (b) A. A. Ovchinnikov, I. L. Shamovsky and K. V. Bozhenko, *J. Mol. Str. (THEOCHEM),* **251,** 141 (1990).

57. S. Rajca and A. Rajca,./. *Am. Chem. Soc,* **117,** 9172 (1995).

58. (a) T. Nakamura, T. Momose, T. Shida, T. Kinoshita, T. Takui, Y. Teki and K. Itoh, *J. Am. Chem. Soc,* **117**, 11292 (1995). (b) M. Matsushita, T. Nakamura, T. Momose, T. Shida, Y. Teki, T. Takui, T. Kinoshita and K. Itoh, *J. Am. Chem. Soc.,* **114,** 7470 (1992).

59. (a) E. Hernandez, M. Mas, E. Molins, C. Rovira and J. Veciana; *Angew. Chem. Int. Edn. Engl.,* 32, 882 (1993). (b) J. Cirujeda, M. Mas, E.

Molins. F. L. de Panthou, J. Laugier, J. G. Park, C. Paulsen, P. Rey, C. Rovira and J. Veciana,./. *Chem. Soc, Chem. Commun.*, 709 (1995).

60. T. Sugawara, M. M. Matsushita, A. Izuoka, N. Wada, N. Takeda and M. Ishikawa, *J. Chem. Soc, Chem. Commun.*, 1723 (1994).

61. (a) W. E. Broderick and B. M. Hoffmann, J. *Am. chem. Soc.*, **113,** 6334 (1991). (b) F. Zuo, A. J. Epstein, C. Vazquez, R. S. McLean and J. S. Miller, *J. Mater. Chem.*, **3,** 215 (1993).

62. P. G. Rasmussen, L. Rongguang, W. M. Butler and J. C. Bayón, *Inorg. Chim. Acta*, 118,7(1986).

# CHAPTER 2

# COMPUTATIONAL STUDIES OF SPIN COUPLING IN ORGANIC CONJUGATED AND NONCONJUGATED RADICALS

## 2.1 INTRODUCTION

The quest for purely organic magnetic materials is one of the actively pursued areas of research today[1]. Several models were proposed to achieve ferromagnetic interactions and ordering in organic materials (having no metal component) and they were discussed in the previous chapter [Section 1.4]. Among these, the topological models put forward by Ovchinnikov[2] and Mataga[3] early on, are very interesting and still very relevant for the design of purely organic magnetic materials. Enormous amount of effort has been put into the design of radical polymers as potential organic magnets. Organic diradicals[4] are of longstanding interest in chemistry, as important reaction intermediates. These are also the basic units of the topological models suggested for organic ferromagnetic materials. Apart from the molecular structure, the features of these diradicals which are relevant to magnetism are: (i) their ground state spin, (ii) the spin density distribution and (iii) the singlet-triplet energy gap.

A triplet ground state for the diradical is indicative of the potential magnetic coupling at the monomeric level, which perhaps can be extended to ferromagnetic interactions at the polymer level. The Zero Field Splitting parameters (ZFS), D and E are the characteristic signatures of the triplet state, which provide information on the molecular structure as well.

Many theoretical and computational studies have addressed the problem of the prediction of the ground state spin in organic $\pi$-conjugated

diradicals.  Ovchinnikov[2] proved that the ground state spin S of an alternant system is given by (N*-N)/2, where N* and N are the number of starred and unstarred carbon atoms in that molecular structure.    Coulson and Rushbrooke and Longuet-Higgins[5] showed that in alternant systems, the ground state spin multiplicity, is given by (N - 2T + 1), where N is the total number of carbon $\pi$-centres and T is the maximum number of double bonds. Tyutyulkov[6] and coworkers generalised this theorem so that heteroatoms and nonalternant systems can also be included.  Borden and Davidson[7] have discussed the spin states of conjugated radicals in terms of the disjoint nature of the nonbonding $\pi$-MOs.  Recently Radhakrishnan[8] has developed a very general rule based on the topology of the molecule concerned, using the spin polarisation picture.

Thus we see that the problem of the ground state spin of di and multiradicals has been addressed by many investigators.  The energy gaps between various spin states have also been subjected to detailed computational and experimental studies.    However, the important characterisation of a high spin state, namely its fine structure constants, D and E, have been rather difficult to compute in good agreement with experiment, although some earlier studies are known[9].

Compared to the extensive computational studies reported on *n*-conjugated di and poly radicals, the literature on the problem of spin coupling in nonconjugated radicals (systems with radical sites separated by saturated carbon atoms) have been sparse.  The higher reactivity compared

to similar conjugated systems and the relatively weaker spin coupling expected in these systems may be the reasons for the paucity of interest in them.

In this chapter the semiempirical quantum chemical studies we have carried out on various conjugated and nonconjugated di and multiradicals are discussed. The first section presents various aspects of the semiempirical quantum chemical methods employed and the configuration interaction schemes invoked. Next we present our computational results on the ZFS parameters of a large number of conjugated diradicals and compare them to experimental and earlier computational results. This study was carried out primarily to test the capability of the AM1 /CI procedure to address spin state problems, in particular to compute spin densities. In the next section we discuss a systematic investigation of the controversial problem of the ground state spin of tetramethyleneethane which again illustrates the utility of the semiempirical quantum chemical approach in this area. The topological dependence of spin coupling in the diradicals are analysed semiquantitatively in the following section and empirical procedures to predict singlet-triplet gaps are developed. The next section deals with the analysis of spin coupling in nonconjugated radical systems and an appraisal of the so-called 'ferrocarbon' model for organic ferromagnets. Concluding section presents an overview of the results and indicates direction for future work, including experimental studies.

## 2.2 THEORETICAL BACKGROUND AND COMPUTATIONAL METHODS

Today a number of methods are available to the quantum chemist to investigate the electronic and geometric structure of molecules. Molecular mechanics methods provide empirical schemes to explore the structure and energetics of very large and complex molecules. Semiempirical methods have evolved into very sophisticated techniques with which extremely reliable predictions of a wide variety of molecular properties can be achieved. With increasing power of computers, very high level of *ab initio* computations can be carried out today utilising sophisticated basis sets. These different techniques find applications in different environments. For many experimentalists interested in large molecules, semiempirical methods still remain one of the optimal methods of choice.

Semiempirical schemes based on the ZDO approximation[10] have evolved through the CNDO[11], INDO[12] and NDDO[13] schemes. Table 2.1 provides a brief summary of some of the popular semiempirical schemes.

Improved parameterisations of INDO and NDDO by Dewar and coworkers have led to the development of the popular MINDO and MNDO methods respectively. The widely successful MNDO procedure was further improved, mainly with respect to the core repulsion functions, to create the

**Table 2.1:** *The various semiempirical methods and the major assuptions involved in them.*

| Method | Basic assumptions |
|---|---|
| CNDO (Complete Neglect of Differential Overlap) | i) ZDO approximation is applied for all two centre orbital products in both overlap and two electron integrals. ii) All three and four centre two electron integrals are neglected. iii) In one and two centre two electron integrals only Coulombic ones are retained. |
| INDO (Intermediate Neglect of Differential Overlap) | i) For all the overlap integrals ZDO approximation is applied. ii) The three and four centre two electron integrals are neglected; among the two electron two centre integrals those of non-Coulombic nature are eliminated. iii) One centre two electron integrals are all retained. |
| NDDO (Neglect of Diatomic Differential Overlap) | i) For all the overlap integrals ZDO approximation is applied. ii) For the two electron integrals ZDO is assumed valid when the atomic orbitals ascribed to a given electron belong to different atoms. |

AM1 code. The semiempirical quantum chemical method, Austin Model 1 (AM1)[14] is one of the most successful computational tool for studying the molecular and electronic structures of moderate to large size organic compounds. It is conceptually simple and computationally inexpensive. We have found that the AM1 calculation involving a reasonable amount of configuration interaction (CI) beyond the HF level provides a fairly accurate prediction of the ground state spin and the magnitude of spin coupling *(ie* energy gap between the ground and excited spin state) in various organic di and multiradicals. We and others[15] have found that the open shell RHF (with CI) procedure is superior to the UHF/CI method in the calculation of the magnitude of spin coupling and the prediction of the ground state spin. The CI procedure employed in the AM1/CI calculations is briefly explained[16] below, using the specific case of a full CI calculation involving 5 MOs (CI = 5) on a diradical.

Suppose there are N occupied levels in the diradical system that is considered for the calculation. These levels are first determined by an SCF calculation. A ground state energy is defined using the lowest N-3 filled MOs. The active space for CI includes the highest occupied molecular orbital, HOMO (N) and the closest lying two filled levels (N-1, N-2), and the lowest two unfilled virtual levels (N+1, N+2). Permutation of six electrons in these five MOs generates 100 configurations (micro states) in a singlet state calculation as follows :

| | | | | | |
|---|---|---|---|---|---|
| 1 | 1 | 1 | 0 | 0 | α |
| 1 | 1 | 1 | 0 | 0 | β |
| | | | | | |
| 1 | 1 | 0 | 1 | 0 | |
| 1 | 1 | 1 | 0 | 0 | |

....................................................

....................................................

| | | | | |
|---|---|---|---|---|
| 0 | 0 | 1 | 1 | 1 |
| 0 | 1 | 0 | 1 | 1 |
| | | | | |
| 0 | 0 | 1 | 1 | 1 |
| 0 | 0 | 1 | 1 | 1 |

Similarly a triplet state calculation involves 50 configurations as follows:

| | | | | | |
|---|---|---|---|---|---|
| 1 | 1 | 1 | 1 | 0 | α |
| 1 | 1 | 0 | 0 | 0 | β |
| | | | | | |
| 1 | 1 | 1 | 0 | 1 | |
| 1 | 1 | 0 | 0 | 0 | |

....................................................

....................................................

| | | | | |
|---|---|---|---|---|
| 0 | 1 | 1 | 1 | 1 |
| 0 | 0 | 1 | 0 | 1 |
| | | | | |
| 0 | 1 | 1 | 1 | 1 |
| 0 | 0 | 0 | 1 | 1 |

Now the **CI** matrix is formed based on empirical rules; the off diagonal elements corresponding to configurations differing by more than two MOs

are neglected. Then the matrix is diagonalised. The ground state energy of the total system is calculated by correcting the ground state energy previously defined using the lowest eigen value of the CI matrix. The various excited state energies are then calculated from the higher eigen values. The CI calculations were invoked in the AM1 procedure, using the keyword, C.I.=n, where n is the number of MOs bracketing the HOMO-LUMO as described above, within which the full CI scheme is invoked.

We have observed in most of the cases, that an open shell configuration was preferred over a closed shell state when the spin state permits both. For example, for a diradical, the singlet state with two unpaired electrons was generally more stable than the one with no unpaired electrons. Technically this meant that for a singlet state calculation, inclusion of the keyword, OPEN(2,2) in the AM1 method led to lower energies, and was employed in all the calculations reported in this thesis.

For the computation of energy gaps between spin states, the following procedure was generally adopted, deviations, if any, are noted at the appropriate places. The geometries are fully optimized for the different spin states of interest. Based on the heats of formation (or the total energy when we have carried out *ab initio* calculations) of these structures, the ground state spin is ascertained. The heats of formation of the other possible spin states for that system are now evaluated at the geometry corresponding to the ground spin state. The differences are quoted as the spin state energy gaps. This procedure therefore provides the spin state gaps

having an experimental relevance, which at the same time takes care of exceptional situations where, the geometries in different spin states are very different. In general we have adopted the convention of defining the energy gaps as the energy of the state with higher multiplicity subtracted from the energy of the state with lower multiplicity. For example, a positive value of $\Delta_{ST}$ indicates that the triplet is stabler than the singlet.

## 2.3 EVALUATION OF ZFS PARAMETERS IN ORGANIC DIRADICALS

In an electron spin resonance (esr) experiment dealing with di and multispin systems, each unpaired electron is affected not only by the applied magnetic field but also by the field associated with the spin of the other unpaired electron(s). The spin Hamiltonian for a triplet state can be written as :

$$H = g\beta H.\,(S_1+S_2) + g^2\beta^2\,(S_1S_2/r^3 - 3(S_1.r)\,(S_2.r)/r^5)$$

where the first term, the Zeeman term, describes the interaction of the spins ($S_1$ and $S_2$) with the applied magnetic field H, while the second term deals with the interaction of the unpaired electron spins with each other. This term, called the spin-dipolar Hamiltonian can be expressed in a more convenient form[17]

$$H_D = D(S_z^2 - 1/3\ S^2) + E(\ S_x^2 - S_y^2)$$

where S is the total spin operator with components $(S_x, S_y$ and $S_z)$ oriented along the principal axes. The D and E values define the energy levels that lead to the observed **fine** structure in an esr spectrum.

A resolved esr spectrum for a randomly oriented triplet molecule, with $D \neq 3E$, will consist of a six line pattern with pairs of lines having separations of 2D, D+3E and D-3E between the outermost, the middle and the innermost lines respectively[18]. From such a spectrum the D and E values can be calculated very easily. They also can be obtained from the diagonalised ZFS tensor $\underline{D}$ whose components $D_{pq}$ are calculated using

$$D_{pq} = (1/2)g^2\beta^2 \sum_{i,j} \rho_i\rho_j\ (r_{ij}^{\ 2}\delta_{pq} - 3p_{ij}q_{ij})r_{ij}^{-5}$$

where $\rho_i$ and $\rho_j$ are the spin densities at atomic sites i and j and $r_{ij}$ is the vector connecting these sites. The eigen values X,Y and Z of the traceless tensor $\underline{D}$, provide directly the D and E values as given below

$$D = -Z + (X+Y)/2$$
$$E = -(X+Y)/2$$

The spin densities in the calculation of the components of the ZFS tensor $\underline{D}$, can be taken either from the experimental hyperfine structure or electronic

structure computations. In this thesis the attention is focussed on the latter approach.

There have been some earlier studies where spin densities obtained from *ab initio*[19] and semiempirical[20] calculations were used to calculate D and E values using the above equations. Particular mention should be made of the fact that the D values calculated from semiempirical methods used by Rule *et al*[20c] were uniformly higher by a factor of 2, than the corresponding experimental values (where available) and the physical basis of this apparently consistent discrepancy is not understood[9]. The computational speed of semiempirical quantum chemical methods and their capability of handling experimentally relevant large molecules, coupled with the accuracy afforded by AM1/CI[8,21] method in predicting the ground state spin of several diradicals prompted us to take up the study of calculating the ZFS parameters using spin densities obtained from open shell RHF AM1 calculations. We were also interested in utilising AM1/CI calculated spin densities in our analysis of the spin polarisation picture to be developed in Section 2.5 later.

Several planar π-conjugated diradicals were considered for this study, based on the availability[20c,20d] of experimental and/or previous computational data on their ZFS parameters. Many of these systems have been discussed in literature as possible coupling units in organic ferromagnets. The molecular graphs are given in Fig. 2.1. The hydrogens are omitted for clarity. The dominant spin sites (other symmetry related

sites are also possible in some of the structures) are labelled in Fig. 2.1. The calculated spin densities at these sites are in good agreement with that expected on the basis of a spin polarisation picture to be discussed at length in Section 2.5, and are presented in Table 2.2. It may be noted that the computed spin densities have to be divided by a factor of 2, to take care of the discrepancy between the AM1 spin densities, which add up to 2 (the total number of unpaired electrons) and the spin densities needed for the calculation of ZFS parameters, which should add up to 1, the total spin quantum number for a triplet state.

The calculated singlet-triplet energy gaps for these molecules are in agreement with previous theoretical estimates where available. There are interesting exceptions though, like tetramethyleneethane (TME, 4) and the Roth's diradical (5)[22]. The detailed investigation of the correct ground state spin prediction for TME is discussed later in this chapter [Section 2.4].

The D and E values calculated using the spin densities obtained from the RHF AM1/CI method are provided in Table 2.3. The superiority of the AM1/CI method over the earlier semiempirical computation methods

**Figure 2.1:** *The diradicals whose ZFS parameters are calculated in this study. The dominant spin sites are labelled.*
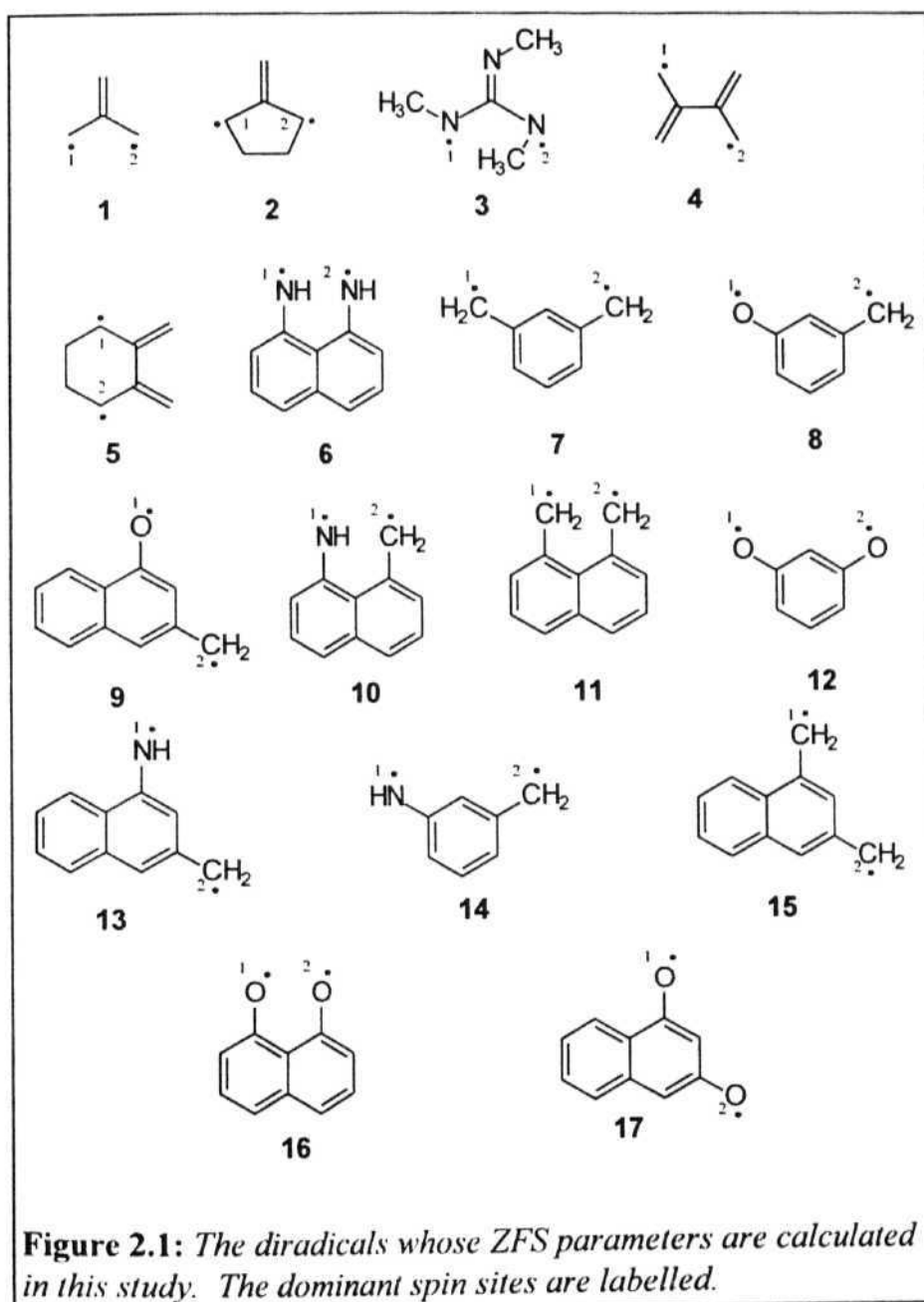
**Table 2.2:** *The calculated spin densities at the labelled sites for the diradicals* **1-17**.

| Molecule | Site 1 | Site 2 |
|:---:|:---:|:---:|
| 1 | 0.33 | 0.33 |
| 2 | 0.64 | 0.64 |
| 3 | 0.57 | 0.57 |
| 4 | 0.24 | 0.24 |
| 5 | 0.53 | 0.53 |
| 6 | 0.24 | 0.24 |
| 7 | 0.50 | 0.50 |
| 8 | 0.19 | 0.53 |
| 9 | 0.14 | 0.53 |
| 10 | 0.22 | 0.41 |
| 11 | 0.38 | 0.38 |
| 12 | 0.21 | 0.21 |
| 13 | 0.21 | 0.15 |
| 14 | 0.15 | 0.26 |
| 15 | 0.20 | 0.25 |
| 16 | 0.14 | 0.14 |
| 17 | 0.21 | 0.10 |

is clearly illustrated by comparing with the experimental numbers where available. The results indicate that **AM1/CI** calculations have in general a good predictive capability as far as the D and E values are concerned.

**Table 2.3:** *The calculated D and E values. Comparison with experimental and previous theoretical data are provided where available*[9,20c].

| Molecule | D (cm$^{-1}$) | | | E (cm$^{-1}$) | | |
| --- | --- | --- | --- | --- | --- | --- |
| | Exptl. | Calculated | | Exptl. | Calculated | |
| | | This Work | Previous | | This work | Previous |
| 1 | 0.0248 | 0.0359 | 0.0520 | ≤0.0003 | 0.0000 | - |
| 2 | 0.0256 | 0.0321 | 0.0470 | 0.0055 | 0.0007 | - |
| 3 | 0.0330 | 0.0255 | 0.0337 | ~0.0000 | 0.0000 | - |
| 4 | 0.0250 | 0.0288 | 0.0490 | <0.0010 | 0.0068 | - |
| 5 | 0.0240 | 0.0255 | 0.0490 | 0.0037 | 0.0065 | - |
| 6 | 0.0257 | 0.0267 | - | <0.0004 | 0.0006 | - |
| 7 | 0.0110 | 0.0279 | 0.0323 | ≤0.0010 | 0.0070 | 0.0047 |
| 8 | 0.0266 | 0.0353 | 0.0543 | 0.0074 | 0.0070 | 0.0087 |
| 9 | 0.0204 | 0.0290 | 0.0438 | 0.0052 | 0.0051 | 0.0076 |
| 10 | 0.0255 | 0.0255 | 0.0356 | 0.0008 | 0.0013 | 0.0111 |
| 11 | 0.0218 | 0.0229 | 0.0377 | 0.0021 | 0.0006 | 0.0111 |
| 12 | - | 0.0415 | 0.0873 | | 0.0054 | 0.0068 |
| 13 | - | 0.0257 | 0.0393 | | 0.0041 | 0.0039 |
| 14 | - | 0.0302 | 0.0459 | | 0.0070 | 0.0043 |
| 15 | - | 0.0242 | 0.0262 | | 0.0049 | 0.0023 |
| 16 | - | 0.0317 | 0.0756 | | 0.0004 | 0.0154 |
| 17 | - | 0.0350 | 0.0708 | | 0.0029 | 0.0052 |

It may be noted that the computed D and E values for the Roth's diradical[23] are in good agreement with the experimental values; however, the reported Curie plot for this compound is in conflict with the AM1 prediction of the stabilization of singlet over triplet by about 5 kcal/mol. In general the calculated D values agree very well with the experimental data. The E values are much smaller in all cases and the agreement with the experimental data is poorer. However, it is to be noted that previous theoretical results deviate much more from the experimental values.

The D and E values can be used as strong signatures of the ground state spin of diradicals. The problem continues to remain rather elusive in the case of TME as discussed in the next section.

## 2.4 THE GROUND STATE SPIN OF TETRAMETHYLENE-ETHANE AND ITS ZFS PARAMETERS

Several simple rules were given to predict the ground state spin of organic diradicals and these have been listed earlier in this chapter [Section 2.1]. However, there are some cases where the prediction of the ground state spin using these simple rules has run into controversies. Even extensive computational studies have not helped to resolve the issue satisfactorily in certain instances. The most famous and notable conflict between theoretical and experimental results is the ground state spin

problem of tetramethyleneethane, TME (4, Fig. 1). Experiments by Dowd *et al*[24] have indicated that TME exists as a triplet ground state species with

**Table 2.4:** *The various singlet-triplet energy gaps reported for TME using a variety of methods.*

| Method of Calculation | Symmetry | $\Delta E_{ST}$ (kcal/mol) |
|---|---|---|
| INDO-S/CI[25] | $D_{2h}$ | -0.6 |
| AM1/CI[8] | $D_{2h}$ | -6.3 |
| PPP[26] | $D_{2h}$ | -5.3 |
| Exact-PPP[27] | $D_{2h}$ | -2.0 |
| SCF-MO/CI[7a] | $D_{2h}$ | -5.3 |
| TCSCF/RHF[28] | $D_{2h}$ | -1.8 |
| SD-CI[28] | $D_{2h}$ | -2.8 |
| MCSCF (2,2)[29] | $D_{2h}$ | -1.7 |
| MCSCF (6,6)[29] | $D_{2h}$ | -3.8 |
| TCSCF/RHF[28] | $D_2$ | 0.1 |
| SD-CI[28] | $D_2$ | -0.4 |
| MCSCF (2,2)[29] | $D_2$ | -0.7 |
| MCSCF (6,6)[29] | $D_2$ | -1.4 |
| TCSCF/RHF[28] | $D_{2d}$ | -2.5 |
| SD-CI[28] | $D_{2d}$ | -2.2 |
| MCSCF (2,2)[29] | $D_{2d}$ | -2.5 |
| MCSCF (6,6)[29] | $D_{2d}$ | -1.9 |

a likely nonplanar geometry ($D_{2d}$) [Fig. 2.2]. The theoretical calculations at various levels [Table 2.4] and the simple rules mentioned above, on the other hand, have consistently predicted a ground state singlet at planar as well as twisted geometries, with varying singlet-triplet energy gaps. It should be mentioned here that the experimentally observed TME species cannot be planar on the basis of the small but finite E value.



**Figure 2.2:** *Representation of the (a) planar($D_{2h}$); (b) twisted($D_2$) and orthogonal ($D_{2d}$) conformations of TME.*
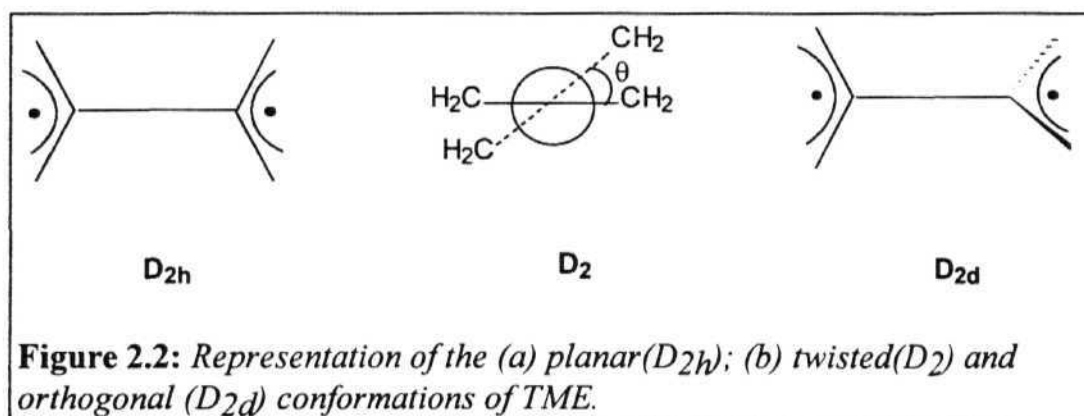
However, Nachtigall and Jordan[30] have shown, using CI+DV2/TZ2P *ab initio* calculations that TME indeed prefers a triplet ground state at a dihedral angle of about 50°.

We were interested in exploring whether the **AM1/CI** method could be utilised to make a correct prediction of the ground state spin of TME, and perhaps even calculate the D and E values agreeable with experimental results. The potential energy surface of TME singlet and triplet state along

the twisting coordinate, 9, was examined invoking $CI = 5$. Each of the two $H_2C\text{-}C\text{-}CH_2$ units were kept planar. At each fixed G, the geometry was optimized. The heats of formation of these optimized structures are plotted against $\theta$ [Fig. 2.3(a)]. The plot clearly shows that the singlet state is preferred at all geometries. However there is a decrease in the magnitude of $\Delta E_{ST}$ as the 0 is increased from 0 to 90 and finally the singlet and triplet states become nearly degenerate in the vicinity of 90°. The results are qualitatively similar to the reports by Borden and Du[28] and Chakrabarthi *et al*[27].

The possible reason for the discrepancy between the AM1/CI calculations and the *ab initio* CI studies of Nachtigall and Jordan could be the inadequacy of the CI scheme used in the AM1 study to represent the correct level of electron correlation. It was envisaged that the inclusion of all the six *n* MOs in the CI may provide better correlation with experimental and high level *ab initio* results. So, the triplet and singlet state potential energy surfaces were re-examined with $CI = 6$. It may be noted here that a $CI = 6$ calculation considers 400 configurations for the singlet and 225 configurations for the triplet state (compared to 100 and 50 configurations considered in a $CI = 5$ calculation). The singlet and triplet heats of formations for the AM1/CI=6 study are plotted against the twisting coordinate 0 [Fig. 2.3(b)]. Clearly the results are quite different with respect to the $CI = 5$ studies. The triplet surface falls steeply at 36° and for 0 = 50 - 90° there is only a minor increase in energy. The singlet surface also falls

steeply but at 44° and crosses the triplet at 50°. From 50 - 90° it remains close to the triplet. The singlet-triplet energy gap at 42° is **10.8** kcaj/mol.
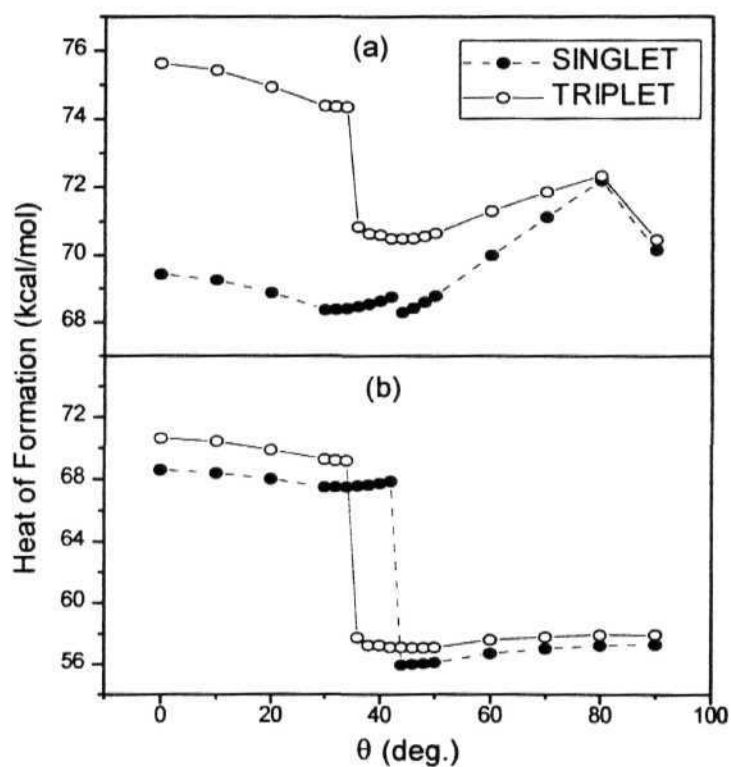


**Figure 2.3:** *Calculated singlet and triplet energy profiles of TME at various twisting geometries for (a) CI = 5 and (b) CI = 6; the lines are only a guide to the eye.*

It may be noted that in the *ab initio* study of Nachtigall and Jordan[30] this energy gap was found to be 1 - 1.5 kcal/mol at 49.5°. The CI = 5 calculations show that the triplet cannot be observed till 6 is 90°, whereas the CI = 6 calculations clearly indicate that the triplet is the ground state at 9 = 40° and the near degeneracy of triplet and singlet above this angle makes it possible to observe experimentally a triplet even above this twisting angle.

After getting satisfactory results which compare well with high level *ab initio* computations in the case of the ground state spin of TME using the AM1/CI=6 method we next proceeded to tackle the problem of calculating the ZFS parameters of TME. From the above results it is clearly understood that the experimentally observed TME diradical, having triplet as the ground state, cannot be planar. This was also suggested by Dowd on the basis of the E value obtained experimentally. Keeping all this in view, the ZFS parameters for the various twisted geometries of TME for $9 \geq 30^o$, were analyzed in detail.

The D and E values calculated from the AM1/CI=6 results are plotted against 9 in Fig.2.4. At $9 = 90^o$ ($D_{2d}$ geometry), E = 0 and D is extremely low compared to the experimental value. The optimal pair of D
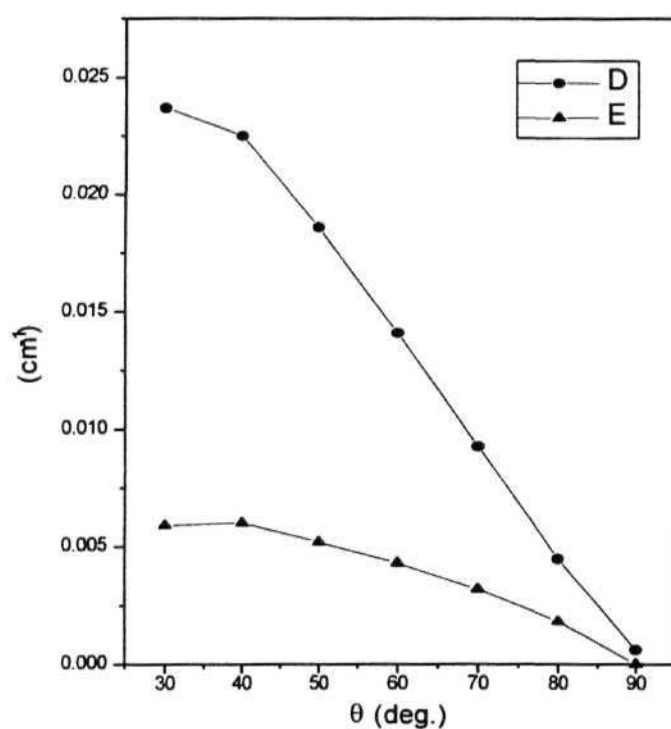
**Figure 2.4:** *The calculated D and E values of TME at various twisting geometries above 30°; the line is only a guide to the eye.*

and E values are obtained for geometries near $\theta = 30$ - $50°$. The D and E values for a fully optimized structure (optimized value of $\theta = 46.5°$) in this region are respectively 0.0179 cm$^{-1}$ and 0.0049 cm$^{*1}$. This seems to be the

closest theoretical description at a semiempirical level, to the experimentally[23] observed TME diradical with $D = 0.025 cm^{-1}$ and $E < 0.001 cm^{-1}$. More detailed analysis like fitting the triplet potential energy surface to a parabola and averaging the D and E values over a Gaussian distribution of several possible conformations likely to be present in the frozen glass (experimental state) were attempted but did not yield any improvement in the computed D and E values.

Thus we conclude that the semiempirical AM1 method can provide correct prediction of the ground state spin even in rather complicated cases like that of TME, provided sufficient CI is involved. We would like to note, however, that in most of the other computational studies we have carried out with the AM1/CI procedure, such sensitiveness of results to the level of CI was not detected. The fine structure splitting values of di- or polyradicals are generally difficult to compute; but AM1/CI (open shell RHF) method appears to be an optimal computational tool to address this problem.

## 2.5 DEPENDENCE OF SPIN COUPLING ON THE *n* - ELECTRON NETWORK IN CONJUGATED DIRADICALS

As explained briefly earlier in this chapter [Section 2.1], several simple rules were put forward to predict the ground state spin of organic $\pi$ - conjugated non-Kekulé systems. A brief mention was also made of a simple general rule suggested by Radhakrishnan[8] based on the spin polarisation

picture utilised earlier by Fukutome[31] in connection with his polaronic mechanism for ferromagnetism. According to the latter model, spin polarisation waves in the polaronic units of a conjugated polymer interfere constructively leading to a ferromagnetic coupling of spins, if the coupling unit has odd chain length and interfere antiferromagnetically if the coupling unit has even chain length. The following rules[8] were given for the prediction of the ground state spin in di and multiradicals.

1. Draw the molecular skeleton graph and insert the maximum number of double bonds such that, radical sites remaining, if any, are separated by the least topological distance (more rigorously, the least number of $n$ - electrons) possible. If the radical sites remaining is zero or 1 the spin state $S = 0$ or $1/2$.

2. On the other hand if the number of radical sites left is two, then (i) $S = 0$, if the shortest path between the two sites is separated by even number of $n$ - electrons or (ii) $S = 1$, if the number of $\pi$-electrons is odd.

3. If the number of radical sites left is more than two; start at any radical site with spin $S_0$: move to the closest radical site with spin $S_1$. The modified spin $S = S_0 \pm S_1$ depending on whether the number of $n$ - electrons on the path is odd or even respectively. Move to the next closest spin site, update $S$ as before. Continue till all the radical sites are covered.

4. In rules 1 and 2, the radical sites are assumed to be spin 1/2 sites. Appropriate modifications have to be made for special systems like carbenic sites; it should also be noted that the number of $\pi_p$ electrons on hetero atoms can be different from 1.

This rule has been tested successfully in several cases by AM1/CI calculations, comparing them with available experimental and/or previous theoretical results. It has also been used to predict the spin states of several controversial nonalternant non-Kekulé systems[32]. Although there are several qualitative rules proposed to predict the ground state spin of diradicals, a systematic quantitative study of the dependence of singlet-triplet energy gaps on the topology of the di or multiradicals has not been carried out previously. If an empirical correlation between the singlet-triplet energy gaps (hence the ground state spin) and the spin density distribution can be worked out, it would provide useful insight into the basic spin polarisation mechanism assumed in the topological models for organic ferromagnetism. A knowledge of the strength of spin interaction in a system reflected in the singlet-triplet gap will be of great use in the design of appropriate model systems to be explored in the ongoing search for organic ferromagnets. For the ferromagnet, one has to design infinite spin systems and understanding the spin coupling at the monomeric level is the crucial first step.

We have carried out AM1/CI computations on several sets of diradicals. Based on the results presented above, we assume that the energy

gaps between spin states and atomic spin densities computed in this method are reliable. Five sets of non-Kekulé structures were considered for this study [Fig. 2.5]. The basic criteria that are kept in view in selecting these molecules are the following. i) For each diradical, the connectivity of the $\pi$-network should allow the choice of a specific shortest topological distance (smallest number of bonds separating them) between the sites with unpaired electrons. ii) Within each sets of diradicals, there should be a regular gradation in the topological distance as well as the number of intervening $n$-electrons, so that a detailed analysis of the dependence of spin coupling with respect to either is possible. iii) There should be systems with odd and even number of intervening $\pi$-electrons between the radical sites so that the mode of spin coupling can also be analyzed.

Molecular graphs of the 26 systems grouped into five sets, considered for this study are provided in Fig. 2.5 (hydrogen atoms are omitted for clarity). A pair of sites with dominant spin densities (not necessarily a unique set in all cases) selected on the basis of Rule 1 above, are also indicated and labelled as 1 and 2. Singlet-triplet energy gaps

**1** (D$_{3h}$)    **2** (D$_{2h}$)    **3** (C$_{2v}$)

**4** (C$_{2h}$)    **5** (C$_s$)

Set 1

**6** (C$_{2v}$)    **7** (C$_s$)    **8** (C$_{2h}$

**9** (C$_{2v}$)    **10** (C$_{2h}$)

Set 2

**11** (D$_{2h}$)    **12** (D$_{2h}$)
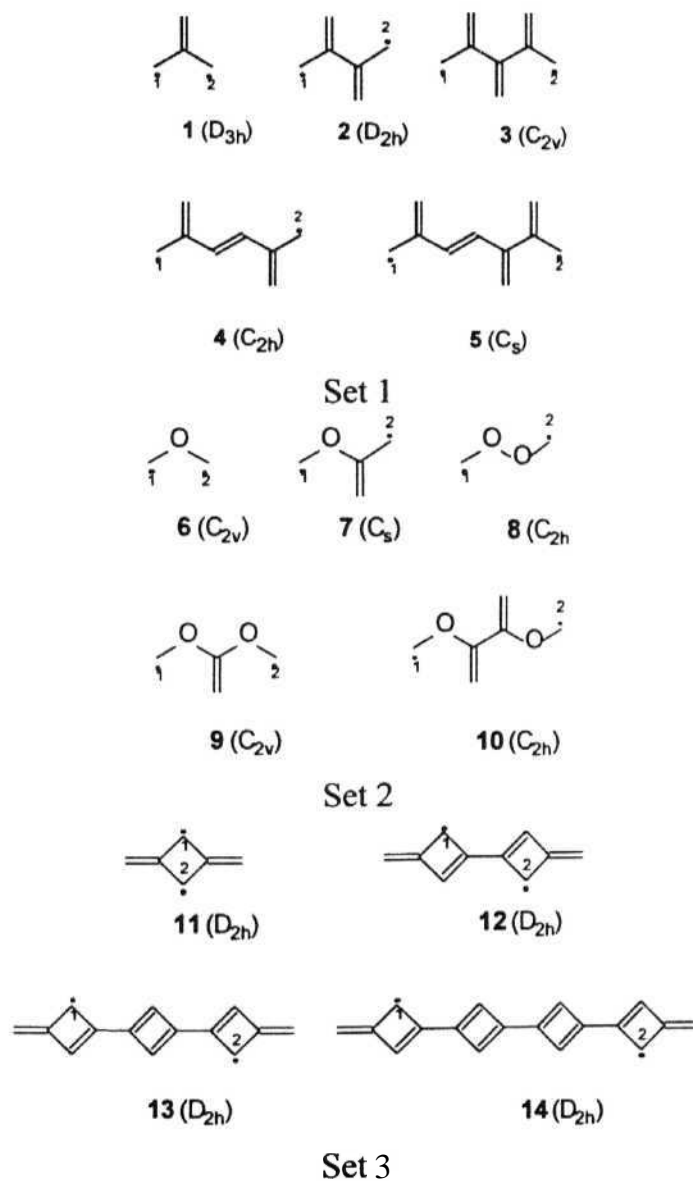
**13** (D$_{2h}$)    **14** (D$_{2h}$)

Set 3

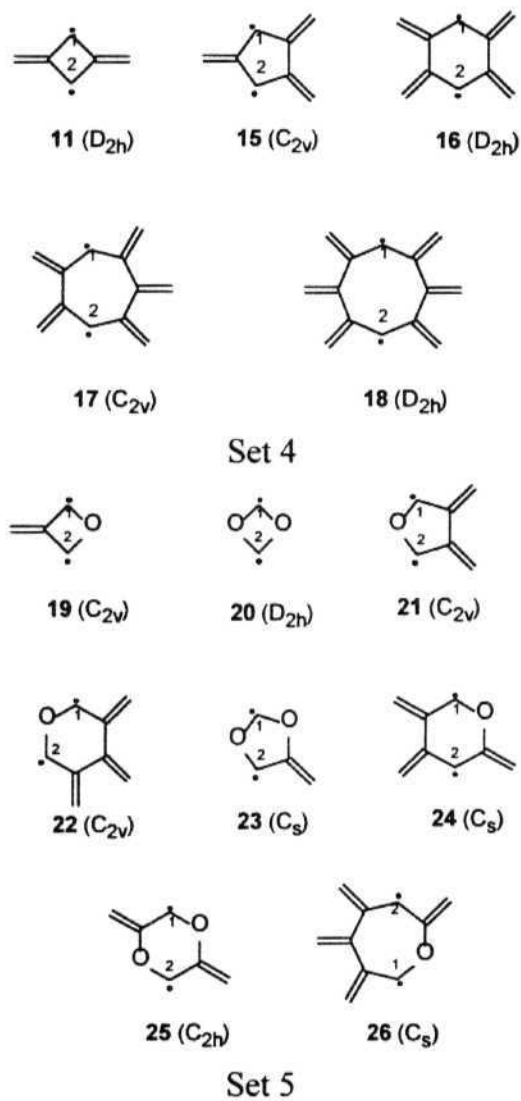**Figure 2.5 (continued on next page):**

**Figure 2.5 (contd.)**: *The diradicals considered in the study of the dependence of spin coupling on the π-electron network.*

computed using the AM1/CI=5 procedure for these systems are collected in Table 2.5.

The first set consists of open chain branched molecules where the radical sites are forced to be at the ends. The topological distance increases from 1 to 5 in these molecules. The number of $\pi$-electrons $n_\pi$, also increases from 1 to 5, oscillating between odd and even. Molecules 4 and 5 are chosen instead of 2,3,4,5-tetramethylenehexatriene and 2,3,4,5,6-pentamethyleneheptatriene, since the latter two tend towards nonplanar structures owing to steric factors and the forced optimization of planar structures led to unphysical geometries, making analysis of the trends in a series meaningless. The singlet-triplet energy gaps of these molecules are plotted in Fig. 2.6 (a). The expected damped oscillation because of the increase in the number of $\pi$-electrons from 1 to 5 and the oscillation between odd and even is clearly observed. It is very interesting to note here that a recent study by Fang *et al*[33] showed very similar results.

The second set is very similar to the first one except that the inclusion of the hetero atom, oxygen, allows the switching of the mode of spin coupling without effecting the topological distance. Fig.2.6 (b) gives the singlet-triplet gap variation with the number of $\pi$-electrons in Set 2. This exercise brought to light a very interesting feature; for similar topological distance, the singlet-triplet gap depends quantitatively on the number of $\pi$-electrons between the radical sites.
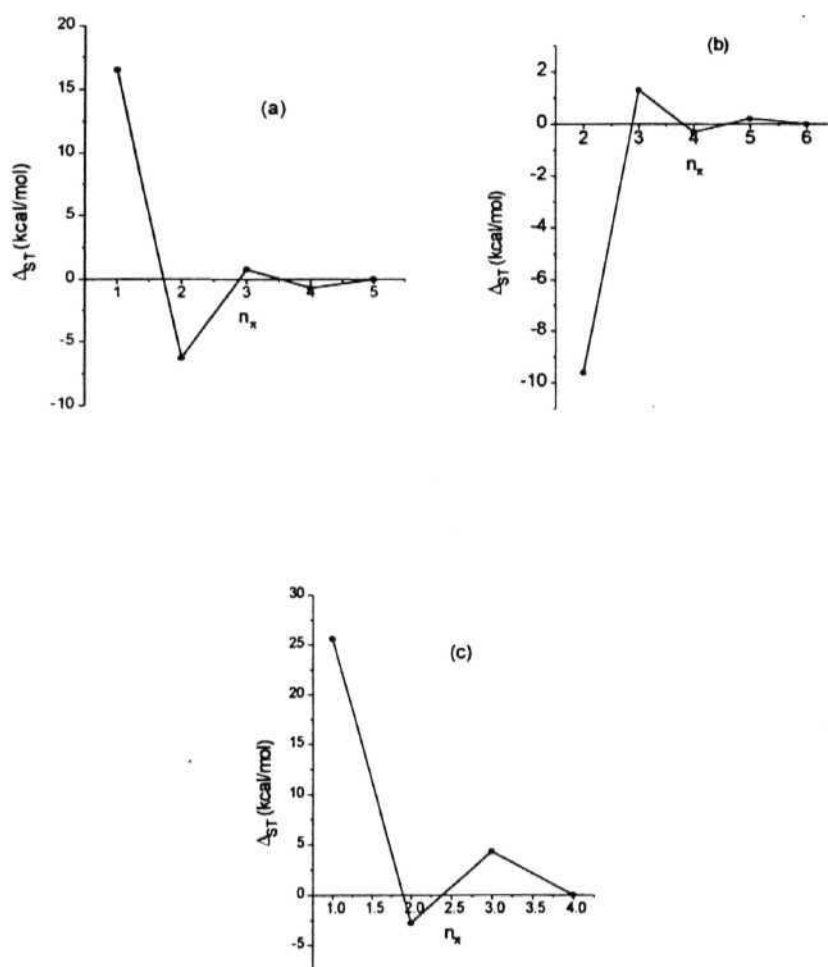
**Figure 2.6:** *The variation in the singlet-triplet energy gap with the number of n- electrons in the **path** for (a) set 1; (b) set 2 and (c) set 3 diradicals in Fig. 2.5; the lines are only a guide to the eye.*

Set 3 consists of poly(cyclobutadienes) with methylene groups attached at 1, 3 positions. Here also there is an increase in the topological distance as well as in $n_\pi$ as we go along the series. Once again the singlet-triplet gaps vary as observed in the previous sets, though there is a slight discrepancy; ie the singlet-triplet gap was slightly higher in magnitude for 13 than 12.

Sets 4 and 5 consist of cyclic systems with methylene groups attached to the ring. These two sets are designed such that there are always two paths possible for the spin coupling, which may be identical or different. In Set 4, the intervening number of $\pi$-electrons (considering both the paths) increase as (1,1), (1,2), (2,2), (2,3) and (3,3)- The net coupling is ferromagnetic for 11, 15 and 18 and antiferromagnetic for 16 and 17. Here the topological distances scale as the intervening number of *n*-electrons and it is clearly seen that the sign of the spin coupling is determined by the number of $\pi$-electrons on the shorter path, when the paths are unequal. In Set 5 on the other hand, the number of $\pi$-electrons increases as (1,2), (2,2), (2,2), (2,3), (2,3), (2,3) and (3,3), whereas the topological distances vary as (2,2), (2,2), (2,3), (2,4) (2,3), (3,3), (3,3), and (3,4). It is very clear from the differences in heats of formations that, the sign of the spin coupling is controlled by the smaller of the two sets of intervening $\pi$-electrons. The dependence of the magnitude of spin coupling may depend on the topological distance or the number of $\pi$-electrons. An analysis of Set 5 may clarify which of the two exerts the dominant influence.

**Table 2.5:** *The singlet-triplet energy gaps for the diradicals* **1-26** *in Fig. 2.5.*

|  | Molecule | $\Delta_{ST}$(kcal/mo1) |
|---|---|---|
| **Set 1** |  |  |
|  | 1 | 16.5 |
|  | 2 | -5.3 |
|  | 3 | 0.8 |
|  | 4 | -0.7 |
|  | 5 | 0.0 |
| **Set 2** |  |  |
|  | 6 | -9.6 |
|  | 7 | 1.3 |
|  | 8 | -0.3 |
|  | 9 | 0.2 |
|  | 10 | 0.0 |
| **Set 3** |  |  |
|  | 11 | 25.6 |
|  | 12 | -2.8 |
|  | 13 | 4.3 |
|  | 14 | 0.0 |

**Table 2.5 (continued)**:

|  | Molecule | $\Delta_{ST}$ (kcal/mol) |
|---|---|---|
| Set 4 |  |  |
|  | 11 | 25.6 |
|  | 15 | 11.8 |
|  | 16 | -4.8 |
|  | 17 | -0.7 |
|  | 18 | 3.2 |
| Set 5 |  |  |
|  | 19 | 5.3 |
|  | 20 | -18.9 |
|  | 21 | -6.3 |
|  | 22 | -4.6 |
|  | 23 | -5.1 |
|  | 24 | -2.3 |
|  | 25 | 4.8 |
|  | 26 | 3.2 |

The singlet-triplet gaps for all the five sets of diradicals are collected in Table 2.5. These results clearly indicate that the computed data are consistent with the predictions of the spin rule and support of the recent study by Fang *et al*[33]. At this point we undertook a detailed analysis to explore possible dependence of the magnitude of the spin coupling (we define below, a parameter to represent this) on the topology and/or the *n-*

**Table 2.6:** *Calculated spin densities for the diradicals **1-26** (Fig. 2.5) at sites 1 and 2.*

| Molecule | Spin density | | Molecule | Spin density | |
|---|---|---|---|---|---|
| | Site 1 | Site 2 | | Site 1 | Site 2 |
| 1 | 0.33 | 0.33 | 14 | 0.13 | 0.13 |
| 2 | 0.24 | 0.24 | 15 | 0.26 | 0.26 |
| 3 | 0.26 | 0.26 | 16 | 0.21 | 0.21 |
| 4 | 0.25 | 0.25 | 17 | 0.21 | 0.21 |
| 5 | 0.25 | 0.25 | 18 | 0.22 | 0.22 |
| 6 | 0.44 | 0.44 | 19 | 0.35 | 0.35 |
| 7 | 0.39 | 0.26 | 20 | 0.42 | 0.42 |
| 8 | 0.42 | 0.42 | 21 | 0.23 | 0.23 |
| 9 | 0.39 | 0.39 | 22 | 0.23 | 0.23 |
| 10 | 0.38 | 0.38 | 23 | 0.37 | 0.25 |
| 11 | 0.34 | 0.34 | 24 | 0.24 | 0.21 |
| 12 | 0.24 | 0.24 | 25 | 0.26 | 0.26 |
| 13 | 0.23 | 0.23 | 26 | 0.22 | 0.23 |

electron network. The spin densities for these molecules are calculated by the AM1/CI open shell RHF procedure. The spin densities for the radical sites (marked 1 and 2 in Fig. 2.5), obtained from triplet state calculations are presented in Table 2.6. The largest spin densities are invariably found at the sites, which are expected to be the radical sites on the basis of simple

resonance structures having the minimum topological separation between them (Rule 1 quoted earlier). For the analysis of the spin coupling, the sign was assigned positive or negative (ferro/antiferro) on the basis of whether the number of intervening $\pi$-electrons is odd or even. When multiple paths in a ring exist the net coupling is evaluated as the algebraic sum.

Initially, we envisaged the spin coupling to be related to the product of the spin densities at the radical sites, weighted by the inverse of topological distance or the number of intervening $\pi$-electrons. When the spin coupling was assumed to be inversely proportional to the topological distance, its correlation with the AM1/CI computed singlet-triplet energy gap, was not very satisfactory (multiple regression coefficient was 0.9). Several other variations of this theme were tried, like powers of topological distance, negative exponential variation in the distance etc. The definition of the spin coupling as an algebraic sum of all the pairwise couplings in the molecule (involving spin densities of all the sites) each weighted with various dependences on the topological distance tried above, was also attempted. However, none of these definitions of the spin coupling gave a better correlation with the singlet-triplet energy gaps.

Next, we explored a definition of spin coupling using the product of the spin densities at the radical sites, weighted with the inverse of the number of intervening $\pi$-electrons. When multiple paths of similar topological distances are present an algebraic sum over the paths was used.

This empirical parameter for the spin coupling, SC, can be formulated as follows.

$$SC = \sum_{P} (-1)^{n_\pi+1} \rho_1 \rho_2 / n_\pi$$

where $n_\pi$ is the total number of intervening $\pi$-electrons in a path and $\rho_1$ and $\rho_2$ are the spin densities at the radical sites 1 and 2. The summation runs over all the conjugated paths, *P,* connecting the radical sites 1 and 2.

The correlation (multiple regression coefficients) of the spin coupling, quantified as above, with the computed singlet-triplet gaps, $\Delta_{ST}$ for each of the sets, described above, as well as the regression coefficient for all the 26 molecules treated as one set are collected in Table 2.7. Except for Set 2, all the others show very good correlation and the regression coefficient for the complete set is also remarkably good considering the varieties of systems considered in this study. The singlet-triplet gap, $\Delta_{ST}$, for the complete set can be related to the empirical parameter SC, using the least square fit equation,

$$\Delta_{ST} \text{ (kcal/mol)} = -0.193 + 112.6 \text{ (SC)}$$

It should be noted here that set 5, as well as molecules 7 and 8 in Set 2 gave a clue for the dependence of spin coupling on the number of intervening $\pi$-electrons rather than on the topological distance between the

spin sites. More detailed algorithms like those described above for the topological distance criterion, produced less satisfactory correlation with the $\Delta_{ST}$.

**Table** 2.7: *Regression coefficients for the linear fit of $\Delta_{ST}$ with SC for individual sets as well as the full set of diradicals* **1-26** *in Fig. 2.5. Regression coefficients when specific molecules are excluded are also provided (see text for details).*

| Set | Number of molecules | Multiple regression coefficient |
|---|---|---|
| 1 | 5 | 0.980 |
| 2 | 5 | 0.846 |
| 2 (excluding 7) | 4 | 0.829 |
| 3 | 4 | 0.996 |
| 4 | 5 | 0.956 |
| 4 (excluding 15) | 4 | 1.000 |
| 5 | 8 | 0.982 |
| Full | 26 | 0.946 |
| Full (excluding 7 and 15) | 24 | 0.964 |

Next we investigated further details of the correlation for the frill data set, to see if the regression coefficient can be further improved by identifying specific problem cases, if any, in the individual sets. The optimized geometries of the singlet and triplet states of every molecule were

compared (in terms of the minimum average deviation of the atomic positions using simple desktop molecular modelling programmes[34]). In all cases, except 7 and 15 an average deviation of less than 0.03A was found, whereas the average deviation was 0.30A for 7 and 0.06A for 15. Therefore, the correlation of the calculated spin coupling parameters to the singlet-triplet energy gaps for the data set excluding these two molecules was determined. In the table, the resulting regression coefficients obtained for Set 2 (excluding 7) and for Set 4 (excluding 15) are also shown. The correlation decreases marginally for Set 2 but increases drastically for Set 4 as well as for the complete set.

A quantitative explanation for the SC dependence on the number of π-electrons may be considered. The spin coupling over a pathway of several 7r-electrons can be viewed as arising out of a series of kinetic exchange[35] interactions between near neighbour sites. The kinetic exchange is directly proportional to the square of the transfer integrals and inversely proportional to the on-site Coulomb repulsion energy. A larger number of π-electrons on the path could decrease the transfer integral since the nuclear charge on the path are screened more effectively. This should lead to a net decrease in the exchange interaction as observed in the above results. Another factor however cannot be overlooked. In the examples that are considered here, the change in the number of π-electrons at a site is associated with oxygen atom substitution for the carbon atom and hence, the modification of transfer integral as well as the on-site Coulomb repulsion. Therefore, delineating the complete picture of the effects of intervening π-electrons on

the spin coupling is complicated. However, this gives a convenient way of predicting, empirically, the singlet-triplet energy gaps in the non-Kekulè systems. Experimental or computed spin densities can be utilised for this purpose as we have discussed. As stated earlier, in the design of an organic ferromagnet, one has to fabricate infinite spin systems; however, studies such as these should prove quite useful for understanding the spin systems at a microscopic level.

## 2.6 SPIN COUPLING IN NONCONJUGATED ORGANIC RADICALS

Considerable amount of theoretical and experimental studies have led to a sound understanding of the nature of spin interactions in $n$-conjugated organic radicals. The various rules developed to predict the ground state in the conjugated systems have been reviewed in Section 2.1. The dependence of spin coupling on the $\pi$-electron network and the empirical procedures to quantify singlet-triplet energy gaps in various non-Kekulé systems are explained earlier in this chapter (Section 2.5). We have shown that open shell RHF calculations using the AM1 /CI method is a suitable semiempirical programme to study these systems.

There have not been many studies directed towards understanding the nature of spin coupling in nonconjugated organic radical systems, where saturated carbon atoms connect the radical sites. These are often more

reactive than their conjugated counterparts and spin coupling in these systems is expected to be very weak making them less amenable to experimental as well as theoretical investigations.

However, there are indications that some of these systems may prove to be very interesting from the point of view of organic ferromagnetism. The spin coupling in these systems is often described as arising from through-space interactions, although there have been instances of through-bond interactions (see examples quoted in Section 1.4.3). The following cases have prompted us to look seriously, at the problem of spin coupling in nonconjugated systems.



1: R = CH₃
2: R = H
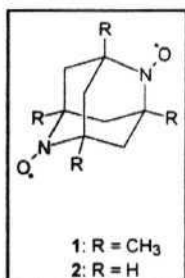
i) In the crystals of Dupeyre-dioxyl 1, the intramolecular spin coupling has been shown to be ferromagnetic, in addition to the intermolecular ferromagnetic spin interactions. This system has been shown to undergo a ferromagnetic transition at 1.48 K[36]. A related system 2 was also reported to have a positive intramolecular exchange interaction, although in the bulk it shows **antiferromagnetic** interactions[37].

ii) Recently there have been a number of reports of ferromagnetic materials obtained by the pyrolysis of hydrocarbons and other organic compounds. Tanaka *et al*[38] reported a ferromagnetic transition in one of the samples prepared by thermal decomposition of adamantane. In another study Murata

*et al*[39] reported a strong stable organic magnet prepared by the pyrolysis of 1,2-diaminopropane, with a saturation magnetisation value of 10.5 emu/g, which is about a third of the value of magnetite, $Fe_3O_4$. There have been several other reports of magnetic materials obtained from pyrolysis of organic compounds, but the origin of cooperative magnetic interactions in these materials is far from clear. Since the molecular species that are pyrolysed are nonconjugated systems, it is impossible to rule out the role of spin interaction between dangling bond ends mediated by σ-bonded carbon networks, in deciding the bulk magnetism of these materials.

iii) There are several recent reports of spin interactions between stable nitronyl nitroxide radicals, some of which are ferromagnetic; in these systems, spin interactions mediated by σ- bonds have been speculated[40].

iv) Ovchinnikov[41] has proposed a few years ago, an interesting model for a carbon-based magnetic material christened as 'ferrocarbon'. He has envisaged a phase of carbon intermediate between graphite and diamond wherein quasi graphite layers of alternately connected $sp^2$ and $sp^3$ hybridized carbon atoms are linked at the $sp^3$ carbons to form a 3-D lattice. He has proposed that such a material would show ferromagnetic alignment of spins at the $sp^2$ radical sites. *Ab initio* quantum chemical calculations carried out by him on model systems (propane- 1,3-diyl and butane-1,4-diyl)[42] with different conformations relevant to the ferrocarbon model indicated that spins would be coupled ferromagnetically.

In view of all these recent developments, and the paucity of any systematic investigation of spin coupling in nonconjugated organic radical systems, we undertook a computational study to analyze the basic spin interactions in these systems. We were also particularly interested in investigating the ferrocarbon model in greater detail.

## 2.6.1 SUITABILITY OF THE AM1/CI METHOD

The successful application of the AM1/CI method for the·study of organic π-conjugated systems has been discussed in the earlier sections. However it was not clear whether this method would be suitable for the computational study of non-conjugated radical systems which we proposed to study here. The prototypical system for the study of spin interaction in nonconjugated systems is propane-1,3-diyl[4b]. This system has been the subject of several earlier theoretical investigations. Hence pilot calculations were carried out on the three main conformations of propane-1,3-diyl labelled by Hoffmann[43] as (0,0), (0,90), (90,90) [Fig. 2.7] using the AM1 /CI procedure and the results were compared with the results of *ab initio* computations. The calculations were full optimizations except for enforcing of the specific conformations and the imposition of $C_{2v}$ symmetry for (0,0) and (90,90) structures and $C_s$ symmetry for the (0,90) conformation. *Ab initio* calculations, the latest one reported by Doubleday

**Figure 2.7:** *The three main conformers of trimethylene (labelling following Hoffmann[43]).*
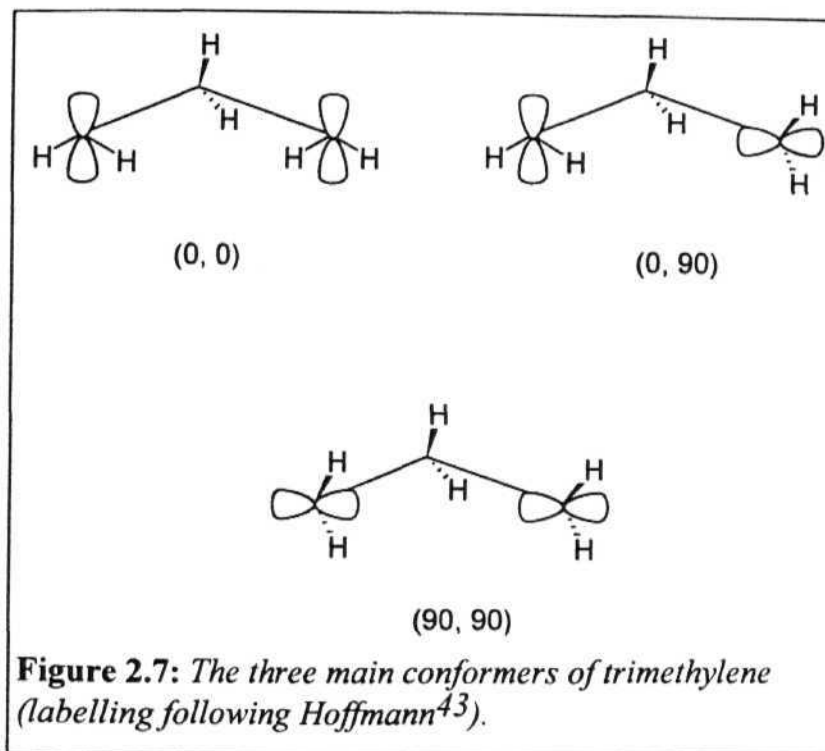
*et al.*[44] using the **4-31** G basis set show that the triplet is favoured over the singlet by 0.61 and 2.04 kcal/mol respectively in the (0,0) and (0,90) conformations. We carried out CASSCF(2,4) (2 electrons in 4 orbitals)/6-31G** calculations (using the Gaussian 94 programme) which show that the (0,0) and (0,90) conformers have a triplet ground state stabilised by 0.62 and 1.88 kcal/mol respectively. In the earlier as well as our present *ab initio* calculations, singlet was found to be stabler in the (90,90) structure. In the AM1 /CI study the (0,0) and (0,90) conformers are found to have a triplet ground state in agreement with the *ab initio* results; however the (90,90)

conformer also showed a triplet ground state, in conflict with the *ab initio* results.    Therefore, a detailed study of the (90,90) conformer was undertaken.

In the (90,90) conformer, optimization of the singlet led to 1-3 bond formation (C-C-C angle = 70.4°) and the AM1/CI singlet-triplet energy gap at this geometry was -73.9 kcal/mol.    Since the diradical character is obtained only at the triplet optimized geometry (C-C-C angle = 111.8°), the singlet-triplet energy gap was evaluated at this geometry which turns out to be 3.3 kcal/mol.  Since the singlet (90,90) conformation shows a tendency to form a bond the singlet and triplet state energies were investigated as a function of the C-C-C angle, using the CASSCF(2,4)/6-31G** and AM1/CI calculations.   The geometries were fully optimized in all cases except for fixing the bond angles and imposing the relevant conformation with $C_{2v}$ symmetry.   The energy surfaces had similar shapes in both calculations as shown Fig. 2.8(a) and Fig. 2.8(b) respectively, with the singlet energies decreasing almost linearly with the C-C-C angle and the triplet energies showing a minimum at about 112° for the AM1 and 115° for the *ab initio* method.   However the point of intersection has important differences in the two cases.   While in the AM1/CI calculation the singlet curve crosses the triplet at 102.5° which is below the minimum of the triplet surface, in the *ab initio* method it crosses at 120°, well above the triplet minimum.   This
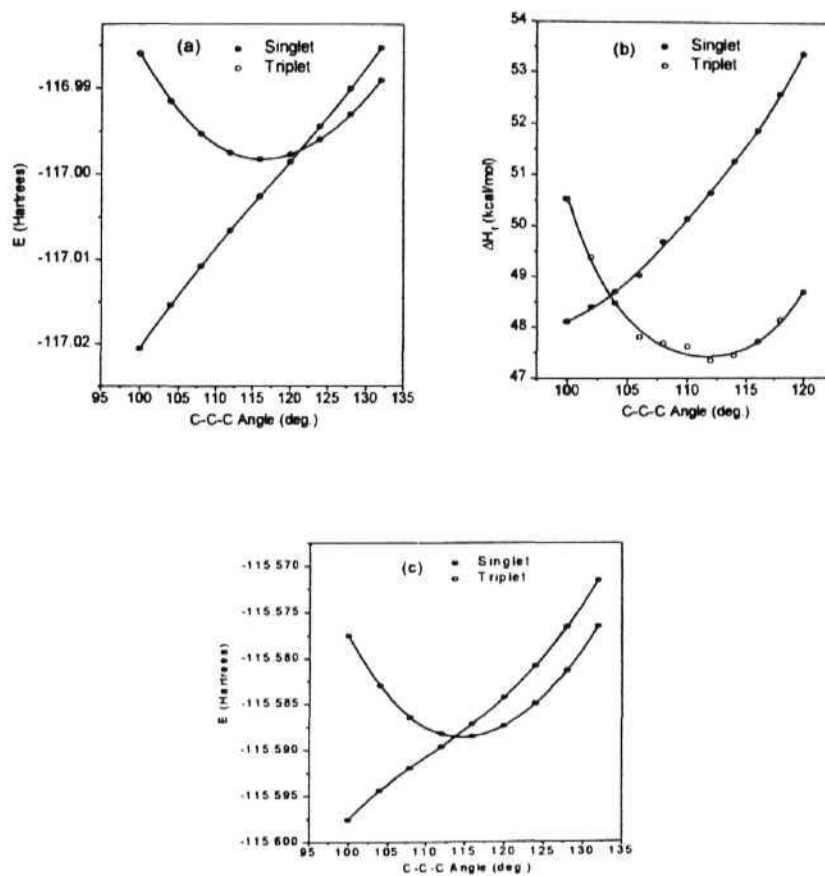
**Figure 2.8:** *Singlet and triplet state energy profiles of trimethylene as a function of the C-C-C angle at (a)* $CASSCF(2,4)/6\text{-}31G^{**}$*; (b) AMJ/CI and (c)* $CASSCF(2,4)/STO\text{-}3G$ *levels of theory.*

means that in the AM1 /CI calculation, the triplet is energetically favoured over the singlet at the minimum of the triplet surface, while in the *ab initio* calculations this is reversed.   Since the 6-31G** basis set provides for greater spatial extension of orbitals, the *ab initio* calculations were repeated using the minimal basis set STO-3G.  Interestingly the trends [Fig. 2.8(c)] were qualitatively very similar to the results of AM1 /CI computations, showing that the triplet is stabler by 0.4 kcal/mol over the singlet at the minimum of the triplet curve.   Thus it is observed that the semiempirical AM1/CI computation provides similar results as a minimal basis *ab initio* calculation.   It should be noted here that the MCSCF calculations by Ovchinnikov[42] showed very large triplet state stabilizations of the order of an eV for propane-1,3-diyl in all the conformations.  We have noticed that similar energy gaps are obtained in HF and CISD calculations, where the singlet optimizations led to unrealistic structures with C-C-C angles of about 130º.

The main focus of our study of spin coupling in nonconjugated radicals (described below) involved spin orbitals oriented towards each other at angles that are constrained by an underlying cyclohexane or related framework.   These have some resemblance to the (0,0) and (0,90) conformers of propane-1,3-diyl but none at all to the (90,90) conformer, which involves orbitals oriented appropriately for bonding interaction. Therefore, we do not consider the failure of the AM1/CI method in the case of the (90,90) conformer a serious setback for the use of this semiempirical procedure for our further studies.   The main question was, whether the

AM1/CI method would be reliable for diradicals which are far from bonding situations. To obtain a relevant appraisal of the efficacy of the AM1/CI method in relation to *ab initio* methods in describing the spin coupling in constrained environments needed for our discussion later in this section, a comparative study of cyclohexane-l,3,5-triyl system was taken up. The AM1/CI calculations were carried out with optimizations of the doublet and quartet states with $C_{2v}$ symmetry. The quartet was found to be energetically lower by 2.2 kcal/mol, and the quartet-doublet energy gap at the quartet geometry was 2.3 kcal/mol. Since the optimization of the cyclohexanetriyl system at the *ab initio* 6-31G** level was found to be computationally expensive, the AM1/CI geometry was used for the CASSCF(3,6)/6-31G** single point calculations. The quartet was stabler over the doublet at this level. On the basis of this result and the earlier computations on the propane-1,3-diyl system, it is clear that the AM1/CI procedure predicts correctly the ground state spin and provides a qualitative and nearly quantitative estimate of spin coupling in the nonconjugated multiradical systems, while it appears to have some limitations in those cases which are close to bonding situations.

## 2.6.2 RESULTS AND DISCUSSION

In conjugated organic multiradical systems, the dominant spin interaction occurs through the delocalised $\pi$-electrons. Our earlier studies have addressed this problem in detail. In the nonconjugated systems on the other hand, the weaker spin couplings are likely to be the cumulative effect

of direct interaction between the spin sites as well as through the mediation of the bonding a-electrons. The basic mechanism of spin coupling through the a-electrons could be visualized using the spin polarization, schematically depicted in Fig. 2.9. **AM1 /CI** UHF calculations (UHF formalism is necessary to reproduce negative spin densities present, if any) on the (0,0) **conformer** gave approximately +0.1 and -0.02 as the spin densities on the $sp^2$ and $sp^3$ carbon atoms respectively, supporting the spin polarization picture. The mutual orientation of the spin bearing orbitals would crucially control the nature of the through-space spin interactions. For analyzing the dependence of spin coupling on the mutual orientation of spin orbitals, the definition of a Pi Orbital Axis Vector **(POAV),** suggested by Haddon[45] was adopted. The POAV used here is the vector which makes



**Figure 2.9:** *Spin polarisation in a nonconjugated diradical*
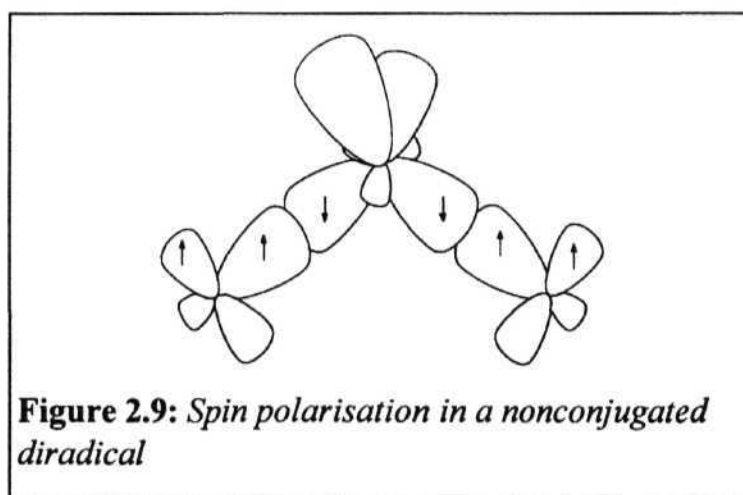
equal angles with the three bond vectors around an $sp^2$ carbon centre bearing the spin. The POAV is readily obtained from the cross product $(\lambda_1 - \lambda_2) \times (\lambda_3 - \lambda_2)$, where $\lambda_1$, $\lambda_2$ and $\lambda_3$ are the unit vectors along the bonds 1, 2 and 3 respectively [Fig. 2.10]. For any pair of radical sites, the direction of the POAVs are chosen such that, the POAVs at site i and j make acute angles with the vectors $i \rightarrow j$ and $j \rightarrow i$ respectively. The angle, $\theta_{ij}$ between these POAVs is computed and utilized as an indicator of the mutual orientation of the spin orbitals. When the two POAVs are parallel the $\theta_{ij}$ is taken as zero.



**Figure 2.10:** *The definition of POAV[45]*
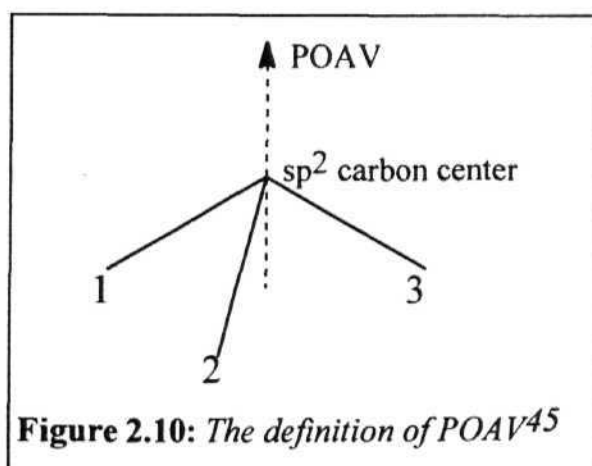
We have carried out all the following calculations using the AM1 programme. In general the geometries of all the radicals were fully optimized for each spin state under consideration. Energies were computed invoking CI = 5, since CI = 6 gave practically identical results in several test
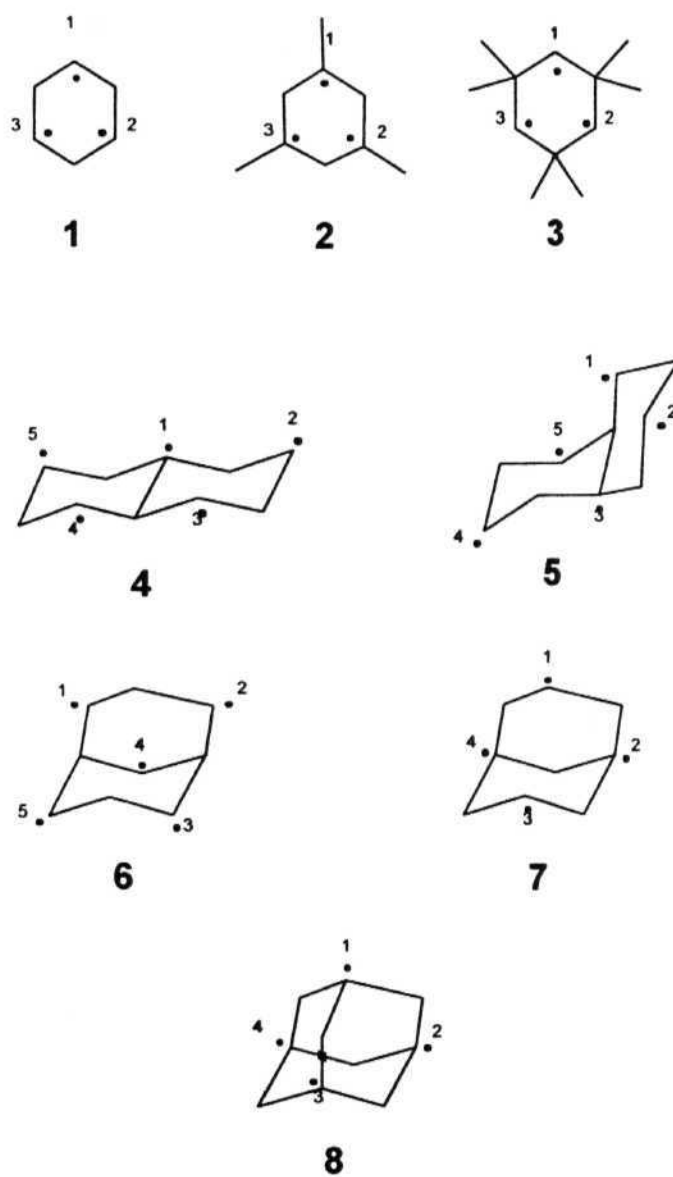
**Figure 2.11:** *The nonconjugated* **multiradicals** *considered in the study; hydrogens are omitted for calrity.*

cases. The ground state spin was determined based on the results of these calculations. The energy gaps that are presented here are the differences in the energies of the various spin states of the radicals calculated with the geometry of the ground spin state determined above.

The set of radical systems represented in Fig. 2.11 consisting of cyclohexane-1,3,5-triyl radicals and related systems in the decalin, [3.3.1]bicyclononane and adamantane framework were considered first. All the systems considered in this set have pairs of radical sites separated by a saturated carbon atom with the spin orbitals sampling a variety of mutual orientations. The cyclohexane framework in particular, also provides radical pairs analogous to the prototypical 1,3-diyl system but now in a more constrained environment, which is more relevant to a discussion of cases like that of 'ferrocarbon'.

Table 2.8 lists the energy gaps for the relevant spin states of the radicals in Fig.2.11. It also provides the various angles, $\theta_{ij}$ between the POAVs at radical sites i and j in these systems. From the table it is clear that except for 7 and 8, the spin coupling is predominantly ferromagnetic. The dominant ferromagnetic coupling in these radical systems, which have radical sites separated by one saturated carbon atom, can be explained by invoking the spin polarization of the $\sigma$- network explained earlier.
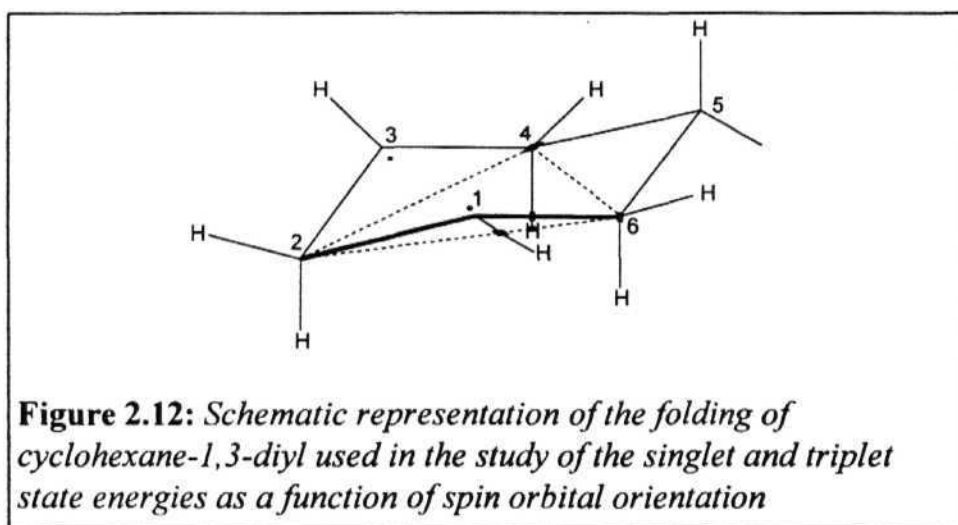
**Table 2.8:** *Relative energies of different spin states and mutual orientations of spin orbitals of nonconjugated multiradicals in Fig. 2.11.*

| Structure Number in Fig.2.11 | Spin State | Relative Energy (kcal/mol) | Angle, $\theta_{ij}$ (degrees) [i-j] | |
|---|---|---|---|---|
| 1 | quartet | 0.0 | 37.9 [1-2]; | 37.8 [1-3] |
|   | doublet | 2.3 | 37.8 [2-3] | |
| 2 | quartet | 0.0 | 35.2 [1-2]; | 35.6 [1-3] |
|   | doublet | 2.9 | 34.5 [2-3] | |
| 3 | quartet | 0.0 | 27.2 [1-2]; | 27.5 [1-3] |
|   | doublet | 2.4 | 31.4 [2-3] | |
| 4 | sextet | 0.0 | 11.3 [1-2]; | 33.5 [1-5]; |
|   | quartet | 1.3 | 13.7 [1-3]; | 41.5 [1-4] |
|   | doublet | 3.0 | 17.5 [2-3]; | 55.2 [3-4] |
|   |   |   | 27.1 [4-5] | |
| 5 | sextet | 0.0 | 27.6 [1-2]; | 9.7 [1-3] |
|   | quartet | 1.9 | 40.1 [1-5]; | 33.6 [2-3] |
|   | doublet | 3.5 | 46.9 [3-4]; | 48.6 [3-5] |
|   |   |   | 20.8 [4-5] | |
| 6 | sextet | 0.0 | 24.0 [1-2]; | 58.6 [1-4] |
|   | quartet | 3.0 | 65.4 [1-5]; | 69.3 [2-3] |
|   | doublet | 4.2 | 55.6 [2-4]; | 55.1 [3-4] |
|   |   |   | 24.0 [3-5]; | 56.0 [4-5] |
| 7 | quintet | 0.0 | 60.6 [1-2]; | 61.3 [1-4] |
|   | triplet | -2.1 | 60.9 [2-3]; | 75.9 [2-4] |
|   | singlet | -2.1 | 60.3 [3-4] | |
| 8 | quintet | 0.0 | 108.9 [1-2]; | 109.9 [1-3] |
|   | triplet | -2.6 | 108.8 [1-4]; | 109.6 [2-3] |
|   | singlet | -14.2 | 108.9 [2-4]; | **110.6** [5-4] |

The exceptional behaviour of 7 and 8 is interesting. The obvious difference between these systems and the rest is that only these have more than one radical site occurring on the bridge atoms. The mutual orientation of the spin orbitals at the bridge sites is quite different from the mutual orientation of other orbitals. The $\theta_{ij}$ values listed in the table can be used to discuss this more quantitatively. In the ferromagnetically coupled spin systems this angle is usually about 30 - 40° with a few cases of lower (10 - 20°) and higher (55 - 65°) angles. However in 7 these angles are found to be about 61° with the 2 - 4 angle (between bridge atoms) being approximately 76°. In 8 all the angles are closer to 109°. Due to programme limitations the high spin heptet state of the hexaradical that can be obtained by placing the radical sites at the nonbridge atoms of the adamantane framework, could not be optimized. However, the $CI = 6$ calculations on the optimized singlet state of this multiradical indicated that the heptet was indeed the ground state. This clearly shows that whenever the radical sites are present on the bridging atoms, there is an increase in the $\theta_{ij}$, leading to an antiferromagnetic coupling of the spins. A careful analysis of the optimized geometries indicates that, in the cyclohexane framework, 0 ij values close to or higher than 70° are associated with a decrease in the distance between the radical sites which possibly leads to some weak overlap of spin orbitals and a bonding interaction resulting in the antiferromagnetic coupling.

The correlation between the nature of spin coupling and the mutual orientation of orbitals was anlyzed more systematically choosing the

cyclohexane-1,3-diyl as the model system [Fig. 2.12]. The variation of the singlet-triplet state energies was investigated as a function of the folding of the plane defined by carbon atoms 2,1,6 and 2,3,4. Geometries were optimized with $C_s$ symmetry constraint, the plane of symmetry passing through carbon atoms 2 and 5 and the four hydrogen atoms attached to them. The angle between the planes defined by carbons 2, 1 and 6 (or 2, 3 and 4 by symmetry) and the plane defined by 2, 4 and 6 was varied from 180° to approximately 120°. When this angle was decreased further, the carbons 1 and 3 get almost bonded and hence such points were not considered. At each fixed value of the angle, the singlet and triplet state geometries were optimized. Fig. 2.13 provides a plot of the



**Figure 2.12:** *Schematic representation of the folding of cyclohexane-1,3-diyl used in the study of the singlet and triplet state energies as a function of spin orbital orientation*
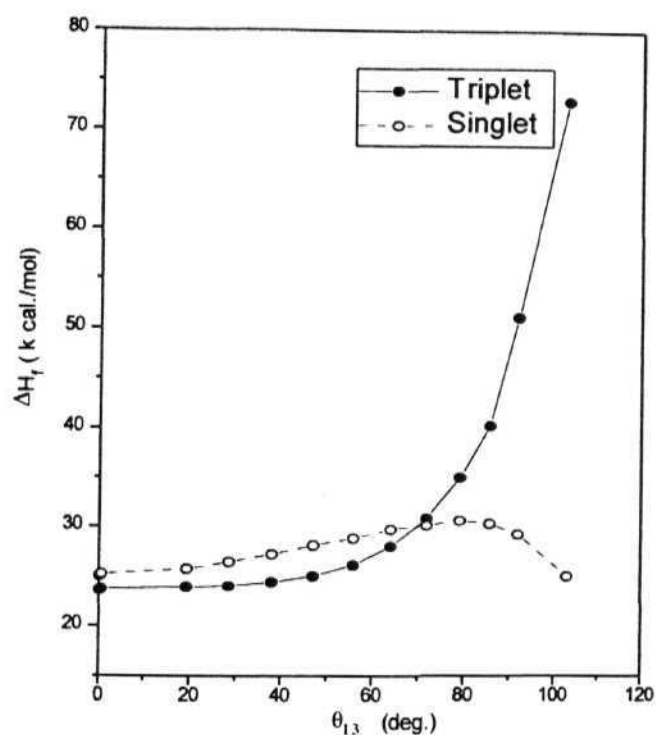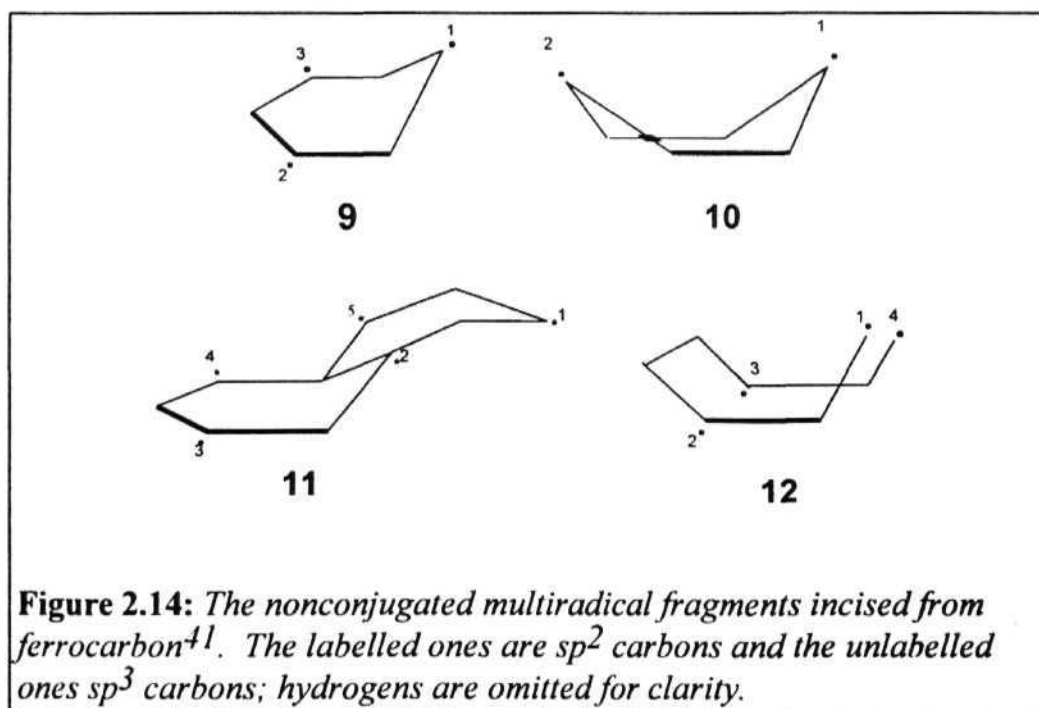
**Figure 2.13** : *Plot of heats of formations of singlet and triplet states of cyclohexane-1,3-diyl as a function of the mutual orientation ($\theta_{13}$)of the spin orbitals (see text for details and the definition of $\theta_{13}$);the lines are only a guide to the eye.*

heats of formation of the singlet and triplet states as a function of $\theta_{13}$. It is clearly seen that the triplet state is preferred when the mutual orientation angle of the POAVs is below 70° and the singlet-triplet energy gap becomes largest when this angle is about 47°. Above 70° the singlet state is lower in energy, eventually leading to bond formation. This result provides a strong support for the conclusions drawn based on the observations made in Table 2.8. Thus this model provides a logical background to visulaize spin interactions in nonconjugated **multiradicals** based on the cyclohexane framework.



**Figure 2.14:** *The nonconjugated multiradical fragments incised from ferrocarbon[41]. The labelled ones are sp[2] carbons and the unlabelled ones sp[3] carbons; hydrogens are omitted for clarity.*

Next the four important fragments from the ferrocarbon model of Ovchinnikov [Fig. 2.14] were taken up for a detailed study. These fragments were incised from the molecular mechanics optimized geometry of the ferrocarbon framework reported by Ovchinnikov. Each fragment along with all the atoms connected directly to it was incised from the lattice; the atoms connected to the fragment were then replaced by H atoms and the C-H distances alone were optimized in the AM1 calculation. Thus these

**Table 2.9:** *Relative energies of different spin states and mutual orientations of spin orbitals of ferrocarbon fragments[4 1] in Fig. 2.14.*

| Structure Number in Fig.2.14 | Spin State | Relative Energy (kcal/mol) | Angle $\theta_{ij}$ (degrees) [i-j] |
|---|---|---|---|
| 9 | quartet | 0.0 | 57.5 [1-2];   57.6 [1-3] |
|   | doublet | 1.7 | 0.2 [2-3] |
| 10 | triplet | 0.0 | 122.6 [1-2] |
|    | singlet | -3.4 | |
| 11 | sextet | 0.0 | 0.1 [1-2];  57.3 [1-5] |
|    | quartet | 1.2 | 57.4 [2-3];  57.3 [2-4] |
|    | doublet | 2.9 | 57.2 [2-5];   0.1 [3-4] |
| 12 | quintet | 0.0 | 57.4 [1-2];   122.6 [1-4] |
|    | triplet | -1.1 | 122.5 [2-3];   57.5 [3-4] |
|    | singlet | -7.8 | |

multiradical systems preserve the relevant bond lengths and all the bond angles and dihedrals from the ferrocarbon lattice. 9 and 10 are model

multiradical systems preserve the relevant bond lengths and all the bond angles and dihedrals from the ferrocarbon lattice. 9 and 10 are model systems for the basic sofa and boat units in the proposed ferrocarbon phase. **11** models a larger fragment made up of two sofa units within the quasi graphite layer. 12 is the model fragment that represents a unit cell connecting the two quasi graphite layers in the ferrocarbon phase. Table 2.9 provides the energies of the various spin states of each fragment as well as the relevant $\theta_{ij}$ angles. From the results it is clearly seen that fragments 9 and 11 show a preference for a ferromagnetic alignment of spins and the mutual orientations of the spin orbitals are either nearly parallel or about 55°. 10 and 12 show **antiferromagnetic** alignment of spins. In 10 the radical sites are separated by two saturated carbon atoms and the $\theta_{ij}$ is about 123°, and both the spin polarization picture (extension of the spin polarization picture in Fig. 2.9 to a **1,4-diradical** would indicate antiferromagnetic coupling of spins; for example, **butane- 1,4-diyl** is known to have a singlet ground state in most of its conformations)[46] and the mutual orientation of spin orbitals support this finding. The case of 12 is interesting. The mutual orientation between orbitals at sites, 1 and 2 (as well as 3 and 4) which are separated by one saturated carbon atom is approximately 58°. This is expected to lead to ferromagnetic coupling of spins within each of these pairs of radical sites. However, these pairs are in turn separated by two saturated carbons and the $\theta$ between 1 and 4 (as well as 2 and 3) is approximately 123°. This leads to overall antiferromagnetic spin interaction and a singlet ground state. This is reminiscent of the application of Rule 3 for extended spin coupling in 7r-conjugated

multiradicals discussed in Section 2.5 above.  Thus the findings of the calculated spin states of these ferrocarbon fragments are quite consistent with the analysis of cyclohexane-1,3-diyl folding problem discussed above. Significantly, in the proposed ferrocarbon model, even though within the quasi graphite layer one may realize ferromagnetic interaction of spins, these calculations predict an antiferromagnetic interaction between the layers.  Thus the realization of a bulk magnetic ferrocarbon is doubtful on the basis of these results.

Our studies above have shown that the cyclohexane skeleton is an interesting framework to install radical sites and study spin coupling to understand the problem of spin interactions in nonconjugated systems. Even from the experimental point of view, this could prove to be very informative.  If a suitable synthetic strategy could be devised to generate 1 [Fig.2.11] or its derivatives from an approximately trisubstituted cyclohexane, the ground state spin could be determined.  Kemp's triacid (l,3,5-trimethylcyclohexane-l,3,5-tricarboxylic acid) or its derivatives could prove to be interesting starting points for such studies.  The triradical 3 should be particularly interesting since the permethylation should prevent any possible 1 - 2 hydrogen atom migrations which could occur in the case of 1 and 2.

In view of its relevance for experimental studies, we have calculated the potential energy surfaces to model the recombination of the two spin sites (1 and 3) in 1, to form [3.1.0] bicyclohexane-3-yl radical.  The
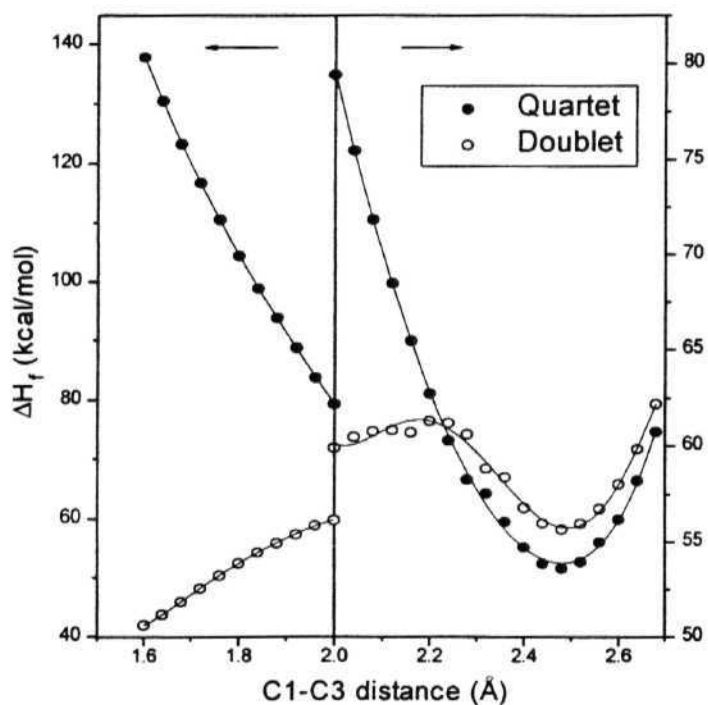
**Figure 2.15** : *Plot of heats of formations of doublet and quartet states of cyclohexane-J ,3,5-triyl as a function of the C1-C3 distance (see text for details); the lines are only a guide to the eye.*

geometries were **fully** optimized at different fixed distances between C atoms 1 and 3 in both the doublet and quartet states. The energy profile is

shown in Fig. 2.15. The doublet is clearly the low energy state at bonding distances *ie,* below C-C distances of 1.6Å. The quartet surface goes through a minimum at the C - C distance of 2.5Å. The energy scales in Fig.2.15 are therefore shown differently for C - C distances below and above 2A, to highlight the quartet minimum. Interestingly, the doublet also shows a minimum at this geometry *albeit* at a higher energy of 2.3 kcal/mol. There is a barrier of about of 6 kcal/mol to go from this minimum to the bonded state along the doublet pathway. For the quartet diradical there is a higher barrier of *ca* 8 kcal/mol to go over to the doublet bicyclic system. Hence if the triradical can be generated at low temperatures, it will be protected by a moderately high barrier from immediate intramolecular recombinations. We believe that low temperature experiments to generate and study the spin state of such nonconjugated radicals would open up new possibilities in the realm of organic magnetic materials.

## 2.7 CONCLUSION

In this chapter we have addressed several problems related to the spin interactions in organic radicals, both conjugated and nonconjugated. The investigations have been primarily based on the AM1 semiempirical procedure. Since we were interested in open shell systems, electron correlation effects arising from interactions of low lying excited states is very important and this has been taken into account through the involvement of configuration interaction in all the calculations. The semiempirical

procedure adopted also allowed us to study several classes of reasonably large radicals systems.   Initial studies related to the calculation of spin densities and fine structure constants derived from them gave a good level of confidence in the methodology.   It was shown that spin densities calculated from open shell RHF calculations have good predictive capability of the ZFS parameters of organic π-conjugated diradicals.   The importance of the CI schemes being used was highlighted by our detailed investigation of the spin state problem in tetramethyleneethane diradical.   Our studies of the correlation between the spin coupling parameter (defined in terms of atomic spin densities and π-electron pathways) and the spin state energy gaps provides an insight into the spin polarisation mechanism in conjugated radicals.   It also led to an empirical approach to the prediction of spin state energy gaps.   We have finally undertaken a detailed analysis of the novel problem of spin interactions in nonconjugated organic radicals.   We believe that this would be an important problem in the field of organic magnetic materials, in the coming days.   Thus the computational studies presented in this chapter are expected to contribute to the ongoing search for organic ferromagnetic materials.

# REFERENCES

1. (a) T. P. Radhakrishnan, *Curr. Sci.*, 62, 669 (1992). (b) T. P. Radhakrishnan in *Strongly Correlated Electronic Systems in Chemistry,* S. Ramasesha and D. D. Sarma (eds.), Narosa Publishers, New Delhi, p.161. (c) H. Iwamura and N. Koga, *Acc. Chem. Res.,* 26, 346 (1993). (d) J. Veciana, C. Rovira, E. Hernàndez and N. Ventosa, *Ann de Quimica*, 73 (1993).

2. A. A. Ovchinnikov, *Theor. Chim. Acta,* **47,** 297 (1978).

3. N. Mataga, *Theor. Chim. Acta,* 10, 372 (1968).

4. (a) A. Rajca, *Chem. Rev.,* 94, 871 (1994). (b) *Diradicals,* W. T. Borden (ed.) Wiley-InterScience, New York, 1982.

5. (a) C. A. Coulson and G. S. Rushbrooke, *Proc. Cambridge Phil. Soc,* **36,** 193 (1940). (b) C. A. Coulson and H. C. Longuet-Higgins, *Proc. Roy. Soc. A,* **191,** 39 (1947). (c) H. C. Longuet-Higgins, J. *Chem. Phys.,* 18,265(1950).

6. (a) N. Tyutyulkov and O. E. Polansky, *Chem. Phys. Lett.,* **139,** 281 (1978). (b) S. Karabunarleiv and N. Tyutyulkov, *Theor. Chim. Acta,* **76,** 65 (1989). (c) N. Tyutyulkov, S. Karabunarleiv and C. Ivanov, *Mol. Cryst. Liq. Cryst.,* **176,** 139(1989).

7. (a) W. T. Borden and E. R. Davidson, *J. Am. Chem. Soc,* **99,** 4587 (1977). (b) J. Pranata, *J. Am. Chem. Soc,* **114,** 10537 (1992).

8. T. P. Radhakrishnan, *Chem. Phys. Lett.,* **181,** 455 (1991).

*9.* J. A. Berson in *The Chemistry of Quinonoid Compounds,* S. Patai and Z. Rappaport (eds.) John Wiley, New York, 1988, Vol. II, Chapter 10, p. 487.

10. I. N. Levine, *Quantum Chemistry,* Third edition, Allyn and Bacon, Boston, 1983, p. 493.

11. J. A. Pople, D. P. Santry and G. A. Segal, *J. Chem. Phys.,* 43, 129 (1965).

12. J. A. Pople, D. L. Beveridge and P. A. Dobosh, *J. Chem. Phys.,* **47,** 2026(1967).

13. (a) D. B. Cook, P. C. Hollis and R. McWeeny, *Mol. Phys.,* 13, 553 (1967). (b) D. B. Cook and P. Palmieri, *Mol. Phys.,* **17,** 271 (1969). (c) A. Golebiewski, J. Mrozek and P. Nalewajski, *Theor. Chim. Acta,*28, 169(1973).

14. M. J. S. Dewar, E. G. Zoebisch, E. F. Healy and J. J. P. Stewart, *J. Am. Chem. Soc,* **107,** 3902 (1985).

15. (a) B. L. V. Prasad and T. P. Radhakrishnan, *J. Phys. Chem.,* 96, 9232 (1992). (b) A. E. Dorigo, D. W. Pratt and K. N. Houk, *J. Am. Chem. Soc,* **109,** 6591 (1987). (b) J. F. Gaw and H. F. Schaefer III, *J. Chem. Phys.,* 83, 1741(1985).

16. J. Sadlej, *Semiempirical Methods in Quantum Chemistry,* Ellis Horwood, Chichister, 1985.

17. A. Carrington and A. D. McLachlan, *Introduction to Magnetic Resonance,* Harper and Row, New York, 1967, p. 81.

18. J. E. Wertz and J. R. Bolton, *Electron Spin Resonance,* McGraw-Hill, New York, 1986, p. 223.

19. (a) D. Feller, W. T. Borden and E. R. Davidson, J. *Chem. Phys.,* **74,** 2256 (1981). (b) S. R. Langhoff, E. R. Davidson and C. W. Kern, *J. Chem. Phys.,* 62, 4672 (1975). (c). E. R. Davidson, J. C. Ellenbogen and S. R. Langhoff, J. *Chem. Phys.,* 73, 865 (1980).

20. (a) A. Gold, *J. Am. Chem. Soc,* **91,** 4961 (1969). (b) M. Godfrey, C. W. Kern and M. Karplus, *J. Chem. Phys.,* **44, 4459** (1968). (c) M. Rule, A. R. Matlin, D. E. Seeger, E. F. Hilinski, D. A. Dougherty and J. A. Berson, *Tetrahedron,* 38, 787 (1982). (d) A good collection of data on D and E values of quinonoid compounds can be found in Ref. 9 also.

21. (a) P. M. Lahti, A. S. Ichimura and J. A. Berson, J. *Org. Chem.;* **54,**958 (1989). (b) P. M. Lahti and A. S. Ichimura, J. *Org. Chem.,* 56, 3030 (1991).

22. W. R. Roth and G. Erker, *Angew. Chem. Int. Edn. Engl.,* 12, 503 (1973).

23. P. Dowd, W. Chang and Y. H. Paik, *J. Am. Chem. Soc,* **109,** 5284 (1987).

24. P. Dowd, W. Chang and Y. H. Paik, *J. Am. Chem. Soc,* **108,** 7416 (1986).

25. P. M. Lahti, A. R. Rossi and J. A. Berson, *J. Am. Chem. Soc,* **107,** 2273 (1985).

26. J. Koutecký, D. Dohnert, P. S. Wormer, J. Paldus and J. Cizek, *J. Chem. Phys.,SO,* 2244 ( 1984).

27. A. Chakrabarthi, I. D. L. Albert, S. Ramasesha, S. Lalitha and J. Chandrasekhar, *Proc. Ind. Acad. Sci.,* **105,** 53 (1993).

28. P. Du and W. T. Borden, *J. Am. Chem. Soc,* **109.** 930 (1987).

29. P. Nachtigall and K. D. Jordan, J. *Am. Chem. Soc,* **114,** 4743 (1992).

30. P. Nachtigall and K. D. Jordan, *J. Am. Chem. Soc,* **115,** 270 (1993).

31. H. Fukutome, A. Takahashi and M. Ozaki, *Chem. Phys. Lett.*, **133,** 34 (1987).

32. (a) T. P. Radhakrishnan, *Tetrahedron Lett.,* **32,** 4601 (1991); (b) T. P. Radhakrishnan, *Chem. Phys. Lett.,* **207,** 15 (1993).

33. Z. Fang, Z. L. Liu, K. L. Yao and Z. G. Li, *Phys. Rev. B,* **51,** 1304 (1995).

34. PCMODEL Version 1.0, Serena Software. Bloomington, IN47402.

35. P. W. Anderson in *Solid State Physics*, F. W. Seitz and D. Turnball (eds.) Academic Press, New York, 1963, Vol. **14,** p. 99.

36. (a) R. Chiarelli, A. Rassat, Y. Dromzee, Y. Jeannin, M. A. Novak and J. L. Tholence, *Phys. Scr.,* **T49,** 706 (1993). (b) R. Chiarelli, M. A. Novak, A. Rassat and J. L. Tholence, *Nature,* **363,** 147 (1993). (c) R. Chiarelli, A. Rassat and P. Rey, *J. Chem. Soc. Chem. Commn.,* 1081 (1992).

37. A. Rassat, R. M. Dupeyre and J. Ronzaud, *J. Am. Chem. Soc,* **96,** 6559 (1974).

38. (a) K. Tanaka, K. Yoshizawa, A. Takata, T. Yamabe and and J. Yamauchi, *Synth. Met.,* **39,** 103 (1990). (b) K. Tanaka, K. Yoshizawa, A. Takata, T. Yamabeand and J. Yamauchi, *J. Chem. Phys.,* **94,** 6868 (1991).

39. K. Murata, H. Ushijima, H. Ueda and K. Kawaguchi, *J. Chem. Soc Chem. Commn.,* 567 (1992).

40. Y. J. Uemura, L. P. Le and G. M. Luke, *Synth. Metals,* **56,** 2845 (1993).

41. (a) A. A. Ovchinnikov and V. N. Spector, *Synth. Metals,* **27,** B615, (1988). (b) A. A. Ovchinnikov and I. L. Shamovsky, *J. Mol. Str. (THEOCHEM),* **251,** 133 (1991).

42. A. Ovchinnikov, I. L. Shamovsky and K. V. Bozhenko, *J. Mol. Str. (THEOCHEM),* **251,** 141 (1991).

43. (a)W. T. Borden, in Ref. 4(b). (b) R. Hofmann, *J. Am. Chem. Soc,* 90, 1475(1968).

44. C. Doubleday, J. W. McIver and M. Page, *J. Am. Chem. Soc,* **104,** 6533 (1982).

45. R. C. Haddon and L. T. Scott, *Pure and Appl. Chem.,* 58, 137 (1986).

46. C. Doubleday, J. McIver and M. Page, *J. Am. Chem. Soc,* **107,** 7904 (1985).

# CHAPTER 3

---

# EXPERIMENTAL INVESTIGATION OF TWO APPROACHES TO MOLECULAR FERROMAGNETISM BASED ON THE SPIN POLARISATION

---

## 3.1 INTRODUCTION

Charge transfer complexes of organic and organometallic compounds and transition metal coordination compounds have played an important role in the growth of molecule-based magnetic materials. Some of the advantages they possess over other systems such as polymer radicals are the following. (i) Solid state structural information is more commonly available in the case of CT complexes, since chances of obtaining single crystals are higher compared to systems such as polymers, though imporant exceptions do exist. (ii) The spins are normally present in delocalised $n$-electron systems and hence in a chemically more stable state. There have been several examples of interesting magnetic properties observed in the case of organometallic complexes, on which complete structural analysis is available. In fact the first molecule-based ferromagnet Fe(Cp*)2-TCNE and other systems in that series have been subjected to detailed structural characterization[1]. A great variety of mechanisms for the fabrication of organic ferromagnets have been proposed based on charge transfer complexes [Section 1.4]. This chapter describes the experimental investigations on two new approaches for achieving ferromagnetic interactions in organic charge transfer complexes and metal coordination polymeric systems. These models make use of the concept of spin polarisation discussed to some extent in connection with organic di and multiradicals in the previous chapter. We present below, a brief review of the phenomenon of spin polarisation. Section 3.2 describes our new proposal for obtaining ferromagnetic interactions in organic charge transfer

complexes. This Section also gives the details of the preparation, characterisation and esr investigations on the magnetic properties of the three new charge transfer complexes, prepared by us in an attempt to investigate this model. In Section 3.3 we propose a simple extension of the topological models described earlier for organic polymeric magnetic systems [Section 1.4], to metal coordination polymers to achieve ferromagnetic interaction between metal ion spins.. The preparation, characterisation and magnetic properties of three new copper(II) complexes motivated by this model, are presented subsequently. In the concluding section we furnish an overview of these results and possible courses for further research.
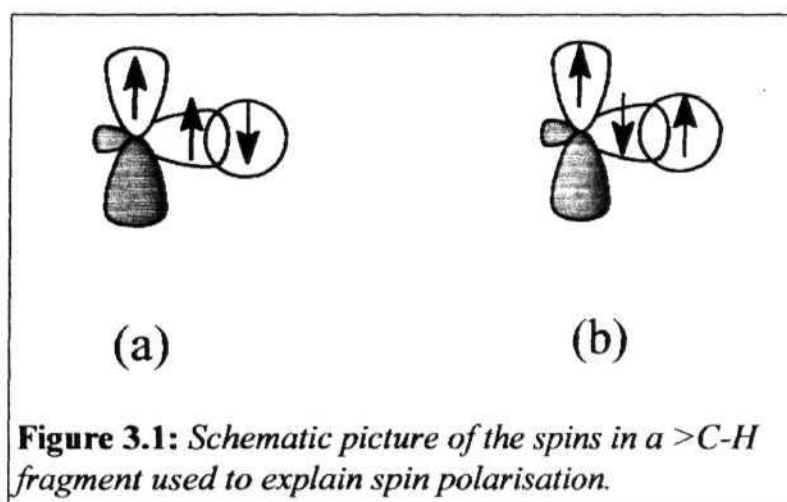
## 3.1.1 SPIN POLARISATION

A simplistic description of spin polarisation would be that it corresponds to a situation in which an unpaired electron, through its exchange interaction with the paired electrons in an adjacent $\sigma$ or $n$ bond, increases the probability of obtaining a spin electron at one atom and $\beta$ spin electron at the other atom participating in that bond. Spin polarisation can usually be visualised using the fundamental notions[2] that (i) two unpaired electrons residing in two noninteracting orthogonal orbitals will tend to have parallel spins (Hund's rule) and (ii) the electrons that form a chemical bond will have antiparallel spins. Usually a valence bond picture can be utilised to explain spin polarisation. Alternatively, a molecular orbital calculation involving configuration interaction of the ground state with

excited states, can be used to explain the experimental observation of spin polarisation.
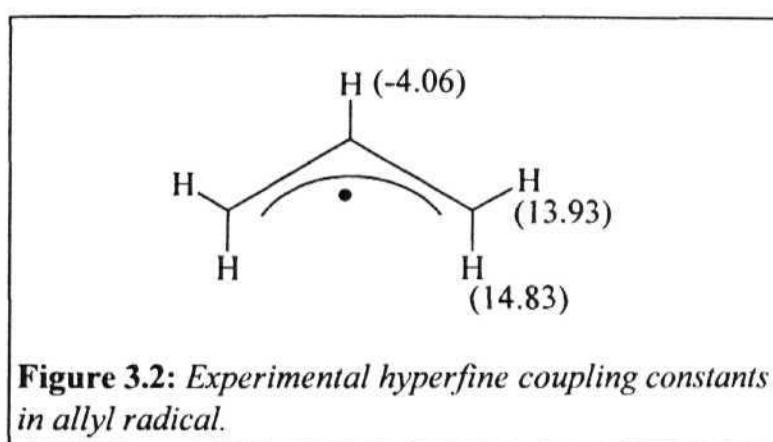
Spin polarisation is normally an intramolecular effect that is extensively used to explain the hyperfine structure observed in esr spectra. A well known case is that of the unpaired electrons in the proximity of ring hydrogens in aromatic nuclei. For example, the benzene radical anion is known to give a seven-line pattern esr spectrum[3], with a splitting constant of 3.75 G. The unpaired electron in this case occupies a delocalized $n$ - orbital which has a node in the plane of the molecule, which contains the hydrogen atoms. Thus the hyperfine structure arising from the proton nuclear spins appears to be an "anomaly"; explained by invoking the phenomenon of spin polarisation.

Consider an isolated >C-H fragment with one $\pi$-electron in it, occupying the $2p_z$ carbon orbital, perpendicular to the plane of the three trigonal bonds. Two different situations are possible with respect to the spins of these electrons, as shown in Fig. 3.1 The electron correlation between the $\sigma$ and $n$ systems leads to the spin configuration (a) being slightly preferred over (b). Hence, if the unpaired electron has spin a, there is slight excess spin a in the carbon $sp^2$ orbital. Thus an a spin in the.carbon $2p_z$, orbital induces $\beta$ spin at the adjacent proton and leads to the observation of the proton hyperfine interaction

**Figure 3.1:** *Schematic picture of the spins in a >C-H fragment used to explain spin polarisation.*

The spin polarisation picture has successfully explained the observed hyperfine coupling constant of odd alternant radicals also; for example allyl radical [Fig 3.2]. The simple molecular orbital model predicts that the unpaired electron occupies the non-bonding MO which has a node at the central carbon atom. Hence, the $n$- electron spin density should be 0.5 on the end atoms and zero in the middle, which contradicts the experimental finding of the 4.06 gauss proton splitting from the central hydrogen atom[4]. This can also be explained by electron correlation effects. Since the unpaired electron in the NBMO is confined to the terminal carbon atoms, electron repulsion is minimized if the electrons of the same spin in the lower bonding MO spends more time on the terminal carbon atoms. Therefore if the unpaired electron has spin a, there will be increased a spin density on the terminal carbon atoms and a finite $\beta$ spin density on the central carbon atom. This polarisation is sometimes termed as **"static** spin

polarisation"[5]. Another problem where spin polarisation picture has been invoked is to explain the ground state of cyclobutadiene[6]. All the available



H (-4.06)

H
(13.93)

H
(14.83)

**Figure 3.2:** *Experimental hyperfine coupling constants in allyl radical.*

experimental evidence indicates that cyclobutadiene has a singlet ground state even at a square $(D_{4h})$ geometry. This is an apparent violation of the application of simple HMO picture and Hund's rule. A spin polarisation picture has been invoked involving admixture of $\pi^*$ antibonding MOs to explain the ground state spin[7] of cyclobutadiene. Since there is no net spin at any carbon as a result of this spin polarisation, in contrast to the allyl radical case, this was termed as "dynamic spin polarisation".

Topological models for organic ferromagnetism in polyradicals utilise the spin polarisation picture extensively, to predict the spin alignment[8]. We have discussed the application of the spin polarisation picture to conjugated and nonconjugated organic radical systems in Chapter

*2.* We describe below, two new models utilising the basic idea of spin polarisation, which are potential approaches to achieve ferromagnetic spin coupling in molecular materials.


## 3.2 A NEW MODEL BASED ON ORGANIC CHARGE TRANSFER COMPLEXES

McConnell's suggestion of a mechanism[9] for ferromagnetic coupling of spins, in a quasi one-dimensional stack of molecular ion radicals, using charge transfer(CT) and configuration interaction(CI) mixing, has generated tremendous amount of experimental work on CT complexes. Several modifications to the basic model proposed by him were made and tested experimentally[10]. A brief overview of the basic idea and the variations on this theme are mentioned in Section 1.4.2. Several good reviews have covered different aspects of this topic[11].
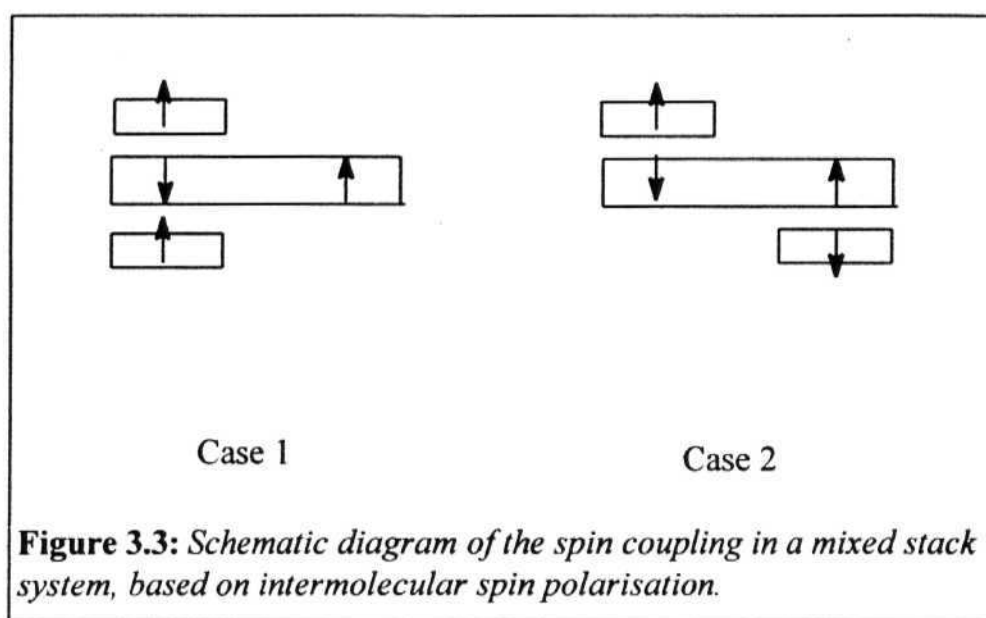
From a synthetic point of view organic CT complexes offer more scope for exploration and realisation of an organic ferromagnet, than the polymer based strategies. Metallocene based charge transfer complexes are good examples of molecular magnetic materials, fully characterized structurally. In these systems, it has been argued that the ferromagnetism arises not due to configuration mixing as was originally concieved, but due to close interactions of atoms with appropriate spin densities[12]. Room temperature ferromagnetism[13] in $V(TCNE)_x.yCH_2Cl_2$ and the soft

ferromagnetism[14] in the TDAE salt of $C_{60}$ are believed to arise from CT interactions and configuration mixing. Recent reports[15] of weak ferromagnetism observed in a lithium-tetrafluorotetracyanoquinodimethanide salt ($T_c < 12$ K) and the ferromagnetic[16] behaviour at room temperature exhibited by a 1:2 complex of TCNQ and its anion radical indicate the continuing relevance of CT complexes to this problem. We have considered a new approach relevant to stacked CT complexes utilising the basic idea of spin polarisation.

Consider a mixed stack of molecular ion radicals and diamagnetic counterion spacers where back charge transfer is energetically costly. The diamagnetic spacer ions should preferably have an extended $\pi$-electron system. If the spins on the radicals can induce spin polarisation in the diamagnetic spacer, depending on the stacking arrangement of the radicals with respect to the diamagnetic spacer, different situations can arise as described below [Fig. 3.3].

<u>Case 1</u>: The spin orbitals of the neighbouring ion radicals have strong overlap with the same region of the diamagnetic spacer so that, they interact with the same set of spin densities on the spacer leading to a ferromagnetic alignment of the ion radical spins.

<u>Case 2</u>: The spin orbitals of the neighbouring ion radicals overlap with different regions of the spacer and if these correspond to opposite spin densities, it results in an overall anti ferromagnetic spin alignment of the ion radical spins.

**Figure 3.3:** *Schematic diagram of the spin coupling in a mixed stack system, based on intermolecular spin polarisation.*

In order to test the concept of spin polarisation induced in an intermolecular fashion and the resulting magnetic interactions we have carried out some model calculations. All the calculations were done with the semiempirical AM1/CI method available in the MOPAC 93 package. We note that, test calculations run using the PM3 parametrisation (we checked this particularly when atoms like Cl are involved) gave nearly identical results. Spin density calculations were carried out using the UHF formulation since presence of negative spin densities have to be explored. Calculation for the singlet-triplet gaps were carried out using a CI scheme wherein all excitations within 5 MOs bracketing the HOMO-LUMO were

included. As discussed in Chapter 2 this procedure gives reliable estimates of the magnetic energy gaps in organic radical systems.

## 3.2.1 MODEL CALCULATIONS

We considered anthracene for the diamagnetic spacer and tetracyanoethylene (TCNE) and cisl,2-dichloro-l,2-dicyanoethylene (DDE) anions for the ion radical part. The latter radical was studied particularly to mimic 2,3-dichloro-4,5-dicyanobenzoquinonide ion considered in experimental studies later. The systems were individually optimized. Anthracene was optimized with $D_{2h}$ symmetry and TCNE and DDE anions were optimized with $D_{2h}$ and $C_{2v}$ symmetry respectively.

The effect of TCNE⁻· and DDE⁻· on the anthracene spacer molecule was examined next, by placing them with their molecular planes parallel to the ring framework in a 7r-stacking fashion. The vertical distance between the spacer and the ion radicals was varied and it was found that 2.2A is the optimal distance where a visible influence of the ion radical on the anthracene moiety is obtained. When the vertical separation is decreased below 2.2A, the charge on the anion gets redistributed with the anthracene taking up part of the charge, indicating that weak bonding interactions are being initiated. Fig. 3.4 depicts the influence of TCNE and DDE anion radicals at a stacking distance of 2.2A on the spin density distributions in anthracene. An important point to note here is that free anthracene being diamagnetic will not show any spin density on its atomic sites. The spin

density distributions depicted in Fig. 3.4 clearly prove that the presence of an ion radical in the vicinity induces a spin polarisation on the **diamagnetic** anthracene molecule. It is seen that when TCNE is in a bond-over-ring position [Fig. 3.4(a)], the spin density distribution on anthracene has six vertical and one horizontal nodal planes. The distribution is alternating and rather complex. In the bond-over-bond conformation, there is a localized spin density distribution in the closest ring with one vertical node alone. It is also clear that $DDE^{-\cdot}$ is able to force a spin polarisation on the anthracene molecule with only vertical nodal planes and regions of alternating positive and negative spin densities are clearly demarcated. The different effects of the two ion radicals appear to arise from the fact that $TCNE^{-\cdot}$ has a symmetric distribution of spin densities whereas $DDE^{-\cdot}$ has an unsymmetric distribution with a node at the central C-C bond.

Having obtained the spin density distributions on anthracene when an ion radical is in its vicinity, we next placed a second ion radical at various positions with respect to the first one, on the other side of the spacer in a mixed stack fashion with the same vertical separation of 2.2A. The singlet-triplet energy separations were computed. The results of our calculations are
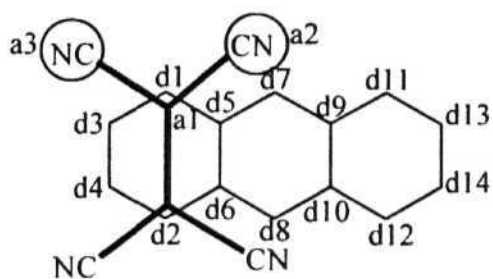
al = +0.40; a2 = a3 = +0.01
dl = -0.50; d2 = +0.50; d3 = +0.50; d4 = -0.50; d5 = +0.50;
d6 = -0.50; *61* = -0.60; d8 = +0.60; d9 = +0.50; d10 = -0.40;
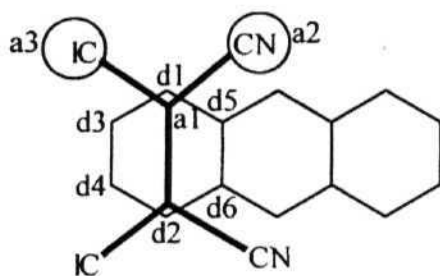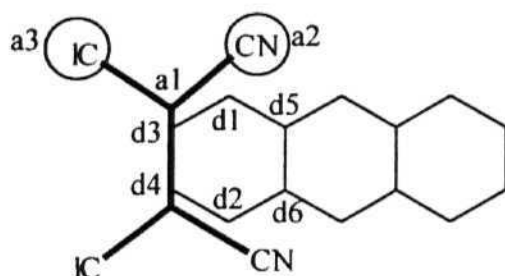dl 1 = -0.40; d12 = +0.40; d13 = +0.40; d14 = -0.40

(a)
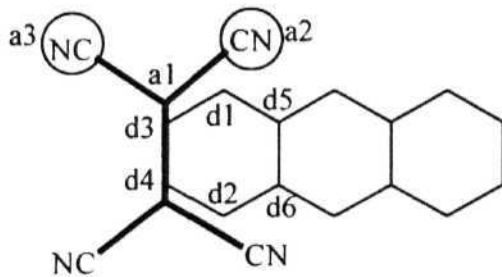


al = +0.40; a2 = +0.05; a3 = -0.01
dl = +0.06; d2 = +0.07; d3 = -0.05; d4 = -0.05; d5 = d6 = 0.00

**(b)**

**Figure 3.4 (continued on next page):**

al =+0.40; a2 = +0.08; a3 =-0.02
**d1** = d2 = -0.02; d3 = d4 =+0.05; d5 = d6 = +0.01

(c)



al = +0.40; a2 = +0.05; a3 = -0.01
dl = d2 = +0.05; d3 = d4 = -0.03; d5 = d6 = +0.01
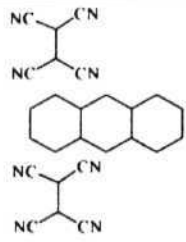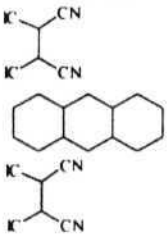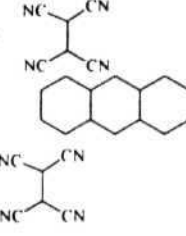
**(d)**

**Figure 3.4:** *Calculated (AMl/UHF) spin densities on the organic acceptor anion radical - anthracene pairs : TCNE"-anthracene in (a) bond-over-ring and (b) bond-over-bond and* **DDE⁻-anthracene** *in (c) bond-over-ring and (d) bond-over-bond conformations; in (b), (c) and (d) the negligible spin denstities observed on two of the rings of anthracene are not shown.*

tabulated in Table 3.1. It is seen that when the spacer spin distribution has simple vertical nodes and the two ion radicals are eclipsed with respect to each other on either side of the molecule so that similar atoms of the ion radical interact with the same atoms of the spacer, the interaction is ferromagnetic [3, 4 and 5 in Table 3.1; refer to Case 1, in Section 3.2.1]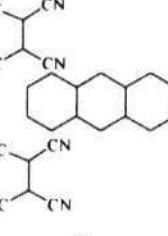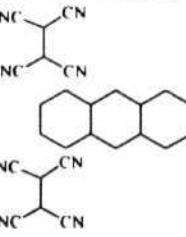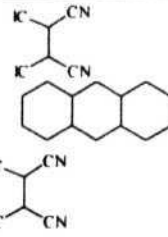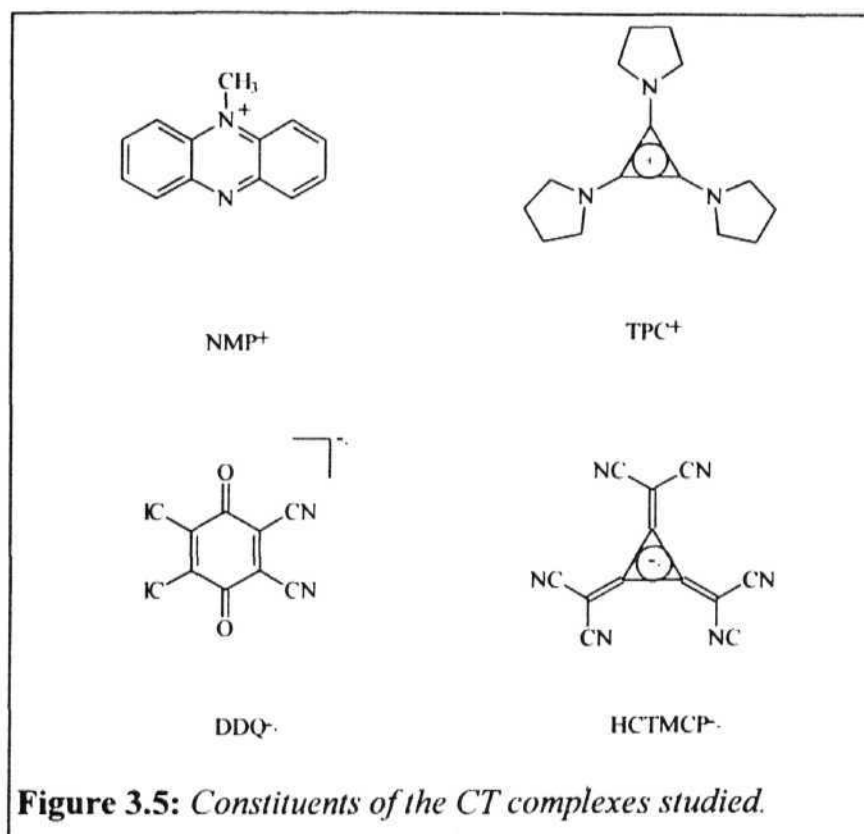. When the two ion radicals are slipped with respect to each other, they interact with different spin regions of the spacer molecule and the interaction is antiferromagnetic [2 and 6 in Table 3.1; refer to Case 2, in Section 3.2.1]. In the case of 1 (Table 3.1) even though the radicals are eclipsed, the spin interaction is antiferromagnetic. This case appears to be complex, and our simple arguments are not applicable, since the spin density distribution in the spacer molecule is complex as seen in Fig.3.4(a). Thus these calculations clearly support the spin interactions we proposed based on the intermolecular spin polarisation picture developed earlier.

Since the calculations have indicated that if the radical anion has an asymmetric structure it is able to enforce a clearer spin polarisation and lead to higher chances of ferromagnetic spin interactions we considered $DDQ^{-\cdot}$ as the ion radical for experimental studies which clearly resembles the hypothetical $DDE^{-\cdot}$ used in the model calculations above. Since N~ methylephenazenium ($NMP^+$) is a well known stable diamagnetic cation having a similar structure as the anthracene used in these calculations, we selected it for the spacer molecule. As contrasting examples to this system we considered a new symmetric cation spacer trispyrrolidine-cyclopropenium ($TPC^+$), and its complexes with asymmetric $DDQ^{-\cdot}$ and a

**Table 3.1:** *Singlet-triplet energy gaps for various molecular model stacks considered in this study (see text for details).*

| Molecular Stacking | $\Delta E_{ST}$ (kcal/mol) | Molecular Stacking | $\Delta E_{ST}$ (kcal/mol) |
|---|---|---|---|
| **1** | -1.9 | **4** | 0.7 |
| **2** | -2.3 | **5** | 1.4 |
| **3** | 1.4 | **6** | -2.6 |

**Figure 3.5:** *Constituents of the CT complexes studied.*

symmetric       anion       radical       hexacyano-trimethylenecyclopropanide
(HCTMCP-) [Fig. 3.5].  The stable cationic species $NMP^+$ and $TPC^+$ also
ensure that the back charge transfer from the anion radicals of DDQ and
HCTMCP would be a highly energetic process.  This is important, since our
spin polarisation picture assumes that complications arising from low-lying
charge transfer states and configuration interaction mixing will not be
present.

## 3.2.2 SYNTHESIS OF THE CHARGE TRANSFER COMPLEXES

The various ionic components for the required CT complexes, $TPC^+$, $DDQ^-$, and $HCTMCP^-$, were prepared following reported procedures as described below. NMP-methosulphate was procured from Fluka chemicals and was recrystallised from acetonitrile. All the solvents were dried prior to the reaction following standard procedures and were stored over $4\text{Å}$ molecular sieves. The details of the synthesis and characterisation are provided below.

Tris(pyrrolidine)cyclopropenium perchlorate was synthesized by adopting the procedure developed by Yoshida and Tawara to prepare tris (dimethylamino) cyclopropenium salts[17]. To 0.7003 g of $C_3Cl_4$ taken in 15ml of dry dichloromethane at 0°C, 0.838 g of pyrrolidine pre-cooled to 0°C, was added with stirring. The solution was stirred at 0°C for 1hr and then at room temperature for 10 hrs. Subsequently it was refluxed for 3hrs. After cooling the reaction mixture to 0°C, 70% perchloric acid was added in excess to the solution. The organic layer was removed. $TPC^+ClO_4^-$ crystallised out from the aqueous layer.

$K^+DDQ^-$ was prepared[18] by reducing DDQ with excess KI in acetonitrile. The solution containing $K^+DDQ^-$ was separated from the excess KI by decantation. The ion radical salt was precipitated by diluting the acetonitrile solution with benzene. The brown coloured $K^+DDQ^-$ was filtered and washed with excess benzene and dried under vacuum.

K$^+$HCTMCP$^-$ was prepared, following the procedure described by Fukunaga[19], by treating $C_3Cl_4$ with sodium hydride and excess of malanonitrile. The dianion is initially formed in the solution and is not very stable. It is converted to the more stable mono anionic form by oxidation with potassium peroxodisulphate.

PREPARATION OF NMP$^\pm$DDQ$^-$: NMP$^+$DDQ$^-$ was prepared by the metathesis reaction of NMP-methosulphate with K$^+$DDQ$^-$ in acetonitrile. In a typical reaction 0.1 g of NMP-methosulphate (0.33 mmol) was dissolved in minimum amount of dry acetonitrile and 0.0886 g of K$^+$DDQ$^-$ (0.33 mmol) dissolved in small quantity of dry acetonitrile was added. The solution immediately turned to dark red colour. Black shining powder of NMP+DDQ- precipitated out on cooling this solution below room temperature for 2 - 3 hrs. It was filtered, washed with benzene and dried under vacuum. m.p. > 300°C. The powder was characterised as follows:

| | |
|---|---|
| **IR** (cm$^{-1}$) | : **2180,** 1560, 1480, 1170, 1030,730 |
| UV-Vis (nm) (CH$_3$CN solution) | : 586, 543, 456, 430, 382, 364 |
| C,H,N analysis (%found) | : 59.41, 2.89, 13.05 |
| (%calculated for NMP+DDQ- ,C$_{21}$N$_4$Cl$_2$O$_2$H$_{11}$ ) | : 59.71, 2.60, 13.27 |

PREPARATION OF TPC$^\pm$DDQ$^-$: TPC$^+$DDQ$^-$ was prepared by the metathesis reaction of TPC$^+$ClO$_4^-$ with K$^+$DDQ$^-$ in water. In a typical

reaction 0.1 g of $TPC^+ClO_4^-$ (0.29 mmol) was dissolved in a small quantity of deaerated distilled water. To this 0.0770g of $K^+DDQ^-$ (0.29 mmol) also dissolved in deaerated distilled water was added. Brown coloured powder precipitated out immediately. The precipitate was filtered under suction and washed several times with deaerated water. It was dried under vacuum at 80°C. The characterisation is as follows:

| | |
|---|---|
| IR (cm$^{-1}$): | : 2959, 2218,2200, 1545, 1456, 1348, 1060,910,878,777, 673 |
| UV-Vis (nm) ( $CH_3CN$ solution) | : 585, 545, 460, 421, 349, 263 |
| C,H,N analysis **(%found)** | : 56.05, 5.42, 13.28 |
| (%calculated for $TPC^+DDQ^-. 0.5H_2O$, $C_{23}N_5H_{24}Cl_2O_{2.5}$) | : 56.21, 5.30, 14.26 |

PREPARATION OF $TPC^+HCTMCP^-$: This compound was prepared by the metathesis reaction of $TPC^+ClO_4^-$ and $K^+HCTMCP^-$. To 0.17 g of $TPC^+ClO_4^-$ (0.5 mmol) in dry acetonitrile, a solution of 0.135 g of $K^+HCTMCP^-$ (0.5 mmol) dissolved in minimum amount of acetonitrile was added. The mixture was stirred well and was diluted with equal volume of deaerated distilled water. Purple coloured powder precipitated out. It was filtered out, washed with water and dried under vacuo at 80°C. The characterisation is as follows:

| IR (cm⁻¹): | : 2878, 2185, 1672, |
|---|---|

IR (cm$^{-1}$):  : 2878, 2185, 1672,
                    1545, 1456

UV-Vis (nm) (CH$_3$CN solution)  : 674, 597, 538, 321,
                    297

C, H, N analysis (% found):  : 65.76, 5.44, 24.76
(% calculated for TPC$^+$HCTMCP$^-$.H$_2$O,
                 C$_{27}$N$_9$H$_{26}$O)  : 65.85, 5.28, 25.60

All the above reactions gave nearly quantitative yields. An important point to be noted is that all the radical anions in these reactions decompose if **kept** in solution for long, hence the CT complexes have to be precipitated out with minimum residence in solution. The ionic composition of all the complexes was confirmed by quantitative UV-Visible absorption spectral analysis by comparing the molar extinction coefficients of the constituent ions and the complex.

## 3.2.4 MAGNETIC PROPERTIES

The magnetic properties of these materials were examined by variable temperature esr studies. The room temperature esr spectra of these complexes are shown in Fig.3.6 and the esr line widths are provided in Table 3.2. All the complexes showed nearly Lorentzian esr line shapes. Therefore the esr signal intensity was calculated using the approximation,

**Table** 3.2: *Room temperature esr linewidths for the three new CT complexes prepared*

| Complex | ESR linewidth (G) at RT |
|---------|------------------------|
| TPC-HCTMCP | 0.625 |
| TPC-DDQ | 10 |
| NMP-DDQ | 2.75 |

(height)x(width)$^2$. These organic ion radical systems have negligible spin-orbit coupling and the usual assumption of the magnetic susceptibility being proportional to the esr signal intensity can be made. Esr spectra were recorded from room temperature down to 120 K for TPC-HCTMCP and down to 50 K for TPC-DDQ and down to 10 K for NMP-DDQ. The last one was the most interesting case, hence the low temperature study employed. The plot of $1/I_{esr}$ for TPC-HCTMCP is shown in Fig. 3.7. This data at temperatures above 120 K follows simple Curie-Weiss law and exptrapolation gives a Weiss constant of -170 K indicating fairly strong antiferromagnetic coupling in this system. The data on TPC-DDQ [Fig. 3.8] shows again Curie-Weiss behaviour with some anomaly at around 100 K. The data above and below 100 K fits Curie-Weiss behaviour with Weiss constants of -84.1 K and -2.5 K respectively. The antiferromagnetic behaviour in these systems may be due to the following reasons.
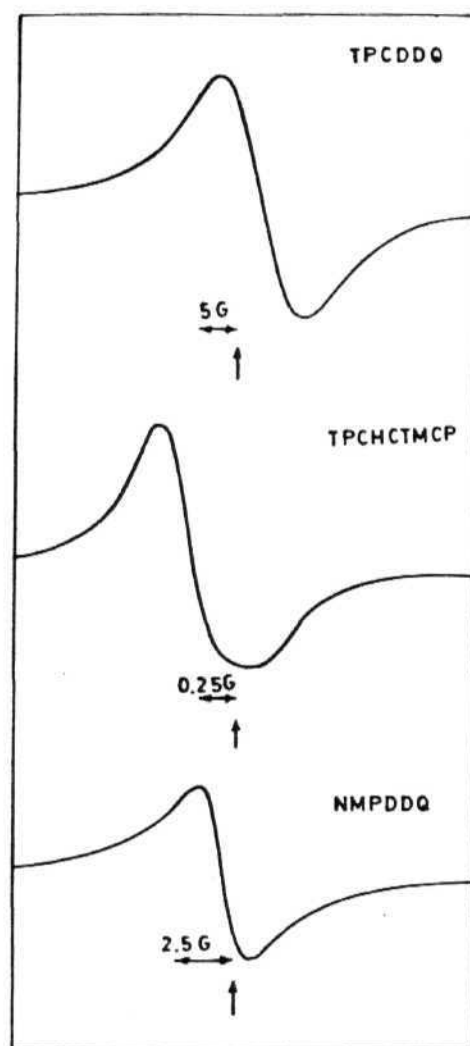
**Figure 3.6:** *Room temperature esr spectra of TPC-HCTMCP, TPC-DDQ and NMP-DDQ.*
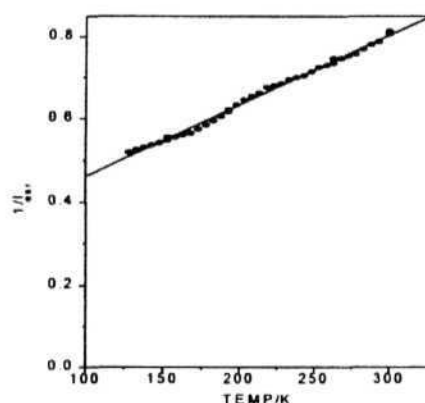
**Figure 3.7:** *$1/\chi_{esr}$ vs T plot for TPC-HCTMCP; least square fit to Curie-Weiss behaviour is shown.*

(i) The complex could be forming a segregated stack instead of a mixed stack in which case, direct exchange interactions between the ion radical spins with out the mediation of the cation spacer would lead to anti ferromagnetic coupling based on kinetic exchange interactions[20].

(ii) The complex may be forming a mixed stack structure; however the spin polarisation in the symmetric cation spacer may not be appropriate for obtaining ferromagnetic spin coupling of the radicals as envisaged in the models classified in Section 3.2.1. Further, in spite of $TPC^+$ being a stable cation, CT interaction between the anion and cation components cannot be ruled out, and such interactions can lead to configuration mixing of excited
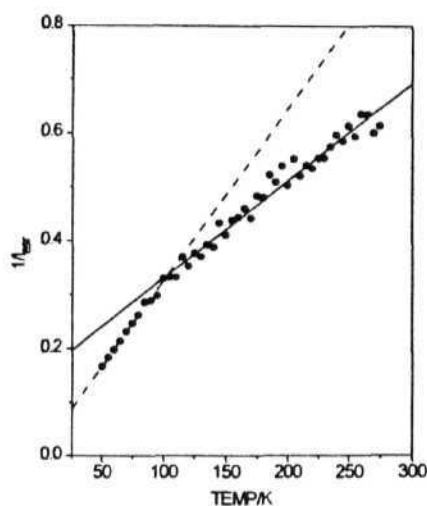
**Figure: 3.8:** *$1/\chi_{esr}$ vs T plot for TPC-DDQ; least square fit to Curie-Weiss behaviour in the temperature regimes, 300 - 100 K (_____) and 100 - 50 K (.........) are shown.*

singlet states and antiferromagnetic spin interaction as described in simple dimer models presented in Section 1.4.2.

In the present circumstances the observed behaviour could be due to the first reason in the case of TPC-HCTMCP, since the esr line widths are very narrow which indicates a strong exchange coupling between the spins. The antiferromagnetic coupling is also very strong as indicated by the large Weiss constant. The antiferromagnetic interaction in TPC-DDQ may be

arising due to the second possibility. The line widths are not very narrow and even the observed anti ferromagnetic coupling is not so strong when compared to the TPC-HCTMCP case. The anomaly around 100K is however difficult to explain in the absence of any structural information.

NMP-DDQ appears to be a better candidate to check the model for reasons explained earlier in Section 3.2.1. Therefore we have carefully examined its variable temperature esr behaviour to very low temperatures. The variation of $1/I_{esr}$ is provided in Fig. 3.9. As can be seen from the plot, the $1/I_{esr}$ follows a very complex pattern, with three different slopes. The data in the region 300 - 100 K follows the Curie-Weiss law with a large Weiss constant of about - 450 K, indicating very strong anti ferromagnetic spin coupling. The behaviour from 100 - 50 K is in strong contrast to the one observed above and has a positive Weiss constant of 24.7 K, indicating a ferromagnetic coupling of the spins in this temperature regime. It is worth noting here that the line widths also start increasing from 100 K [Fig. 3.10], which is the main cause for the increase in the esr intensity. Below 10 K, however, the $1/I_{esr}$ seems to follow a simple Curie paramagnetic behaviour, with a small Weiss constant of +4.3 K. The unusual ferromagnetic behaviour of $NMP^+DDQ^-$ in the limited temperature range may be arising
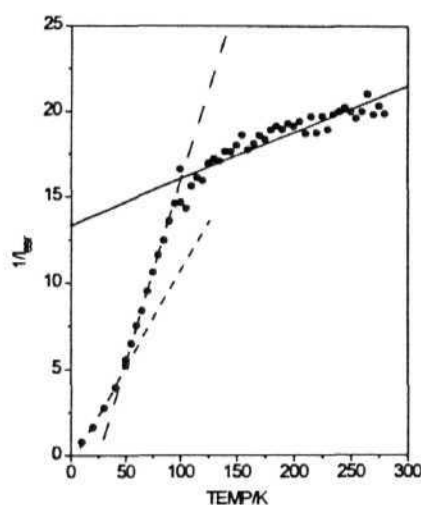
**Figure 3.9:** *1/$\chi_{esr}$ vsT plot of NMP-DDQ; least square fitting of the data to Curie-Weiss behaviour in different temperature regimes 300 - 100 K (_____), 100-50K(-~), and 50 - 10 K (- -) are shown,*

due to the spin polarisation effects discussed earlier in this chapter. The antiferromagnetic behaviour at higher temperature and the change at 100 K may be explained by structural modifications that may occur around 100K. The sudden rise in linewidths below this temperature also supports this hypothesis. As we saw in Section 3.2.2, small variations in the relative stacking arrangement of the ion radical and diamagnetic spacer could result in the reversal of magnetic interaction leading to the complex behaviour of
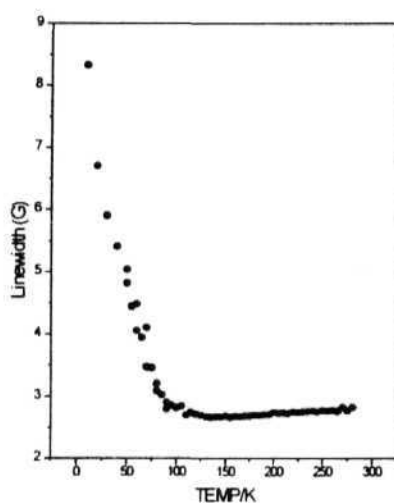
Figure **3.10:** *Variation of esr line width of NMP-DDQ with temperature.*

the magnetism of $NMP^+DDQ^-$. The near cancellation of the ferromagnetic interaction below 50 K may be arising due to interstack anti ferromagnetic interactions which set in at low temperatures. Since $NMP^+$ is not very stable in solution we were unable to grow good quality crystals of this compound. The lack of structural information prevents us from speculating further the reasons for this complex behaviour. However, the variation in the esr linewidths strongly suggests that NMP-DDQ is undergoing some structural modifications at around 100 K.

Though the lack of structural information is a major impediment in fully understanding the systems described above, these studies have provided some novel organic CT complexes and indicate possible new directions for the search for molecule-based magnetic materials..

## 3.3 COPPER(II) COMPLEXES OF 4,5-DICYANOIMIDAZOLE

The main drawback of the polycarbene/ployradical systems based on the topological models for purely organic ferromagnets, is their chemical reactivity, which often leads to low spin concentrations in the bulk material. If carbon based radical sites in these systems could be replaced by paramagnetic transition metal ions, it may be possible to overcome this difficulty. Transition metal coordination polymers with interesting magnetic, electrical, nonlinear optical and ferroelectric properties has been the subject of intense research. Focus has been mainly on one-dimensional coordination polymers[21]. The general strategy of design of ferromagnetic interactions between the metal ion spins in these polymeric systems has been to make the magnetic orbitals of adjacent metal ion centres orthogonal by using a variety of ligands[22]. But this has proved to be a synthetically challenging proposition. Alternatively, the propensity for antiferromagnetic coupling has been used to design ferrimagnetic chain structures [23]. Two important classes of such type of materials have been i) the metal-organic free radical and ii) ordered heterometal structures. Since ferromagnetism is a bulk property, the $T_C$ in these one-dimensional polymers will depend on

the magnitude of the interchain 2-D and 3-D inetractions. Realising this, many groups have been trying to incorporate 2-D and 3-D spin interactions by a variety of methods. We mentioned some of these methods in Section 1.3.3 and also in Section 4.2 A few reports have appeared recently, of Cu(II) assembled in 2-D and 3-D networks; these systems have shown anti ferromagnetic spin interactions[24]. Different ligands which can mediate ferromagnetic inetractions between metal ion spins are being investigated[25]. If a ligand bridging two paramagnetic metal ions can provide a short odd *n*-electron path, it could serve as a ferromagnetic coupling unit (recall the topological models based on spin polarisation) for the metal ion spins provided the metal ion spin orbitals are in conjugation with the ligand $\pi$-system. In principle, imidazoles which are capable of ligating to two metal ions through their N atoms should be suitable candidates for this purpose. However reports of imidazolate bridged Cu(II) ions indicate that the metal ion spins are usually antiferromagnetically coupled[26]. 4,5-dicyanoimidazole (DCI) would be an interesting variant to investigate in this connection since it is more acidic than imidazole and therefore capable of forming the corresponding imidazolate ion more easily. We are aware of only one report[27] with structural information on a metal complex with DCI as a ligand; a polymeric structure involving Cu(I) and DCI was suggested for this complex. Earlier studies in our laboratory[28] have shown that water soluble Cu(II) salts readily react with DCI to give complexes with a probable polymeric structure. Variable temperature esr studies on these compounds showed that the signal intensity decreased continuously on cooling suggesting anti ferromagnetic coupling between Cu(II) spins. These

materials were all amorphous and no structural information could be gathered. Therefore we attempted the synthesis of smaller Cu(II) clusters by blocking some of the coordination sites of the Cu(II) ion. Since 2,2'-bipyridil (bipy) is known to form very stable complexes with Cu(II) we chose bipy as a ligand. In this Section we present our experimental investigations on the preparation, characterisation, structural analysis and magnetcic susceptebility studies of three new copper coordination complexes with DCT and bipy as the ligands.

## 3.3.1 SYNTHESIS AND CHARACTERISATION

Initially we tried a simple reaction protocol of directly mixing the ingredients, the Cu(II) salt, bipy and DCI; the copper salt we started with was $Cu(NO_3)_2.3H_2O$. However, the ir spectrum of the product showed that the anion NO3" is still present in the complex. We followed two different routes to overcome this problem : i) using a starting copper salt with a counterion such as sulphate which does not form a good ligand and ii) doing the reaction in an acidic buffer solution. Thus we obtained three novel Cu(II) complexes, which we refer to as CUBD-I, CUBD-II and CUBD-III. Below we provide the preparation, characterisation and magnetic susceptibility studies of these three complexes. We were able to grow good quality single crystals in the case of CUBD-I and CUBD-II and the structural analyisis of these two complexes are also provided.

PREPARATION OF CUBD-I:    In a typical reaction 0.1 g of $Cu(NO_3)_2.3H_2O$ (0.41 mmol) was dissolved in 5ml of distilled water and warmed.  To this a warm solution of 0.13 g. (0.83 mmol) of bipy in 10ml of ethanol was added.  The pale blue colour of copper nitrate turns to dark blue immediately.  To this, a hot solution of 0.05 g. (0.42 mmmol) of DCI in 5 ml of ethanol was added and stirred for 10 minutes.  The solution was then allowed to cool and then subjected to slow evaporation.  Large, prsim-shaped crystals separated out in 2 - 3 days.  They were filtered and washed with cold ethanol and water.  This product is labelled as CUBD-I.  It was found that, addition of DCI to $Cu(bipy)_2(NO_3)_2$ prepared separately, also produces CUBD-I.  The ir spectra showed broad peaks around 1354 $cm^{-1}$ indicating the presence of NO3" remaining in the complex; the cyano peak at 2239 $cm^{-1}$ indicates that the DCI is unlikely to be in a deprotonated form (compare with CUBD-II discussed below).

| | |
|---|---|
| IR $(cm^{-1})$ | : 3474, 3074, 2239, 1599, 1444, 1354, 1026,777 |
| C, H, N analysis (%found ) | : 47.97, 3.23, 21.97 |
| (% calculated for $Cu(bipy)_2(DCI)(NO_3)_2.0.5H_2O$, $CuC_{25}N_{10}H_{19}O_{6.5}$ ) | : 47.87, 3.03, 22.34 |

PREPARATION OF CUBD-I 1 : In a typical reaction 0.5 g (2 mmol) of $CuSO_4.5H_2O$ was dissolved in 10ml of water and warmed.  To this a hot solution of 0.63 g (4 mmol) of bipy dissolved in 10ml of distilled water was

added. Pale blue colored precipitate formed almost immediately. The IR spectrum of this compoud matches well with the one reported[29] for a polymeric $[Cu(bipy)(SO_4)]_n$. This was filtered out. To the rest of the solution which was still blue. a warm solution of 0.24 g (2 mmol) of DCI in 5 ml of ethanol was added and stirred for 10 minutes. On cooling, a pale blue crystalline precipitate formed. However, good quality crystals could not be grown with this method. This product was partially soluble in water but was highly soluble in organic solvents such as ethanol and acetonitrile. Hence, this product was recrystallised from acetonitrile-water mixture. Pale blue platelets separated out as the organic solvent evaporates off. These were filtered and washed with plenty of water. The ir spectra did not show any peaks corresponding to $SO_4^{2-}$; the cyano peak is found at a frequency markedly lower than that of free DCI, indicating the formation of DCI".

| | |
|---|---|
| IR (cm$^{-1}$) | : 3109, 2226, 1601, 1442, 1109, 769 |
| C, H, N analysis (%found ) | : 56.00, 2.72, 32.69 |
| (% calculated for $Cu(bipy)_2(DCI^-)_2(DCI).H_2O$ $C_{35}N_{16}H_{23}O$) | : 56.25, 3.08, 30.00 |

PREPARATION OF CUBD-III : This was also prepared from $Cu(NO_3)_2.3H_2O$ but in presence of an acidic buffer. 0.1 g (0.41 mmol) of $Cu(NO_3)_2.3H_2O$ was dissolved in 5 ml of distilled water and was warmed. To this 2 ml of the freshly prepared acetic acid/sodium actetate buffer was added. The solution immediately turns dark blue. To this warm solution a

solution of 0.13 g (0.83 mmol) of bipy in 10 ml of warm ethanol was added. 0.050 g (0.42 mmol) of DCI dissolved in 10 ml of warm ethanol was added next. The solution was cooled to room temperature and the solvents were slowly evaporated. Pale blue hemispherical beads separated out over a period of 2 - 3 days. The product was filtered and washed with water. The IR spectra did not show the presence of $NO_3^-$; the cyano peak again indicates the presence of DCI'' formation. This compound also was not very soluble in water. All our elTorts to grow crystals of this compound were unsuccessful.

| | |
|---|---|
| IR ($cm^{-1}$) | : 3117, 2227, 1604, 1442, 1300, 1111, 769 |
| C, H. N analysis (%found ) | : 47.33, 2.66, 27.02 |
| (% calculated for $Cu(bipy)(DCl)_2(H_2O)_3$, $C_{20}N_{10}H_{16}O_3$) | : 47.29, 3.15, 27.58 |

## 3.3.2 CRYSTAL STRUCTURE AND MAGNETIC STUDIES

As indicated above, single crystals of two of the copper complexes could be grown and their structures were analysed. Table 3.3 describes the details of the structure determinations of CUBD-I and CUBD-II. Both crystals belong to the triclinic space group. The molecular structure of the CUBD-I complex is provided in Fig.3.11. The structure of this complex is very similar to the reported structure of $Cu(biypy)_2(NO_3)_2$[30]. However, the dicyanoimidazole has been incorporated in the structure. It is clearly seen

that the DCI does not coordinate to the Cu(II) ion. The DCI appears in the structure because of a H-bond that links its acidic H atom to the O of the $NO_3^-$ which is not ligated to Cu(II). It is interesting to note here that the ir cyano stretch frequency in CUBD-I is $2239cm^{-1}$, which is shifted to lower

**Table 3.3:** *Crystallographic data far CUBD-I and CUBD-II.*

|  | CUBD-I | CUBD-II |
|---|---|---|
| Molecular Formula | $CuC_{25}N_{10}H_{22}O_7$ | $CuC_{35}N_{16}H_{20}$ |
| Space group | $P\bar{1}$ | $P\bar{1}$ |
| a, Å | 12.398 | 9.803 |
| b, Å | 13.679 | 19.666 |
| c, Å | 8.837 | 9.276 |
| α, deg. | 100.77 | 101.45 |
| β, deg. | 100.39 | 100.11 |
| γ, deg. | 103.40 | 99.36 |
| z | 2 | 2 |
| $\mu$ ($CuK_\alpha$), $cm^{-1}$ | 6.01 | 6.01 |
| no. of reflections | 4249 | 4550 |
| R | 0.051 | 0.034 |
| $R_w$ | 0.066 | 0.054 |

frequency than the peak in pure DCI, which appears as a doublet at 2245 and 2258 $cm^{-1}$. This shift is not as large as that found when the DCI is

deprotonated and may be arising from the effect of the H-bonding interaction. Since we were mainly interested in getting DCI to coordinate to the Cu(II) ion, we proceeded in two different ways as mentioned above. In the first of these methods, we proceeded on the basis that it would be difficult to get rid of the strongly coordinating ligands such as NO3" if present in the starting Cu salt making it difficult for DCI to coordinate. Hence we used $Cu(SO_4)_2$, instead of cupric nitrate. As can be seen from the structure of CUBD-II (Fig.3.12) we were successful in making the DCI coordinate to the copper(II) ion. The charge balance is maintained by one uncoordinated DCI" present in the crystal lattice; interestingly, a neutral DCI is also present, H-bonded with the DCI". An important point to be noted here is the ir cyano stretch frequency: it moves further down with respect to CUBD-I and now appears at 2226 $cm^{-1}$. Perhaps this could be taken as an indication of DCI" formation and its coordination to the metal. Surprisingly the cyano stretch frequency expected for the neutral DCI in the complex is not seen in the ir spectrum.

Even though the coordination around the Cu(II) are different, the crystal structures of CUBD-I and CUBD-II are very similar in many respects. In both cases, we find that the Cu(II) is pentacoordinated, a rather common feature, and is in a highly distorted square pyramidal geometry. No peculiar bond lengths are seen around the Cu(II) ion (Table 3.4) or in the bipy ligands. We have examined the packing diagrams of CUBD-I and CUBD-II

**Figure 3.11:** *ORTEP of the molecular structure oft 'UBD-I.*
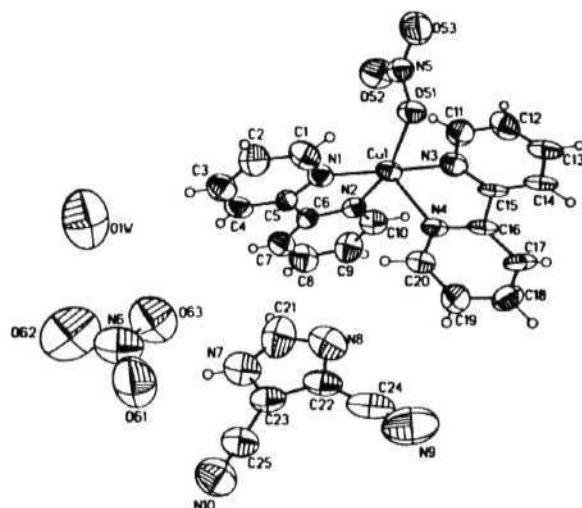


**Figure 3.12:** *ORTEP of the molecular structure oft 'UBD-II.*

**Table 3.4 (a):** *Relevant bond lengths and bond angles in CUBD-I; standard deviations are provided in paranthesis.*

|              | Distance (A) |
|--------------|--------------|
| Cu - O(51)   | 2.078(3)     |
| Cu-N(1)      | 1.980(4)     |
| Cu - N(2)    | 2.032(3)     |
| Cu-N(3)      | 2.008(4)     |
| Cu - N(4)    | 2.185(3)     |

|                    | Angle (deg.) |
|--------------------|--------------|
| O(51) - Cu - N(1)  | 92.5(1)      |
| O(51) - Cu - N(2)  | 161.5(1)     |
| O(51) - Cu - N(3)  | 88.1(1)      |
| O(51) - Cu - N(4)  | 90.8(1)      |
| N(1)-Cu-N(2)       | 81.1(1)      |
| N(1) - Cu - N(3)   | 176.7(1)     |
| N(1)-Cu-N(4)       | 104.2(1)     |
| N(2)-Cu-N(3)       | 97.4(1)      |
| N(2)-Cu-N(4)       | 107.5(1)     |
| N(3)-Cu-N(4)       | 79.0(1)      |
| Cu - O(51) - N(5)  | 107.0(2)     |
| Cu-N(1)-C(1)       | 125.6(3)     |
| Cu-N(1)-C(5)       | 115.6(3)     |
| Cu - N(2) - C(6)   | 113.9(2)     |
| Cu-N(2)-C(10)      | 127.1(3)     |
| Cu-N(3)-C(11)      | 122.8(3)     |
| Cu - N(3) - C(15)  | 116.9(3)     |
| Cu-N(4)-C(16)      | 111.8(2)     |
| Cu - N(4) - C(20)  | 129.5(3)     |

**Table 3.4 (b):** *Relevant bond lengths and bond angles in CUBD-II.*

|  | distance (A) |
|---|---|
| Cu-N(1) | 1.993(2) |
| Cu-N(2) | 2.043(2) |
| Cu-N(3) | 2.003(2) |
| Cu-N(4) | 2.162(2) |
| Cu-N(5) | 2.001(2) |

|  | Angle (deg.) |
|---|---|
| N(1)-Cu-N(2) | 80.79(7) |
| N(1)-Cu-N(3) | 173.04(7) |
| N(1)-Cu-N(4) | 96.08(7) |
| N(1)-Cu-N(5) | 94.16(7) |
| N(2)-Cu-N(3) | 95.92(7) |
| N(2) - Cu - N(4) | 98.83(7) |
| N(2)-Cu-N(5) | 145.28(7) |
| N(3)-Cu-N(4) | 78.29(7) |
| N(3) - Cu - N(5) | 92.01(7) |
| N(4)-Cu-N(5) | 115.88(7) |
| Cu-N(1)-C(1) | 124.9(2) |
| Cu-N(1)-C(5) | 115.2(1) |
| Cu - N(2) - C(6) | 113.6(1) |
| Cu-N(2)-C(10) | 128.0(1) |
| Cu - N(3) - C(11) | 122.7(1) |
| Cu-N(3)-C(15) | 118.1(1) |
| Cu - N(4) - C(16) | 113.1(1) |
| Cu - N(4) - C(20) | 128.9(2) |
| Cu-N(5)-C(21) | 127.8(2) |
| Cu-N(5)-C(23) | 127.2(1) |

crystals. The Cu(II) - Cu(II) distances are all very large. It was found that a **unique** closest Cu(II) - Cu(II) distance of 7.1 A and 8.2A occurs **in CUBD-I**
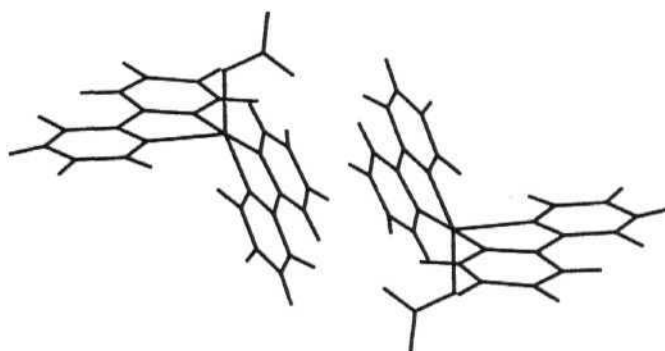


(a)
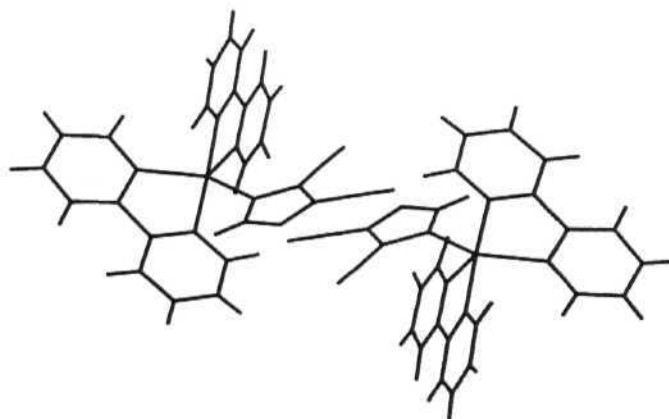


(b)

**Figure 3.13:** *Dimeric structures in (a) CUBD-I and (b) CUBD-II crystals.*

and CUBD-II respectively (Fig.3.13). In fact these shortest distances define a weak dimer structure for these complexes.

Since $HNO_3$ would be the biproduct during the reaction of copper nitrate with DC1 (which is also fairly acidic), in the second startegy that we adopted to get DCI to coordinate to Cu(II), we used an acidic buffer which will ensure the pH to be maintained at an optimal level say. 4.0. It may be noted here, that a similar procedure was reported in the preparation of a chloaranilic acid complex of Cu(II)[24]. We were not able to grow single crystals of CUBD-II I; but the cyano strech frequency (at $2227cm^{-1}$, very similar to that one of CUBD-II) indicates that probably in this case also the DCI" is formed and is coordinated to Cu(II). The peculiar hemispherical bead-like morphology and the low solubility in water displayed by CUBD-III indicate that it perhaps has a polymeric structure.

Room temperature esr spectra of the three complexes showed normal Cu(II) signals. Magnetic susceptibility of these three complexes (as powder samples) were measured on a SQUID magnetometer, from 300 K to 3 K at a field of 10 kG. The data are plotted as $\chi^{-1}$ against T in Fig.3.14. It is seen that the behaviour in the case of CUBD-I and CUBD-II are very close to Curie paramagnetic. but shows a small but clear deviation towards lower susceptibilities. This can be taken as evidence for a weak antiferromagnetic interaction[31]. The room temperature magnetic moment estimated for these two complexes were respectively, 1.63 and 1.64 B.M,
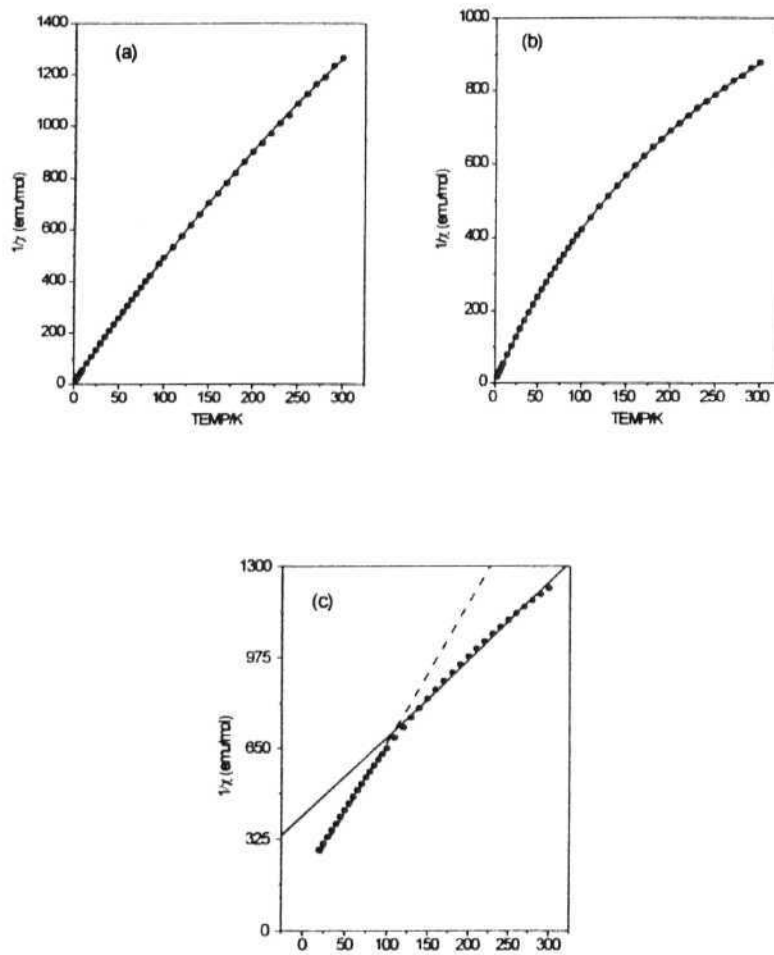
**Figure 3.14:** *l/χvs T plots of (a) CUBD-I, (b) CUBD-II and (c) CUBD-III; the lines are fits to the isotropic Heisenberg model in (a) and (b) and to Curie-Weiss law [300 - 100 K (_____); 100 -3 K (. . . . .)] in (c).*

again indicating a weak anti ferromagnetic interaction of S = 1/2 ions. The data for both these complexes could be fit quite well using the simple isotropic Heisenberg model within a dimer picture[32]. The latter approximation could be justified in view of the crystal structure described above. The best fit lines shown in Fig.3.14(a) and (b) are obtained for small values of J = -0.72 and -0.22 cm$^{-1}$ respectively in the two cases. These fits assumed a fixed g value of 2.0023 and showed that only about 50% of the Cu ions contributed to the susceptibility; contribution of a temperature independent paramagnetism (TIP) of 1.6x10$^{-4}$ and 5.3x10$^{-4}$ emu/mol respectively was also necessary to obtain the good fit shown in the figure. Attempts to fit the data by fixing the participation of Cu(II) ions at 100% led to very unphysical J values or very high TIP contributions. We do not at present understand the low percentage of the Cu(II) spins contributing to the susceptibility. The data analysis nevertheless indicates that the Cu(II) ions in both CUBD-I and CUBD-II are coupled by a very weak anti ferromagnetic interaction, obviously, a consequence of the large Cu-Cu distances observed.

The situation with CUBD-III was very different, however. The Heisenberg dimer model does not fit the $\chi^{-1}$ *vs* T data in any reasonable manner. Among the various analysis we attempted, we found that the data can be fit well, only if we assume Curie-Weiss behaviour with two different 0 values. -34.9 K and -162.7 K for the temperature ranges 3 - 100 and 100 - 300 K. This implies that CUBD-III has fairly strong extended anti ferromagnetic interactions, and behaves very differently from the other

two complexes. Again this points to the possibility of a polymeric structure for this complex. The anomaly in the magnetic data at 100 K is not understood; it is possible that some structural phase transition takes place at this point. We believe that in CUBD-III we are beginning to see a Cu(II)-DCI⁻-Cu(II) structural unit emerging. It is quite possible that due to the steric repulsions of the cyano groups on the DCI, these chains have strongly nonplanar structures. Further, it is also likely that the spin on Cu(II) does not reside in a d-orbital that is appropriate for conjugation with the π-system of DCI. Hence the simple topological models for spin coupling through *n*-electron pathways may not be realised here. Further work including elucidation of structure on a coordination polymer would be required to extend this scheme for the realisation of a magnetic material.

## 3.4 CONCLUSIONS

In this chapter we described our experimental investigations on different organic CT complexes and metal coordination compounds based on the general idea of spin polarisation to achieve ferromagnetic alignment of spins. The proposed ferromagnetic alignment of spins based on intermolecular spin polarisation was supported by model calculations on stacked organic acceptor anions and diamagnetic spacers with extended π-electron conjugation. Variable temperature esr studies on three organic CT complexes are described. While the complexes TPC-HCTMCP and TPC-DDQ seem to follow simple anti ferromagnetic Curie-Weiss type behaviour,

NMP-DDQ shows a very complex behaviour, with ferromagnetic spin alignment in limited temperature regimes. It was suggested, based on the esr line widths and the temperature dependence of esr signal intensity, that, TPC-HCTMCP may be forming a segregated stack while TPC-DDQ and NMP-DDQ may have mixed stack structures. We believe that DDQ" fails to force a spin polarisation on $TPC^+$ whereas in the case of the more extended structure of $NMP^+$, the spin polarisation picture we have proposed may be operating.

Three new copper(II) complexes have been prepared. It was expected that when $DCI^-$ acts as a bridging ligand between paramagnetic metal ions, by coordination at its N (1 and 3 positions) atoms, it will be able to mediate a ferromagnetic spin coupling through the odd $\pi$-conjugation path. Structural analysis indicates that in CUBD-I, DCI is not coordinated to Cu(II). Using different synthetic procedures we succeeded in preparing complexes where DCI is coordinated to the Cu(II) ion. Magnetic susceptbility studies however, does not indicate any ferromagnetic interactions between copper(II) spins. While there seems to be negligible interaction between Cu(II) spins in CUBD-I and CuBD-II, the behaviour of CuBD-III indicates strong anti ferromagnetic interactions. As far as we are aware these are the first complexes of Cu(II), or any paramagnetic metal ion for that matter, with DCI" as a ligand. This should open up a new class of metal complexes with the potential to develop novel magnetic materials.

## REFERENCES

1. (a) J. S. Miller, J. C. Calabrese, H. Rommelmann, S. Chittipeddi, J. H. Zhang, W. M. Reiff and A. J. Epstein, *J. Am. Chem. Soc.*, **109,** 769 (1987). (b) S. Chittipeddi, K. R. Kromack, J. S. Miller and A. J. Epstein, *Phys. Rev. Lett.*, 58, 2695 (1987).

2. A. Carrington and A. D. McLachlan, *Introduction to Magnetic Resonance*, Chapman and Hall, London, 1967, Chapter 6.

3. T. R. Tuttle and S. I. Weissmann, *J. Am. Chem. Soc,* **80,** 5342 (1958).

4. W. T. Borden, *Modern Molecular Orbital Theory for Organic Chemists,* Prentice-Hall, New Jersey, 1975, Chapter 5.

5. T. Bally and S. Masamune, *Tetrahedron,* 36, 343 (1980).

6. W. T. Borden in *Diradicals,* W. T. Borden (ed.), Wiley-Interscience, New York. 1982, Chapter 1.

7. (a) W. T. Borden, *J. Am. Chem. Soc,* 97, 5968 (1975). (b) H. Kollmar and V. Staemmler, *J. Am. Chem. Soc,* 99, 3583 (1977).

8. (a) H. Fukutome, A. Takahashi and M. Ozaki, *Chem. Phys. Lett.,* **133,** 34 (1987). (b) T. P. Radhakrishnan, *Chem. Phys. Lett.,* **181,** 455 (1991).

9. H. M. McConnell, *Proc Robert A. Welch Foundation Conf. Chem. Res.,* **11,** 144 (1967).

10. R. Breslow, *Pure and Appl. Chem.,* 54, 927 (1982).

11. For example see T. P. Radhakrishnan, *Curr. Sci.,* 62, 669 (1992).

12. A. Zheludev, A. Grand, E. Ressouche, J. Schweizer, B. G. Morin, A. J. Epstein, D. A. Dixon and J. S. Miller, *J. Am. Chem. Soc,* **116,** 7243 (1994).

13. J. M. Manriquez, G. T. Yee, R. S. McLean, A. J. Epstein and J. S. Miller, *Science,* **252,** 1415 (1991).

14. P. M. Allemand, K. C. Khemani, A. Koch, F. Wudl, K. Holczer, S. Donovan, G. Gruner and J. D. Thompson, *Science,* 253, 301 (1991).

15. T. Sugimoto, M. Tsujii, H. Matsuura and N. Hosoito, *Chem. Phys. Lett.,* **235,** 183(1995).

16. K Ueda, T. Sugimoto, S. Endo, N. Toyota, M. Kohama, K. Yamamoto, Y. Suenaga, H. Morimoto, T. Yamaguchi, M. Munakata, N. Hosoito, N. Kanehisa, Y. Shibamoto and Y. Kai, *Chem. Phys. Lett.,* **261,** 295 (1996).

17. Z. Yoshida and Y. Tawara, *J. Am. Chem. Soc,* 93, 2573 (1971).

18. Y. Matsunaga, *J. Chem. Phys.,* 41, 1609(1964).

19. T. Fukunaga, *J. Am. Chem. Soc,* 98, 611 (1976).

20. P. W. Anderson in *Solid Stale Physics,* F. Seitz and D. Turnbull (eds.), Vol. 4, Academic Press, New York, 1963, p. 99.

21. C. T. Chen and K. S. Suslick, *Coord. Chem. Rev.,* **128,** 293 (1993).

22. R. D. Willett in *Magneto-Structural Correlations in Exchange Coupled Systems,* R. D. Willett, D. Gatteschi and O. Kahn (eds.), NATO·ASI Series, Vol. **140,** Reidel, Dordrecht, 1983, p. 389.

23. O. Kahn, *Angew. Chem. Int. Edn. Engl.,* **24,** 834 (1985).

24. S. Kawata, S. Kitagawa, M. Kondo, I. Furuchi and M. Munakata, *Angew. Chem. Int. Edn. Engl.,* **33,**1759(1994).

25. S. Mitsubori, T. Ishida, T. Nogami, H. Iwamura, N. Takeda, M. Ishikawa, *Chem. Lett.,* 685 (1994).

26. (a) J. Avrey in *Understanding Molecular Properties*, J. P. Dahl (ed.), D. Reidel, Hollard, 1987, p. 187. (b) P. G. Rasmussen, J. B. Kolowich and J. C. Bayón, *J. Am. Chem. Soc.*, **110,** 7042 (1988). (c) G. Kolks, S. J. Lippard, J. V. Waszczak and H. R. Lilienthal, *J. Am. Chem. Soc,* **104,** 717 (1982). (d) M. Z. Wan, H. Q. Wei, T. W. Xia, L. S. Xiaung, W. Z. Min, H. J. Ling, *Polyhedron,* 15, 321 (1996). (e) P. G. Rasmussen and J. E. Anderson, *Polyhedron,* 2, 547 (1983).

27. P.G . Rasmussen, L. Rongguang, W. M. Butler and J. C. Bayón, *Inorg. Chim. Acta,* **118,** 7 (1986).

28. Satya Prasanna, Ph. D. Thesis, University of Hyderabad, 1996.

29. W. R. McWhinnie, *J. Inorg. Nucl. Chem.,* 26, 21 (1964).

30. (a) R. J. Fereday, P. Hodgson, S. Tyagi and B. J. Hathaway, *J. Chem. Soc, Dalton Trans.,* 2070 (1981). (b) H. Nakai, *Bull. Chem. Soc Jpn.,* 53, 1321 (1980).

31. K. S. Hagen, T. D. Westmoreland, M. J. Scott and W. H. Armstrong, *J. Am. Chem. Soc,* **111,** 1907(1989).

32 C. J. O`Connor, *Progr. Inorg. Chem.,* 29, 203 (1982).

# CHAPTER 4

---

# NOVEL MAGNETIC MATERIALS BASED ON ORGANIC RADICALS IN HOST LATTICES

---

## 4.1 BACKGROUND

Molecular magnetic systems such as metal complexes, organic free/ion radicals etc. have been mainly studied in solution state or in the crystalline solid state. If the solutions are dilute, the spin systems are practically isolated and spin exchange interactions can be induced between them by increasing the concentrations. In the crystalline state, the radicals are either paramagnetic or involved in some cooperative magnetic interactions such as antiferromagnetism, ferromagnetism etc.. Organic radicals are by and large para or antiferromagnetic in the crystalline state and specific design techniques lead to ferromagnetic systems as discussed in Section 1.4. We envisaged that introduction of organic free or ion radicals into some kind of host lattices in appropriate concentrations would give rise to magnetic interactions not normally seen in the solution or pure crystalline state, and hence novel magnetic materials. The hosts may or may not play an active part in the magnetic interactions. Inclusion of the organic spin systems in an interacting host environment may lead to specific tailored dimensionalities for magnetic couplings which would be determined by the dimensionality of the host lattice.

It is well known that short range interactions in a purely one-dimensional array cannot lead to any ordering phase transitions at finite temperatures[1]. This is due to the fact that the entropy associated with the introduction of a point of disorder always wins over the energetics associated with it. However, in two or higher dimensions, phase transitions

are possible at finite temperatures. Consider an arrangement of N Ising spins in a square lattice with L segments forming a boundary between regions of up and down spins. In such a lattice, Peierls[1c] has shown that, since both the energy and entropy vary as the first power of L, a temperature can be found for which the energy overwhelms the entropy and ferromagnetic ordering of the spins is possible. Hence introducing 2-D and 3-D spin interactions is of fundamental significance in the design of magnetic materials. Many metal coordination complexes and the recent metal-organic free radical coordination compounds have demonstrated the utility of 3-D spin interactions. Recently several hydroxylated[2] organic free radicals which have appreciable 2-D and 3-D interactions based on the H-bond networks have been synthesized and studied. There has also been efforts to synthesize polycarbenes which branch out into 2-D lattices[3]. However, we have not come across a model that deliberately imposes a built in 2- or 3-dimensionality on the spin interactions between organic free/ion radicals, to fabricate molecule-based magnetic materials.

Intercalation compounds is one of the areas of host-guest chemistry which has been actively pursued. Intercalation is the insertion of an atomic or molecular species (guest) into a rigid lattice (host) which possesses or creates voids to accommodate these guest species. Here rigidity means that only minor structural and chemical modifications occur upon intercalation and that the identity of the host is in some sense preserved. Graphite, clays, transitional metal dichalcogenides and zeolites are well known examples of host materials, which have two- or three- dimensional van der Waal's voids

*ie,* regions in space where no significant chemical bonding is present. Inclusion of guests in the interstices of closely packed structures (certain metal nitrides, carbides and hydrides) are also considered as intercalation compounds. Graphite intercalation compounds (GIC's) which are formed by the insertion of guest atoms/molecules into the interlayer spaces of graphite, have been known for over a century and have been studied in very great detail[4].

In this Chapter we have focussed mainly on the synthesis, structure and magnetic properties of novel graphite intercalation compounds wherein organic ion radicals are present as intercalates and where, we believe, the graphite host is intimately involved in the spin interactions. Towards the end of this chapter we also discuss some studies of the organic free radical, DPPH, distributed in polystyrene films in different concentrations. The polymer host appears to be only weakly involved in the magnetic interactions. However, the radical-radical interactions are found to be quite different from what is found in the solution or crystalline state.

## 4.2 GRAPHITE INTERCALATION COMPOUNDS

Graphite, an allotropic form of carbon, has a planar two-dimensional sheet structure [Fig. 4.1], with voids between the sheets. These interlayer van der Waal's spaces arise from the strong in-plane covalent bonding and the weak interplane bonding interactions. A large number of atoms, ions

and molecules have been included as guests (generally called intercalates) into these interlayer spaces to give graphite intercalation compounds. A significant characteristic of graphite is its ability to accommodate even two different intercalates resulting in ternary



**Figure 4.1:** *Schematic picture of graphite (host) and intercalate (guest).*
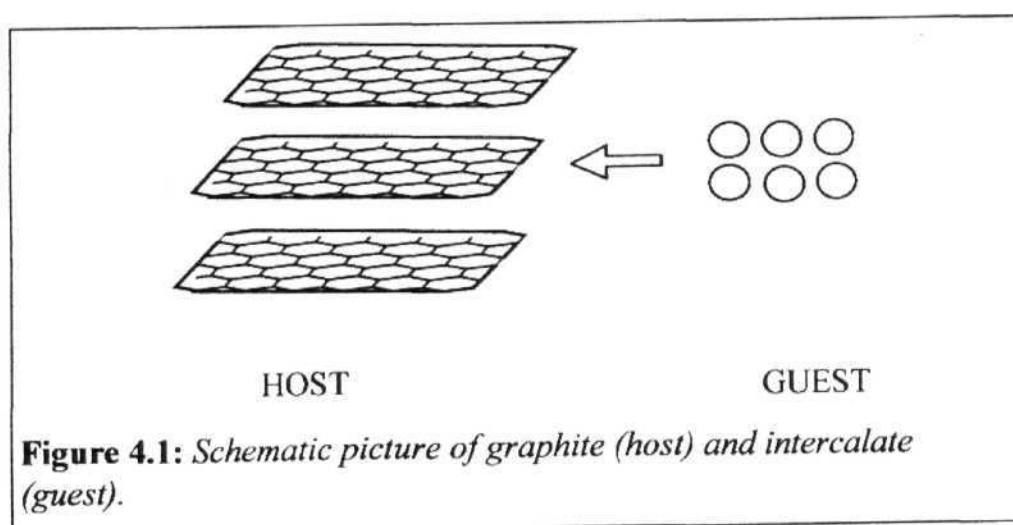
intercalation compounds. Another important feature of GIC's is the long range structural ordering in the stacking direction, the so called *staging* phenomenon. It is characterized by the ratio of host layers to the guest layers. For example, in a "first stage compound" every interlayer void is filled, resulting in the alternate stacking of graphite sheets and the intercalate layers. In a similar fashion the GIC which has 'n' layers of graphite between the intercalate layer is called the $n^{th}$ stage compound [Fig. 4.2]. In pristine graphite the interlayer spacing, the c-axis repeat distance, is $c_0 = 3.35A$. Intercalation of atoms or molecules into graphite requires an

increase in this interlayer spacing to a significantly larger value. While the distance, $d_s$, between the graphite sheets sandwiching the intercalate layer increases from $c_0$, the distance between graphene layers with no intercalate layer in between remains practically the same as $c_0$. Thus the c-axis repeat distance $I_c$ in the $n^{th}$ stage compound is given by

$$I_c = d_s + (n-1)\, c_0$$

Since as noted above, the c-axis repeat distance $I_c$, depends on the intercalate and the stage number, n, the $(00l)$ X-ray diffraction from the c-axis repeat distance is a convenient tool for the characterization of the GIC's.



**Figure 4.2:** *The ideal staging phenomenon in GIC's.*
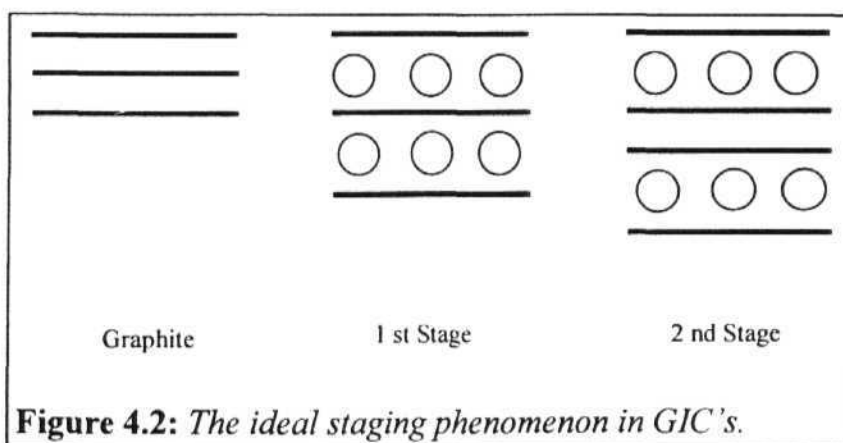
In an ideal staging structure, as explained above, the graphene layers which contain intercalate layers between them and the layers which do not

contain any intercalate layers can easily be distinguished. However it is more likely, as Daumas and Herold[5] have argued, that the intercalate is always distributed in all the graphitic galleries and forms a domain structure [Fig. 4.3]. This could easily explain the absence of a change in diffusion coefficient during a stage transformation, because this model does not require large intercalate migration during stage transformations[6]. This model received further support when Thomas *et al* directly observed[7] a domain structure for graphite-FeCl$_3$ using lattice imaging with a transmission electron microscope.



**Figure 4.3:** *Daumas-Hérold[5] model for the staging phenomenon in GIC's.*
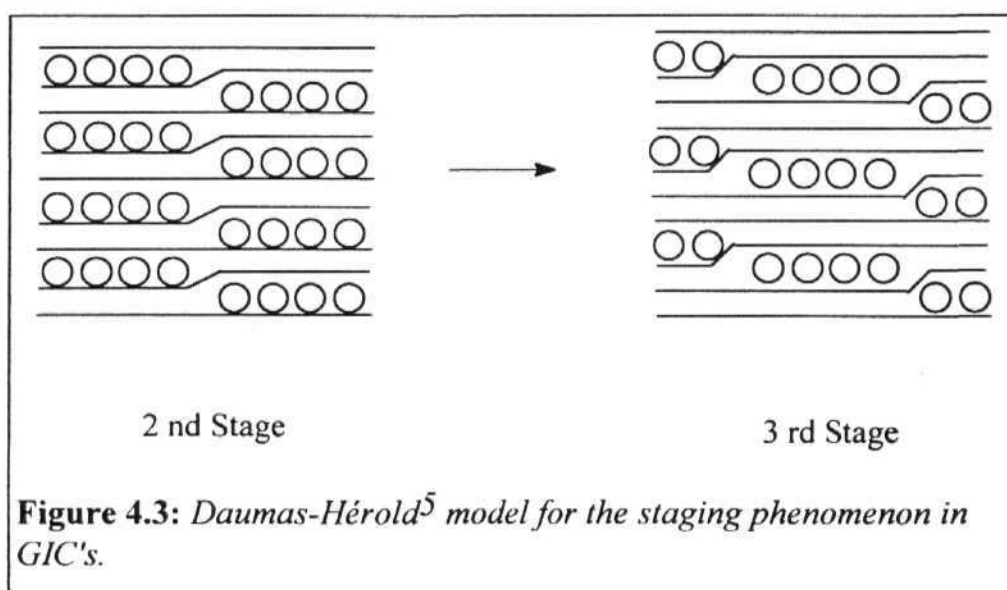
Among the host materials, graphite is unique in that it has both donor and acceptor nature. The direction of charge transfer either from or to

graphite layers classifies GIC's as acceptor or donor-type compounds respectively. This charge transfer modifies the electronic structure of the graphite. One of the significant outcome of this charge transfer is the increased electrical conductivity of many GIC's with respect to graphite. For example, though graphite is a semimetal, the in-plane conductivity of the second stage $AsF_6$-graphite intercalation compound exceeds that of copper metal[8]. Further, the first stage potassium-graphite ($C_8K$), shows a superconducting transition below 1K, even though both pristine graphite and potassium metal do not undergo such a transition[9].

Several paramagnetic species have been intercalated into graphite as part of fundamental research on magnetism and in the search for new magnetic materials. The coexistence of the localized magnetic moments and the conduction $\pi$-electrons of graphite may provide novel systems displaying RKKY[10] type of interactions. The first stage europium-GIC ($C_6Eu$) is an interesting case where magnetic properties of GIC's has been investigated. In this GIC, the interplanar separation, $d_s$, is about 4.87A. Because of this small distance and the strong interaction between conduction electrons of graphite and the $Eu^{2+}$ spins, $C_6Eu$ exhibits antiferromagnetism with Néel temperature of 40 $K^{11}$.

Some of the intensely investigated magnetic GIC's are the binary $CoCl_2$-GIC and $NiCl_2$-GIC and their random mixture graphite intercalation compounds (RMGIC's), namely stage-2 $Co_cNi_{1-c}Cl_2$-GIC's, stage-1 $Co_cMg_{1-c}Cl_2$-GIC's, stage-2 $Co_cMn_{1-c}Cl_2$-GIC's and stage-2 $Ni_cMn_{1-c}Cl_2$-

GIC's, where c is the Co or Ni concentration $(0 \leq c \leq 1)$[12]. Since the second stage $CoCl_2$-GIC and $NiCl_2$-GIC have well-defined magnetic layers these are considered to be good candidates for the 2D-XY system and the magnetic transitions of these compounds are explained by the transition proposed in the 2D-XY system with six-fold anisotropy[13]. The RMGIC's provide a variety of opportunities to study magnetic phase transitions of 2D random spin systems. In the stage-2 $Co_cNi_{1-c}Cl_2$-GIC systems there are ferromagnetic intraplanar exchange interactions between $Co^{2+}$ spin pairs and $Ni^{2+}$ spin pairs[14]. Suzuki *et al*[15] have shown that in the stage-2 $Co_cMn_{1-c}Cl_2$-GIC's, the intraplanar exchange interactions between $Co^{2+}$ spin pairs is ferromagnetic, while the exchange interaction between $Mn^{2+}$ pairs is anti ferromagnetic. The magnetic behaviour of stage-2 $Ni_cMn_{1-c}Cl_2$-GIC's is similar to that of stage-2 $Co_cMn_{1-c}Cl_2$-GIC's, with intraplanar ferromagnetic interactions between $Ni^{2+}$ spin pairs and anti ferromagnetic intraplanar interactions between $Mn^{2+}$ spin pairs[12].

Several organic molecule-alkali metal-graphite intercalation compounds have been reported in literature[16]. But the main focus of these reports has been the catalytic properties of alkali metal-graphite binary intercalation compounds in the dehydrogenation and polymerization reactions of the organic intercalates. Magnetic studies involving organic radical intercalated systems have not been reported earlier.

## 4.2.1 APPROACH TO GIC'S CONTAINING ORGANIC ION RADICALS

Charge transfer complexes of 7,7,8,8-tetracyanoquinodimethane (TCNQ), tetracyanoethylene (TCNE) and 2,3-dichloro-4,5-dicyano-p-benzoquinone (DDQ) have been subjected to detailed studies due to their interesting magnetic properties. We envisioned that if the ion radical salts of these compounds could be intercalated into graphite interesting magnetic interactions between the spins, mediated by the conduction electrons of graphite may be realized. This situation could be very similar to the RKKY type of interactions mentioned above for the transition metal ion-graphite intercalation compounds. The interesting structural features of GIC's *viz.* staging phenomenon and the ability to form ternary intercalation compounds could be utilised effectively to control and vary the intercalate concentration and the conduction electron population in the graphite bands, thereby creating and regulating the various cooperative magnetic interactions. Here, graphite ensures the two-dimensionality of the spin system. There have been few reports of organic radical/radical ion insertion into interlayers of inorganic lamellar compounds. DPPH-saponite clays, DPPH-montmorillonite[17], TTF-MPS$_3$ (M = Fe, Mn and Cd)[18] and N-alkyl pyridinium nitronyl nitroxide-saponite calys[19] are some of them. However, there is no definite role played by these lamellar compounds in mediating the magnetic interactions of the radicals except helping them to form a molecular packing different from that present in their crystalline state. This may be concluded, since all these intercalated materials have shown simple

Curie paramagnetic behaviour. Therefore, graphite with its possible role in mediating the magnetic interactions holds much promise as a unique host lattice compared to other layered inorganic hosts.

Enoki and coworkers have benn investigating the intercalation of oxygen molecule (S = 1) into alkali metal graphite intercalation compounds, where the localized magnetic moments of oxygen molecule coexist with the conduction $\pi$-electrons of graphite and are expected to lead to interesting magnetic material[20]. However, it was found that the delocalized nature of the high density oxygen in graphitic galleries leads to non-magnetic systems[20d].
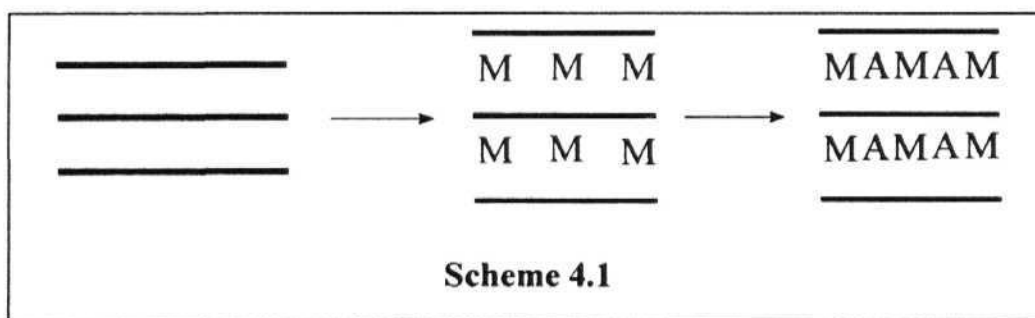


**Scheme 4.1**

We envisaged an approach that involves the intercalation of a suitable electron donor like alkali metal (M) into graphite, followed by the intercalation of a strong organic acceptor (A) [Scheme 4.1]. The electrons donated to graphite in the initial step would be subsequently transferred (partially or fully) to the organic acceptor. The net result would be the

production of the alkali metal-organic acceptor ion radical salt as an intercalate in graphite. Intercalation of a Lewis acid followed by an organic donor would be a parallel approach.

## 4.2.2 EXPERIMENTAL

*Preparation of ternary GIC's*

We have used both HOPG (highly oriented pyrolitic graphite) as well as graphite flakes to prepare the GIC's reported in this thesis. However, most of the detailed studies discussed below have been carried out on the GIC's prepared from HOPG. We chose potassium as the first intercalate because of the following reasons ; (i) K-GIC's are some of the best studied intercalation compounds, (ii) they are relatively easy to prepare and, (iii) potassium is known to form ion radical salts with most of the strong π-acceptors that we were interested in introducing as the second intercalate.

Initially we attempted to prepare potassium-GIC's *via* solution techniques. In this process, potassium and graphite were taken in solvents like dry benzene and refluxed extensively. We also tried the liquid ammonia route where a vacuum line was set up and liquid ammonia distilled over onto the graphite and potassium, kept at low temperature. Both these techniques led to the formation of the second stage $C_{24}K$. The first stage $C_8K$ could not be prepared by these methods. Since we were

interested in looking at different stage GIC's in a consistent fashion, we abandoned these routes.

We next adopted the sublimation of potassium onto graphite in a controlled way to prepare $C_8K$ or $C_{24}K$. Preliminary idea about the formation of either is indicated by the bronze colour of the former and the bluish colour of the latter. Initially we developed a simple 1-pot, 2-stage procedure to prepare the potassium-graphite-organic acceptor compound by modifying the two bulb[21] technique used to prepare the alkali metal GIC's. This method avoids the separate preparation of the reactive K-GIC's. The details of our new experimental procedure are provided below.
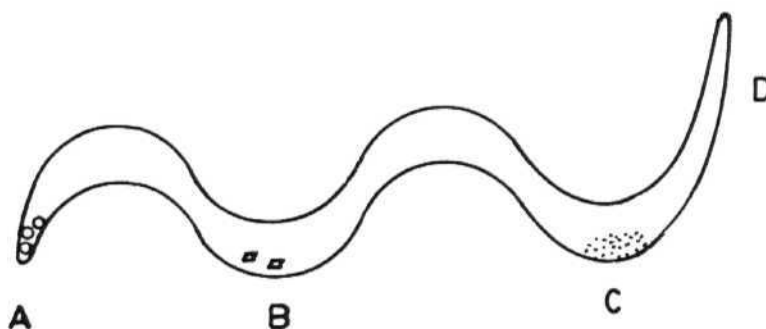


**Figure 4.4:** *Schematic diagram of the bent glass tube used to prepare the ternary GIC''s.*

Freshly cut potassium pieces (always taken in excess), absolutely dried graphite (flakes or HOPG cut into approximately 2 x 1 x 0.5mm pieces) and the recrystallised or resublimed organic acceptor, X, were carefully loaded in that order into the three regions A, B and C of a bent glass tube [Fig. 4.4]. The tube was sealed under vacuum (approximately $10^{-4}$ mm Hg). A kanthal wire coil wound uniformly around the tube in the A-B region was used to heat the potassium and intercalate it into graphite. The temperature around the graphite region was varied using more or less number of turns in the coil, so that the first stage $C_8K$ or second stage $C_{24}K$ can be prepared[22]. The stage of the potassium intercalation into the graphite in this step was monitored by observing the formation of the uniform colour of the K-GIC as stated earlier. The organic acceptor zone, C, was kept at a low temperature with the help of an ice bath through out this step to inhibit the reaction of potassium with the organic acceptor vapours. In the next step the kanthal wire coil was moved to the B-C-D region to sublime the organic acceptor onto the $C_8K$ or $C_{24}K$ formed in the first step. Finally the region B alone was heated for some time to remove any unreacted organic acceptor on the graphite. Time and temperature for heating in both the steps were varied depending on the stage of the potassium-graphite required and optimal conditions were determined based on the reproducibility of the final products. The temperature used to sublime the organic acceptor is generally not more than 250°C and it is a safe assumption that at this temperature the deintercalation of potassium GIC's, a highly activated process does not occur. All the final products

were relatively stabler than the potassium-GIC's but still had to be handled under inert atmosphere.

In order to characterize the intermediate $C_8K$ and $C_{24}K$ we have also carried out the general two zone procedure. In the two zone[21] method the temperatures of graphite and intercalate were regulated at $T_G$ and $T_I$ respectively, ensuring $T_G > T_I$[22].

*Characterization of GIC's*

The general characterisation studies that are done on the above GIC's are the weight uptake, X-ray diffraction and infrared and esr spectroscopy. The weight uptake of the graphite was carefully monitored before and after the intercalation reaction and the weight change was used to estimate the final composition assuming that a uniform first stage or second stage GIC is formed, as the case may be, after the first step. This assumption was validated by stopping some test reactions after the first step and characterising the K-GIC's formed. X-ray diffraction experiments were carried out either on samples ground under a coating of vacuum grease, or on single pieces of HOPG under a coating of apezone grease. IR spectra were recorded with pellets prepared from samples ground with KBr. But the IR spectra always indicated that some moisture was picked up by the samples during the preparation of KBr pellets. For magnetic susceptibility measurments the samples were handled in a glove box with argon

atmosphere and were encapsulated and sealed in a quartz tube, in order to avoid decomposition of the sample.

### 4.2.3 ATTEMPTED INTERCALATION OF TCNQ

Our initial experiments involved the strong organic acceptor TCNQ as the third component in the ternary GIC. When TCNQ was sublimed at around 250°C for nearly 3 hrs. onto CgK, the bronze colour of $C_8K$ changed to a black colour and the product had a rough appearance in contrast to the smooth appearance of HOPG and $C_8K$. The weight increase indicated that the final product had a nominal composition $C_8K(TCNQ)$. Powder diffraction studies showed extremely broadened peaks indicating lack of crystallinity in the product [Fig. 4.5]. ESR signals were symmetric Lorentzian curves, with a linewidth of 0.6 G, very close to that observed for pure $K^+TCNQ^-$· It is necessary to note here that esr signals for all the $C_nK$ compounds as well as compounds[23] having appreciable conduction electron population in the graphite bands show Dysonian type lines. This proves that in the $C_8K(TCNQ)$ compound there is practically no conduction electron population. The variation of esr signal intensity with temperature was investigated for $C_8K(TCNQ)$ and $K^+TCNQ^-$· (synthesised separately following known procedures) for a control study. Both of them were exact reproductions of the spin-Peierl's behaviour reported[24] in $K^+TCNQ^-$·. These results suggest that the $K^+TCNQ^-$· formed probably destroys the graphite's layered structure resulting in an amorphous product which is

finally a physical mixture of the ion radical salt and graphite. A possible
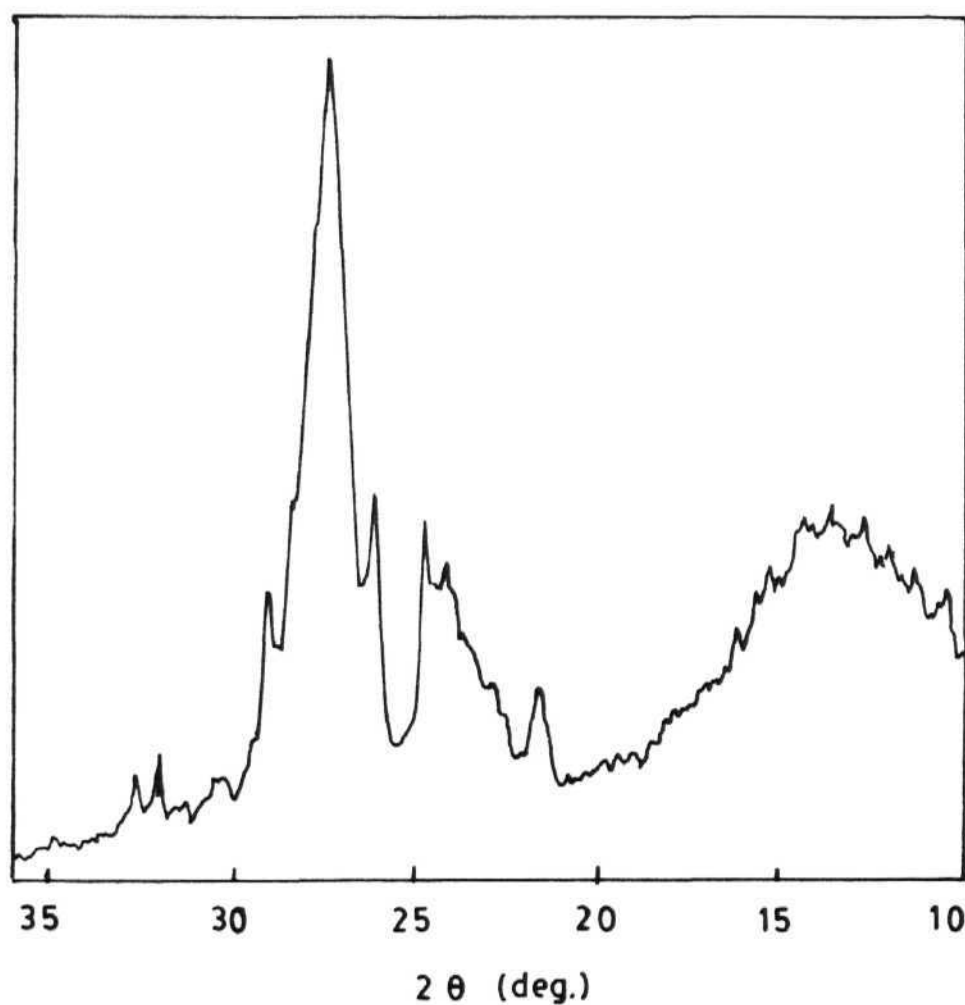reason for the exfoliation of graphite is the large size of TCNQ which



**Figure 4.5:** *Powder X-ray diffraction pattern of C$_8$K(TCNQ).*

cannot be accommodated in the limited space available between the $K^+$ ions present in $C_8K$. Since the graphite galleries appear to be destroyed due to the intercalation of the organic species, TCNQ, we did not pursue the intercalation of other large acceptor molecules such as DDQ and chloranil and instead shifted our attention to the smaller TCNE molecule.

## 4.2.4 TCNE INTERCALATION INTO $C_8K$

TCNE intercalation into CgK resulted in two characterisable stoichiometries, depending on the extent of time CgK is exposed to TCNE vapours. When the sublimation of TCNE onto CgK at 100°C is stopped after 6hrs, the bronze colour of $C_8K$ completely transforms to a dark greenish blue colour. The product shows a weight increase of 70 to 75% from the initial HOPG taken. This corresponds to a nominal composition of $C_8K(TCNE)_x$ with x = 0.22 - 0.26 [sample A]. On sublimation of TCNE for 24 hrs onto CgK, the colour change is, as observed earlier, to dark greenish blue but the net weight increase is about 90 to 95%. The compositions now corresponds to $C_8K(TCNE)_x$ with x = 0.37 - 0.41 [sample B]. It is interesting to note here that when graphite flakes were used the weight increase was always nearly 95%.

The IR spectra of both samples A and B show cyano stretches at 2168 and 2083 $cm^{-1}$, while the cyano stretch[25] of neutral TCNE is at 2200 $cm^{-1}$ and of $K^+TCNE^-$ is at 2190 $cm^{-1}$. Based on the IR data, we believe that TCNE is present as the monoanion in the ternary GIC system and that
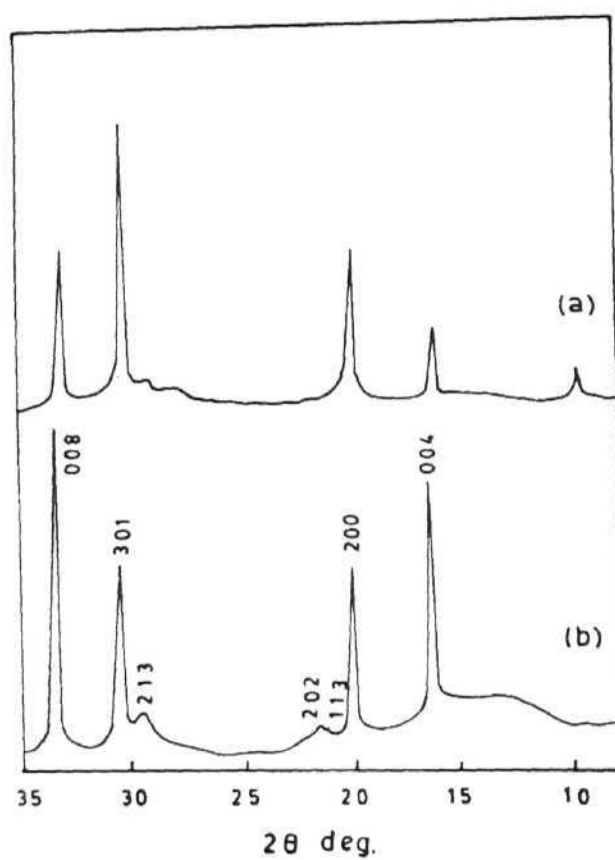
**Figure 4.6:** *Powder X- ray diffraction pattern of (a) Sample A and (b) Sample B.*

the enhanced lowering of the CN stretch frequency seen in these spectra may be due to slight modification of the force constants of this stretching mode in the intercalated state. The formation of TCNE dianion is ruled out since the characteristic vibration of the dianion at 1250 cm$^{-1}$ is completely absent[26].

Powder diffraction patterns of samples A and B were recorded by grinding the samples under a coating of vacuum grease [Fig. 4.6a and 4.6b respectively]. While the peak positions in both the patterns occur at similar angles they differ in their relative intensities. We have analyzed the pattern for sample B by indexing its peak positions to a hexagonal unit cell, assuming that the final product retains the ($A\alpha A\beta A\gamma A\delta$) structure observed for alkali metal GIC's. The peak positions indexed well to a unit cell with cell parameters a = 10.218A and c = 21.038A. Table 4.1 compares the indexing of CgK and sample B. In Fig.4.7 we present a plausible structure of a hexagonal unit cell which is in reasonable agreement with the cell parameters determined above; TCNE is assumed to lie flat with its molecular plane parallel to the graphene sheets, so that the c parameter does not vary much from that in $C_8K$. This phase represented here has a nominal composition of $C_{32}K(TCNE)_3$, which agrees well with the weight increase of 90-95% observed experimentally. However the observed formation of TCNE" can be explained only by invoking an unusual donation of three electrons from $C_{32}K$. The weight increase and diffraction pattern could also be explained by the formation of a mixed phase of composition [CgK + $C_{32}K(TCNE)_3$]. This would also explain the increased intensity of peaks

**Figure 4.7:** *A model structure of* $C_{32}K(TCNE)_3$.
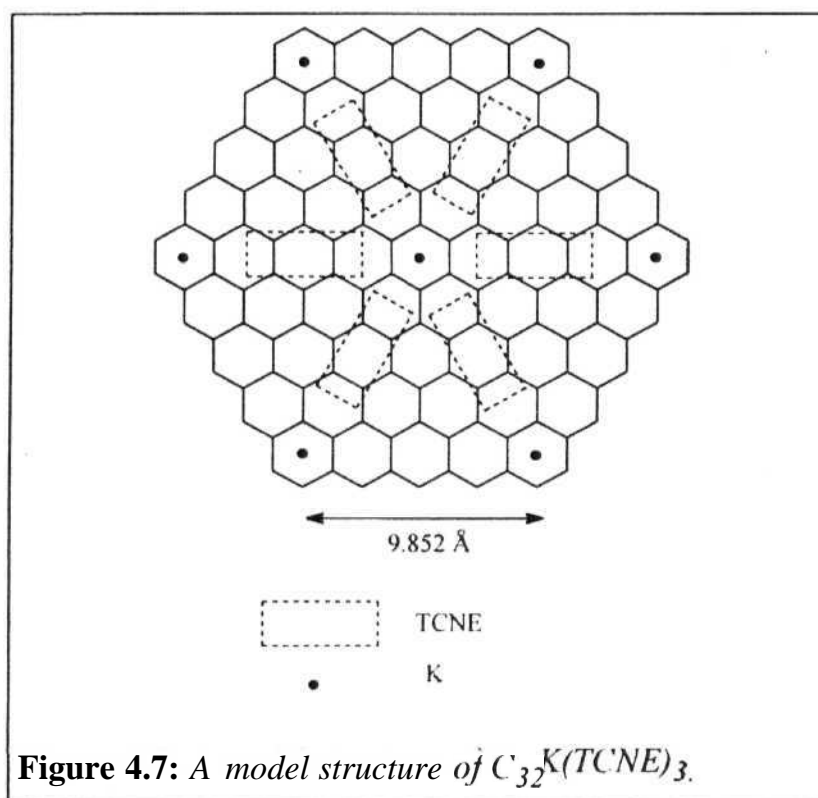
The room temperature esr spectrum of sample A and sample B show typical Dysonian line shapes observed for samples with appreciable conduction electron population. A typical lineshape for sample B at room temperature is shown in Fig. 4.8 (definition of linewidth and A, B parameters are also shown). Table 4.2 lists the parameters both at room temperature and at 150 K for samples A and B and compares these data **with** corresponding to d = 5.28A and 2.63A (assignable to $C_8K$ phase as well[27])

**Table 4.1:** *Indexing of the powder pattern of $C_8K$ and $C_{32}K(TCNE)_3$.*

| $C_8K^{27}$ | | | | $C_{32}K(TCNE)_3$ | | | |
|---|---|---|---|---|---|---|---|
| d Å | *h* | *k* | *l* | d Å | *h* | *k* | *l* |
| 5.40 | 0 | 0 | 4 | 5.26 | 0 | 0 | 4 |
| 2.70 | 0 | 0 | 8 | 4.43 | 2 | 0 | 0 |
| 1.80 | 0 | 0 | 12 | 4.13 | 1 | 1 | 3 |
| 1.35 | 0 | 0 | 16 | 4.08 | 2 | 0 | 2 |
| | | | | 3.02 | 2 | 1 | 3 |
| | | | | 2.93 | 3 | 0 | 1 |
| | | | | 2.63 | 0 | 0 | 8 |
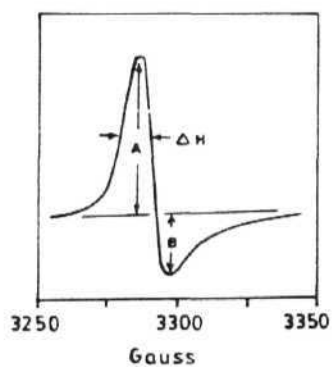


**Figure 4.8:** *Room temperature esr spectra of a typical $C_8K(TCNE)_x$ sample.*

in the powder patterns as one goes from sample A to sample B those available for $C_8K$ in the literature. A comparison of the values for A/B parameters and the linewidths clearly shows the difference between CgK and samples A and B. While there is a considerable decrease in the linewidth for CgK as the temperature is lowered, the line width for sample A slightly increases and the linewidth of sample B remains unchanged. The esr signal intensity which is proportional to the spin susceptibility (noted henceforth as $\chi_{esr}$) can be calculated using the approximation height x (width)$^2$. We note that this approximation has been used[28] for several $KH_x$-GIC's which have similar small A/B parameters. Since there is no linewidth change for sample B the height of the signal is taken as a measure of $\chi_{esr}$. The variation of $\chi_{esr}T$ as a function of temperature for sample A and

Table 4.2: *Comparison of g value, line width and A/B parameters of Sample A and B with C'$_8$K.*

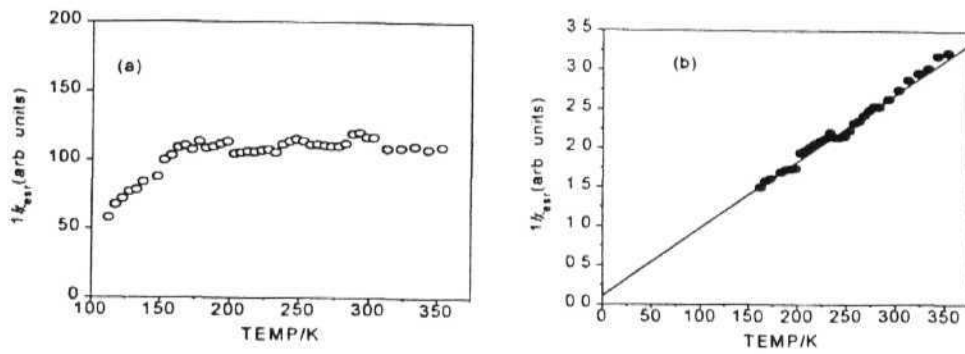| Compound | 298 K | | | 150 K | | |
|---|---|---|---|---|---|---|
|  | g | AH (G) | A/B | g | AH(G) | A/B |
| $C_8K^{23}$ | 2.0016 | 11.4 | 2.5 | - | 6.1 | 3.3 |
| A $C_8K(TCNE)_{0.23}$ | 2.0037 | 6.5 | 2.9 | 2.0013 | 7.5 | 3.1 |
| B $C_8K(TCNE)_{0.38}$ | 2.0026 | 8.5 | 2.2 | 2.0012 | 8.5 | 2.5 |

**Figure 4.9:** *The (a) $\chi_{esr}T$ v$T$ and (b) $1/\chi_{esr}$ vs $T$(350 - 150K) plots of sample A; least square fit to Curie-Weiss law is shown.*
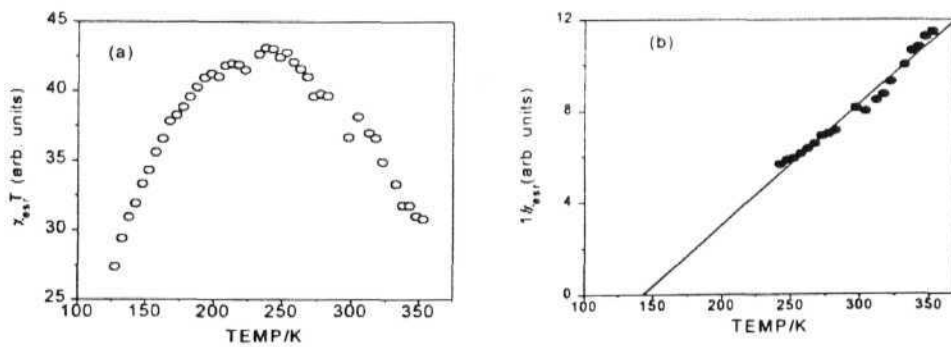


**Figure 4.10:** *The (a) $\chi_{esr}T$vs $T$ and (b) $1/xesr$ vs $T$ (350 - 240Kplotsof sample B; least square fit to Curie-Weiss law is shown.*

sample B are given in Fig. 4.9(a) and Fig. 4.10(a) respectively. The intensities were reproducible under temperature cycling proving the sample stability during the experiment and absence of any hysterisis behaviour. The features were confirmed by repeating the experiment on several samples. It is worth noting here that the esr signal intensity for CgK. decreases continuously as the temperature is lowered[29].

The $\chi_{esr}$ for sample A follows within experimental error, the simple Curie paramagnetic behaviour from 80°C to -110°C, in contrast to the gradual decrease in signal intensity reported for CgK. The $1/\chi_{esr}$ *vs* temperature plot which confirms this is shown in Fig. 4.9(b). However, below -110°C. the intensity saturates and then slowly decreases. We note that the magnetic susceptibility of $CoCl_2$-GIC and $NiCl_2$-GIC have been reported to follow a similar behaviour at low temperatures[30]. The esr intensity behaviour of sample B is more interesting. Here, there is a sharper increase in $\chi_{esr}$ from 80 to -30°C following a Curie-Weiss behaviour. The plot of $1/\chi_{esr}$ w T shows a positive $\theta$ of 120 - 150 K [Fig. 4.10(b)]. This range of 0 was obtained from the several samples studied. Below -30°C the signal intensity becomes constant and then decreases as observed for sample A. The data in this region could be fitted to a single-triplet two level behaviour with $\Delta E_{ST}$ ($E_T$ - $E_S$) = 250 K which indicates antiferromagnetic coupling of dimeric spins in the low temperature regime. The above facts clearly show that the ternary potassium-graphite-tetracyanoethylene intercalation compounds are markedly different from the parent binary compound $C_8K$. We discuss possible explanations for this unusual

magnetic properties of an organic radical-based intercalation material, after presenting the results on $C_{24}K(TCNE)_x$ below.

As mentioned earlier, there were questions of the extent of homogeneous intercalation of TCNE into $C_8K$, since the diffraction data could be explained on the basis of mixed phases as well. To investigate this aspect, the ternary compound HOPG sample was cleaved along the plane perpendicular to the c-axis keeping the sample inside a glove box, it showed the $C_8K$ bronze colour inside the sample, indicating that the product formed is inhomogeneous. However, when the sample was coated with apezon grease and mounted for (*00l*) diffraction study with the top surface facing the X-rays, the diffraction pattern showed some new peaks indicating the formation of a new phase at least on the surface. Detailed *in situ* (*00l*) diffraction study over extended time periods would be needed to follow the intercalation process in greater detail and arrive at the optimal conditions needed to obtain a homogeneous product.

The probable reason for the inhomogeneous intercalation of TCNE into $C_8K$ is the high density of potassium ions which perhaps hinders the entry of TCNE ions. Since the samples do not appear to be homogeneous it would be premature to attempt a detailed analysis of the ferromagnetic coupling of spins observed in sample B. However, the effect observed is very interesting and warrants more detailed research on this class of compounds. Therefore we decided to probe in greater detail the intercalation of TCNE into $C_{24}K$, which has a lower density of $K^+$ ions.

## 4.2.5 TCNE INTERCALATION INTO $C_{24}K$

This reaction also was carried out initially, following the similar procedure as for $C_8K(TCNE)_x$ compounds described above without isolating the intermediate phase of $C_{24}K$. The final weight changes could be interpreted as corresponding to the composition $C_{24}K(TCNE)$. This material showed slightly asymmetric esr signals with an A/B value of 2.4 at room temperature which decreased to 1.7 at 150 K. The linewidth was large (15G) and temperature independent. These properties were in contrast to those reported for $C_{24}K$ which has a narrow linewidth of 2.8 G and large A/B value of 5.5 at room temperature. The strong decline in A/B again indicated the transfer of conduction electrons from the K-GIC to TCNE. Variable temperature esr studies indicated that the signal intensity remained nearly constant down to -100°C in contrast to the decreasing signal intensity of $C_{24}K$. Since, as in the previous case of $C_8K$-TCNE reaction, we were not certain about the phase composition, we have carried out a multistep procedure to prepare these compounds and measured magnetic susceptibility to lower temperature regions.

$C_{24}K$ was obtained from the $C_8K$ which in turn was prepared using the standard 2-bulb method. The $C_8K$ was characterised by its powder diffraction pattern [Fig. 4.11 (a)], which is in agreement with the reported one[27]. It was annealed[31] with graphite at 350°C for 48 hrs. in a sealed tube when the following reaction takes place.

$$C_8K + 16C \quad \rightarrow \quad C_{24}K$$

$C_{24}K$ formed was characterised by the X-ray diffraction pattern [Fig. 4.1 l(b)j which matches very well with the known data[27]. The $C_{24}K$ thus prepared was exposed to TCNH vapours at 85°C for 48 hrs. in a sealed tube.
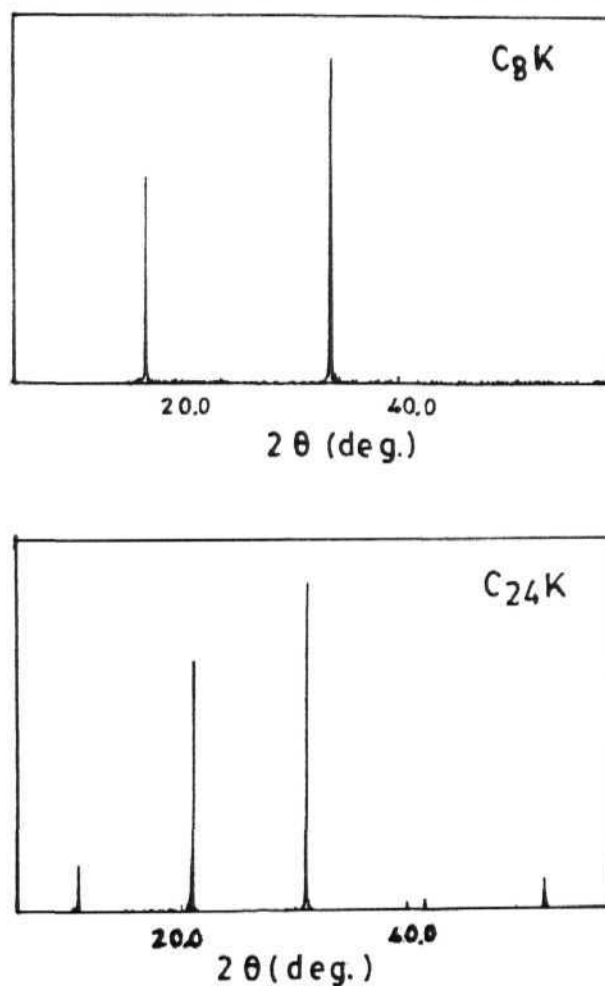


Figure 4.11: *The (00l) X-ray diffraction pattern of (a) $C_8K$ and (b) $C_{24}K$.*
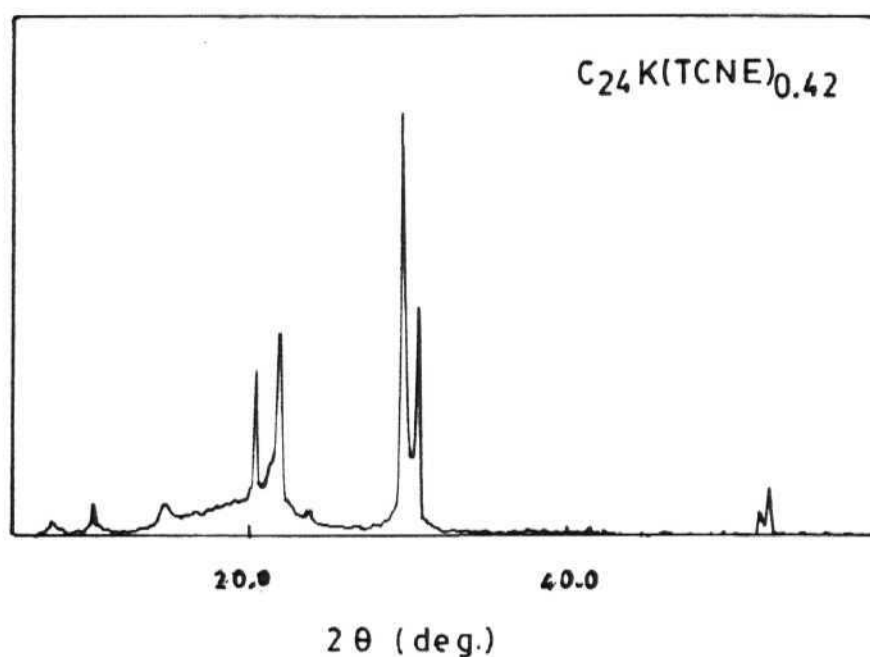
**Figure 4.12:** *The (00l) X-ray powder pattern of C$_{24}$K(TCNE)$_{0.42}$.*

The blue colour of C$_{24}$K turned to a greenish shade. The (*00l*) X-ray pattern |Fig. 4.12] showed a set of peaks with a repeat distance of 11.7Å, in addition to the C$_{24}$K peaks. It may be noted that the I$_c$ in C$_{24}$K is 8.4 A. The weight uptake corresponds to a composition C$_{24}$K(TCNE)$_{0.42}$. This indicates that the product from our single-pot method mentioned earlier might not be exactly the composition inferred there. The magnetic susceptibility studies were carried out parallel to the c-axis. $\chi$ was
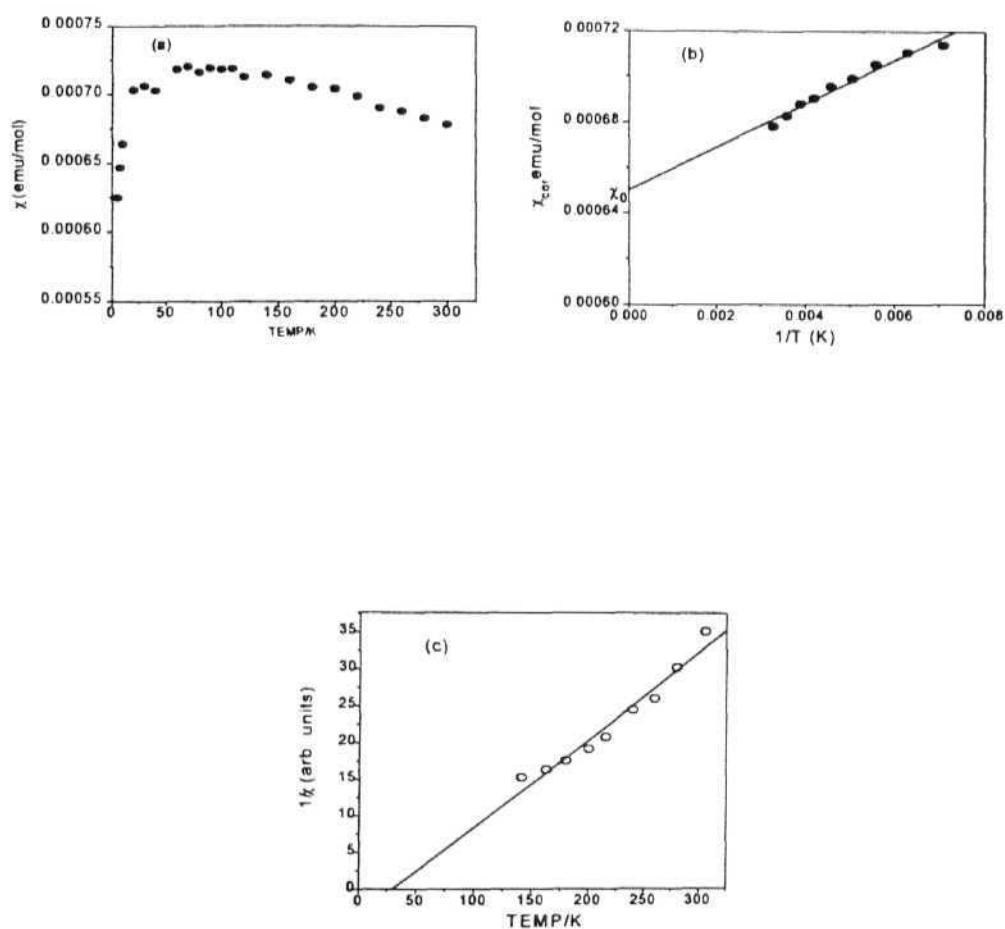
**Figure 4.13:** *The (a) $\chi$ vs T for the full temperature range (b) $\chi$ vs 1/T and (c) 1/(x-X()) vs T in the temperature range 300-140 K for $C_{24}K(TCNE)_{0.42}$.*

estimated from M *vs* H plots for H in the range 10kG. Diamagnetic corrections using Pascal's constants for the composition mentioned above was applied. The susceptibility variation with T for $C_{24}K(TCNE)_{0.42}$ is shown in Fig. 4.13. While it was reported[32] that the susceptibility of $C_{24}K$ remains constant in the temperature region 300 K - 50 K, the susceptibility of $C_{24}K(TCNE)_{0.42}$ clearly shows an increase before it starts saturating and then decreasing at low temperatures. The initial rise in the susceptibility clearly proves the presence of localized magnetic moments in addition to the conduction electrons present in $C_{24}K$. $\chi_0$, the susceptibility at infinite temperature was determined by extrapolation of the $\chi$ *vs* 1/T plot [Fig.4.13(b)]. The spin only magnetic susceptibility ($\chi-\chi_0$) is plotted as 1/($\chi-\chi_0$) *vs* T in the temperature region 300-140 K in Fig.4.13(c) and shows that the susceptibility follows a Curie-Weiss behaviour with a positive Weiss constant of 29.4 K which indicates the ferromagnetic exchange between the localized magnetic moments. This result is qualitatively similar to the esr result obtained for the inhomogeneous $C_8K$ described earlier and the $CoCl_2$-GIC and $NiCl_2$-GIC reported by earlier workers[30]. The susceptibility for all the samples show strong decline at very low temperatures indicating the onset of antiferromagnetic interactions. We have not come across any reports on the magnetic susceptibility studies or variable temperature esr studies on $K^+TCNE^-$. Due to the extreme reactivity of this material, our attempts at isolating and studying $K^+TCNE^-$ in solid state were also unsuccessful. However, we expect that the coupling between $TCNE^-$ spins will be antiferroamgnetic as a result of the kinetic exchange[33] interactions commonly seen in simple organic ion radical/CT

salts. Hence it appears that the $K^+TCNE^-$ formed inside graphite behaves in an unusual way different from $C_nK$ and $K^+TCNE^-$. It is possible that the itinerant graphite conduction electrons mediate a superexchange interaction between the localized spins of $TCNE^-$. The mean free path of these conduction electrons would be sensitive to changes of temperature thereby changing the spin coupling they mediate. This could explain why the samples exhibit simple paramagnetic (recall sample A of $C_8K(TCNE)$) or ferromagnetic behaviours at higher temperature regimes, and anti ferromagnetic interactions at low temperatures. An alternate explanation to this unusual magnetic behaviour may be given in terms of two different exchange interactions, (i) a short range ferromagnetic, within a layer leading to small magnetic islands and (ii) a longer range anti ferromagnetic interaction across layers. Such models have been used to explain similar magnetic behaviour observed in second stage Ni and Co chloride GIC's[30c]. Detailed studies of the electrical properties would be useful to understand in greater detail, the electronic structure and magnetic properties of our novel ternary systems. Even though the ternary K-graphite-organic acceptor systems arc much stabler than the parent K-GIC's, they still are not amenable to routine experimental procedures. Handling the materials in controlled atmosphere is necessary. This makes extensive experimentation on these systems difficult.

Recently there were reports of modelling studies on graphite intercalation compounds using semiempirical and *ab initio*[34] calculations on small cluster units. Some efforts are already under way in our laboratory to

model the systems we studied above, using semiempirical and *ab initio* computations to understand the basis for spin interactions in these systems[35]. Our AM1/CI calculations on model systems like anthracene and TCNE and DDL anions described in Section 3.2 also give some clues about the spin polarisation and spin coupling that may be operational in these systems.


## 4.3 GRAPHITE INTERCALATION COMPOUNDS OF ORGANIC DONORS

As indicated earlier, studies on Lewis acid-graphite-organic donor ternary intercalation systems would be a parallel approach to the one described in the previous Section. As noted earlier, graphite acts as electron acceptor or donor in the various binary intercalation compounds. There are many reports of graphite-Lewis acid intercalation compounds. The systems that have particularly attracted our attention, for further intercalation studies of organic donors are graphite-bromine, graphite-perchlorate, graphite-terafluoroborate and graphite-hexafluorophosphate, since these intercalate species can form charge transfer salts with typical organic π-electron donors. The graphite-bromine system is known to lose bromine as soon as it is removed from the bromine atmosphere. Hence we focussed our attention on the other systems. This Section describes our attempts to synthesize "graphite-organic donor-CT salt" ternary systems. Though we were able to devise simple approaches to the intercalation of the Lewis

acids, we were unsuccessful in subsequent intercalation of the organic donors into these binary systems. Therefore, the results presented in this Section are significant only in terms of graphite intercalation chemistry and not in terms of novel magnetic systems.

There have been several procedures described in the literature for the synthesis of binary intercalation compounds with graphite as the electron donor. The typical procedures used to prepare intercalation compounds of metal halides, $MX_n$, involve the use of a strongly oxidizing atmosphere of $X_2$, the relevant halogen gas. Electrochemical methods are used to prepare the other Lewis acid intercalation compounds but still they are also carried out in presence of strong acids[36] or the more reactive nitrosonium salts[37]. We developed a simple and mild electrochemical procedure to prepare the Lewis acid-graphite intercalation compounds that we are interested in, using the respective tetrabutylammonium salts as the electrolyte. The general procedure to prepare these compounds is described below.

In a 'TT shaped electrochemical cell a weighed specimen of a piece of HOPG ($2 \times 1 \times 1$ mm) formed the anode plate. A copper wire inserted into the HOPG and held in place by drop of molten wax, provided the electrical connection. A 1M solution of the appropriate electrolyte in dry dichloromethane was taken in the cell so that it just covers the HOPG piece [Fig. 4.14]. A platinum wire formed the cathode. A constant current of ~ 100 $\mu$A was passed through the electrolyte for about 6 hrs. using a Keithly Model 224 Constant Current Source. The colour of the graphite piece

turned to blue indicating the formation of a second stage Lewis acid-graphite species. After the electrolysis, the graphite was carefully removed from the copper wire; the wax drop is easily removed, and the GIC was washed several times with dichloromethane and dried at room temperature under vacuum. The net weight increase normally conforms to the formulation $C_{20}X$. This indicates that most likely a second stage compound is formed along with intercalation of some solvent (a normal second stage



**Figure 4.14:** *H-shaped electrochemical cell used for the preparation of Lewis acid-Graphite intercalation compounds.*
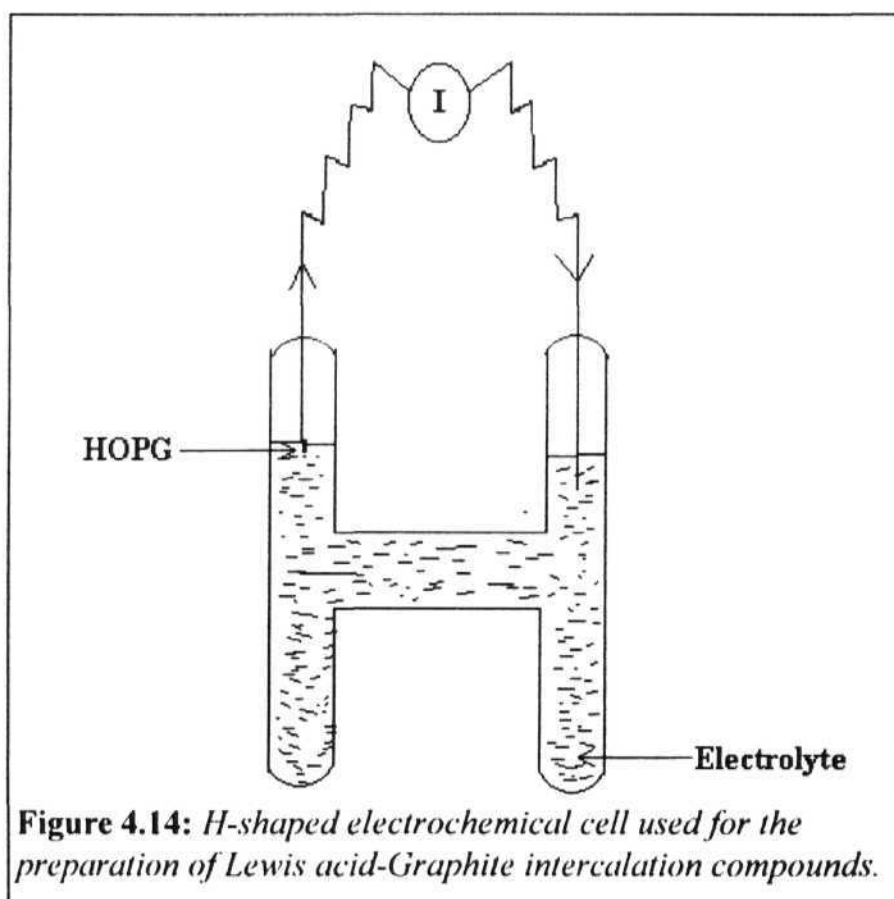
compound would correspond to $C_{24}K$, and hence a lower % increase in weight).

We have carried out the intercalation of three ions, tetrafluoroborate ($BF_4^-$), perchlorate ($ClO_4^-$) and hexafluorophosphate ($PF_6^-$) using the respective tetrabutylammonium salts as the electrolyte. We note that though the former two have been studied in some detail earlier[36], the latter one has not been subjected to any serious investigation. The products are quite air-stable and the IR spectra could be recorded [Fig. 4.15]. The IR spectra clearly showed the presence of the X" ions intercalated. Esr spectra of the GIC's were recorded. The parameters observed for the room temperature spectra of these compounds are provided in Table 4.3. Strong assymetry is found only in the case of the perchlorate-GIC.

**Table 4.3:** *Room temperature esr parameters of Lewis Acid - GIC's'.*

| Compound | A/B | line width (G) |
|----------|-----|----------------|
| GIC-BF$_4$ | 2.6 | 3.5 |
| GIC-ClO$_4$ | 11.0 | 3.5 |
| GIC-PF$_6$ | 2.3 | 3.0 |

Subsequent attempts to intercalate organic donors such as tetrathiafulvalene (TTF) and N,N,N',N'-tetramethyl-1,4-phenylenediamine (TMPD) by sublimation onto the Lewis acid GIC's always resulted in
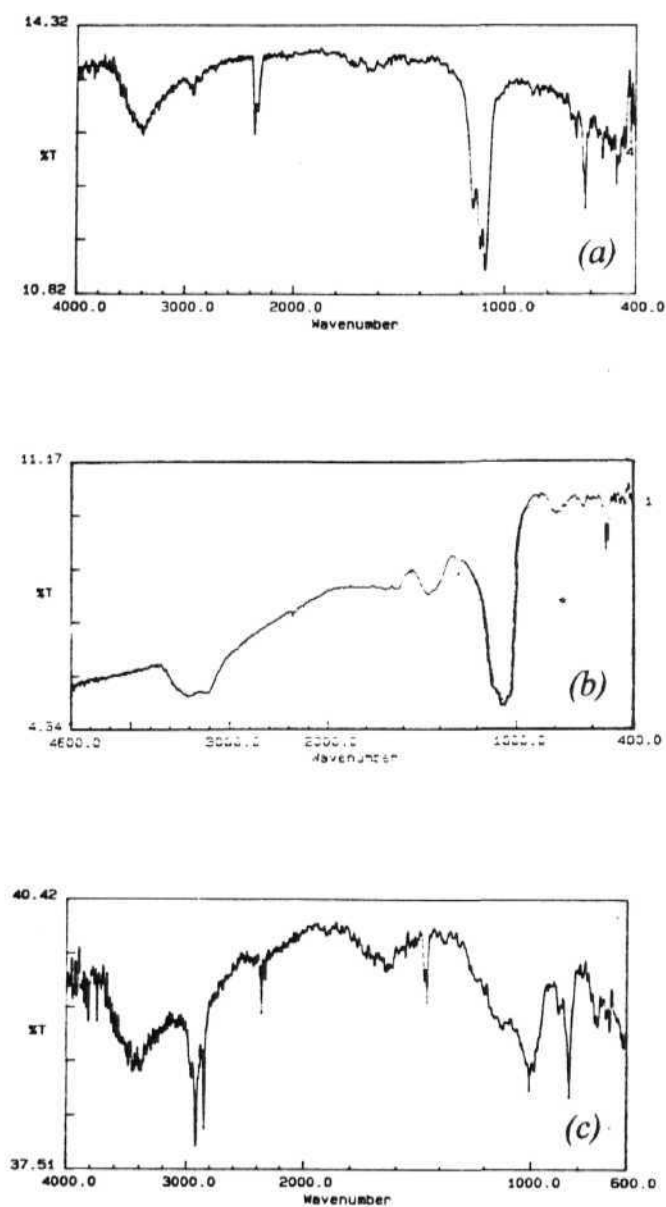
**Figure 4.15:** *IR spectra of $ClO_4$ '(a), BF4' (b) and $PF_6^-$ (c) intercalated second stage GIC's.*

exfoliation of the graphite.  This appears to result from the decomposition of the intercalated anions and expulsion of the gaseous products from the graphite galleries at the higher temperatures (70°C or higher) used for organic donor intercalation.  Attempts were made to intercalate the organic donors in solution; however the intercalated anions leached out forming the organic donor - anion charge transfer complexes in the solution rather than as intercalates inside graphite.  Thus our attempts to prepare the ternary organic donor intercalated GIC's as a parallel class of materials to the organic acceptor intercalated GIC's, was not successful.   However, the present work was useful in developing a convenient procedure for the preparation of second stage Lewis acid - GIC's.

## 4.4 ORGANIC FREE RADICALS IN NONGRAPHITIC HOST LATTICES

Above we have described our investigations on organic ion radicals intercalated into the graphite host lattice, which could mediate the spin interactions between the paramagnetic dopants.   Interesting cases of localized spins interacting in unusual ways have been observed in the $KC_nTCNE$ systems.  We have mentioned in Section 4.2.2 about the several reports on the insertion of organic free/ion radicals into various noninteracting media such as saponite clays and other inorganic lamellar compounds.  These host lattices only provide a medium where the guests are in a different environment than in their bulk state.   We were also

interested in investigating the nature of spin interactions of organic free radicals between the extreme limits of isolated molecules in solution and the bulk crystalline state. For this purpose we identified various matrices such as silica gel, polymers like polystyrene which form good films and the conducting polymers such as poly(3-hexylthiophene) (PTP) and polyphenylacetylene (PPA). It was expected that the first two hosts would be generally inert spectators and the conducting polymer host may perhaps exert some influence on the magnetic interactions of the radicals embedde within. One can also imagine that the host matrix may have an indirect influence on the magnetic interactions by inducing a specific arrangement of the radical species with respect to each other so that novel direct spin interactions may be achieved, which are not possible in the pure crystalline state. Spin dilution could however, be a detrimental factor from the point of view of fabrication of a magnetic material.

The first approach we attempted was the insertion of free radicals in silica gels prepared through the sol-gel technique. Tetraethylorthosilicate (TEOS) is known to form gels when hydrolysed with catalytic amounts of acid/base[38]. We had come across an interesting report where Cu(II) spins were included in silica gels through this technique and very interesting magnetic properties including ferromagnetic transition and hysterisis for Cu(II) based materials was observed[39]; there was no clear information on the structural aspects however. We prepared silica gels using a similar technique with the stable organic free radical, diphenylpicrylhydrazide (DPPH) as the dopant. TEOS was hydrolyzed by adding to it a mixed
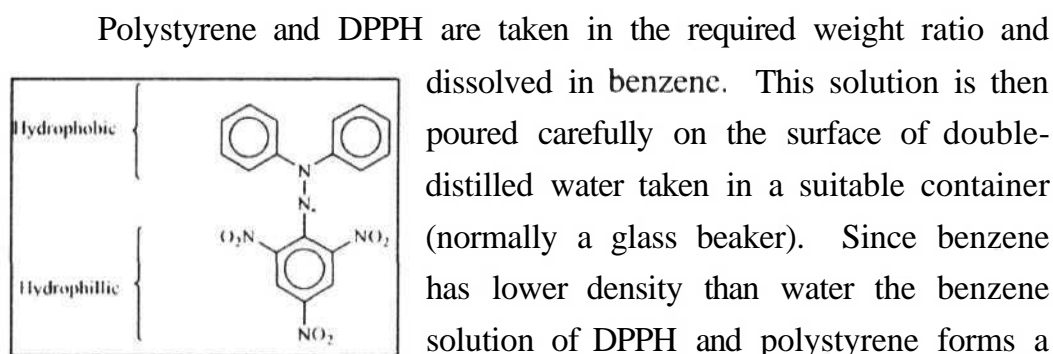
solution of $H_2O$, $C_2H_5OH$ (typically the $TEOS:C_2H_5OH:H_2O$ molar ratio was 1:5:5) and a few drops of acid or base. Required amount of DPPH in $CH_3CN$ was added. Brown clear glasses were obtained after a weeks time. This colour suggested that the DPPH is being partially destroyed, since pure DPPH has a dark violet colour. We have taken ground samples of the glass and recorded the esr spectra which showed very weak signals and the intensity corresponds to approximately 3% spin retention during the glass formation. When the glass is heated in ethanol, free DPPH gets extracted out, and the esr spectra of the solution indicated that small amounts of DPPH remains intact. Two explanations are possible for the low spin concentrations observed in these silica glasses : i) the acid used in the hydrolysis has reacted with the free radical and destroyed the free spins or (ii) DPPH reacts with the free Si-0 bonds while the gel is being formed thereby forming covalent bonds and destroying the spins. We therefore repeated the gel formation without using the acid catalysis, utilising only water and alcohol in the process. However again the glasses formed had very low spin concentrations indicating that probably the second mechanism is in operation. Since the spin species are largely destroyed in the gel formation process, we did not pursue further these materials.

We next turned our attention to the conducting polymers. These systems when doped with free radicals could be visualised as being somewhat similar in nature to the graphite intercalation compounds, since the possibility of the conduction electrons of the host matrix mediating the magnetic interactions exists. However, various attempts made to grow

homogeneous films of conducting polymers with organic radicals incorporated within were not successful. For example, we attempted the doping of TCNE into PTP hoping that TCNE ion radicals could form by electron donation from the conducting polymer. Only black powder materials which were paramagnetic could be obtained. Another experiment we tried was the doping of $Li^+TCNE^-$ salt in PPA. Again good films could not be obtained.

Since one of the difficulties with the conducting polymers was the formation of good uniform films we concentrated our studies on the popular film forming polymer polystyrene. We chose DPPH as the spin species. Conventional film growing techniques like dissolving the polymer and dopant in an organic solvent and slowly evaporating the solvent were tried initially. However, this procedure does not allow sufficiently large concentrations of the dopant to be included in the film which is essential to initiate strong magnetic exchange between DPPH radical species. When DPPH and polystyrene are dissolved in benzene and the solvent slowly evaporated good quality, homogeneous films formed only if the DPPH concentration did not exceed 20% by weight of the polystyrene. Esr spectra of these films showed the well-known 5-line hyperfine structure of DPPH indicating that the exchange between DPPH spins is still very poor and that the radicals exist almost as though they were in dilute solution. We developed a very simple procedure which allowed us to include sufficiently higher concentrations (up to 50%) necessary to observe exchange couplings of DPPH in polystyrene. This simple technique involved the formation of

the film on water surface.  The detailed procedure to prepare these films is given below.

Polystyrene and DPPH are taken in the required weight ratio and dissolved in benzene.  This solution is then poured carefully on the surface of double-distilled water taken in a suitable container (normally a glass beaker).  Since benzene has lower density than water the benzene solution of DPPH and polystyrene forms a layer on top of the water surface.  Benzene is now allowed to evaporate slowly producing the polystyrene film with the required concentration of DPPH on the water surface.  Dark violet films of DPPH-doped polystyrene were formed.  We believe that the DPPH molecule with its hydrophilic picryl moiety is held at the water-benzene interface, allowing higher concentration of DPPH to be distributed in the polymer film as it is formed. The C, H and N analysis of three representative films containing 20%, 30% and 40% DPPH are given in Table 4.4.  Though the agreement between the observed and expected values is not perfect, the deviations are small (maximum 1.2%).  The small discrepancies may be arising due to the inclusion of traces of benzene and/or water.  The important point is that the expected amount of DPPH is present.  This was supported by esr spectroscopic studies on the films with relatively low concentrations of DPPH where spin interactions between the radicals is negligible.  The spin concentration of the films was checked by quantitative comparison of the
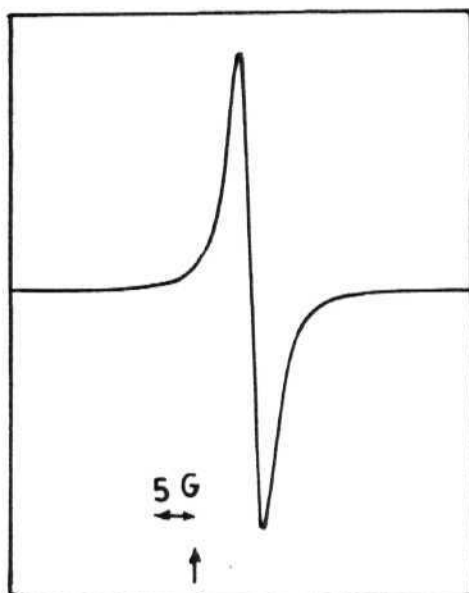
**Figure 4.16:** *Room temperature esr spectrum of pure crystalline DP PH.*
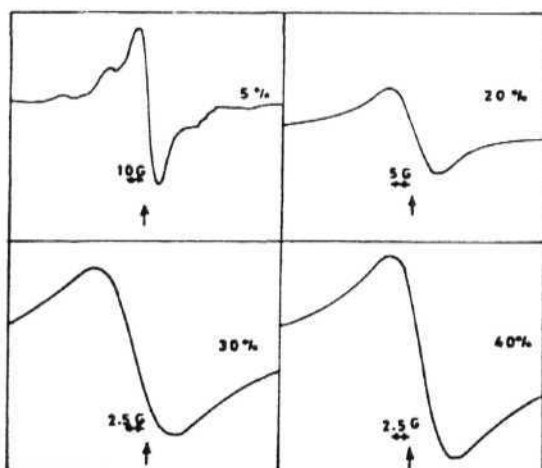


**Figure 4.17:** *Room temperature esr spectra of DPP H-doped polystyrene films at 5%, 20%, 30% and 40% doped levels.*

esr signal intensity with a standard sample of pure DPPH. Expected amount of DPPH was observed in the films within experimental error, indicating that the radicals did not undergo any decomposition during the film formation.

**Table 4.4:** *Comparison of expected and observed C,H, N % in DPPH-doped films.*

| Compound | | %C | %H | %N |
|---|---|---|---|---|
| 20% | Expected | 86.82 | 6.17 | 2.95 |
| | Observed | 86.85 | 7.33 | 2.16 |
| 30% | Expected | 84.0 | 5.93 | 4.08 |
| | Observed | 85.01 | 7.14 | 3.02 |
| 40% | Expected | 82.26 | 5.73 | 5.06 |
| | Observed | 83.11 | 6.86 | 3.98 |

The magnetic properties of these films were investigated by variable temperature esr experiments. The room temperature esr spectra of four specific compositions are provided in Fig. 4.17 along with that recorded for a sample of pure crystalline DPPH [Fig. 4.16]. The hyperfine structure observed for the films at lower *viz. 5%* concentration is clearly seen. The 20% film indicates the collapsing of the hyperfine structure showing that there is some exchange coupling developing between the DPPH spins. However, the exchange interaction in 20%, 30% and 40% is very different

from the very strong exchange present in the bulk solid as can be seen from the line widths. The esr intensity w temperature for the 5%-doped sample follows the Curie law and all the other concentrations studied follow the Curie-Weiss law, with negative Weiss constants (0) [Fig. 4.18]. In Table 4.5 we compare the AH and 0 for the four DPPH-doped films with that of a pure sample of DPPH we have analysed. We note here that the esr spectra of DPPH is known to be strongly influenced by the solvents used to recrystallise it[40]; the data we have presented were obtained on DPPH we have purified by recrystallisation from benzene. The variation of the intensity of the central line was taken as representative of the total intensity variation in the 5%-doped sample (this linewidth does not change much with T), while the intensity using the approximation $(height)x(width)^2$ was used in the case of samples with other concentrations.

**Table 4.5:** *Esr line widths and Weiss constants observed for pure solid-DPPH and DPPH-doped polystyrene films.*

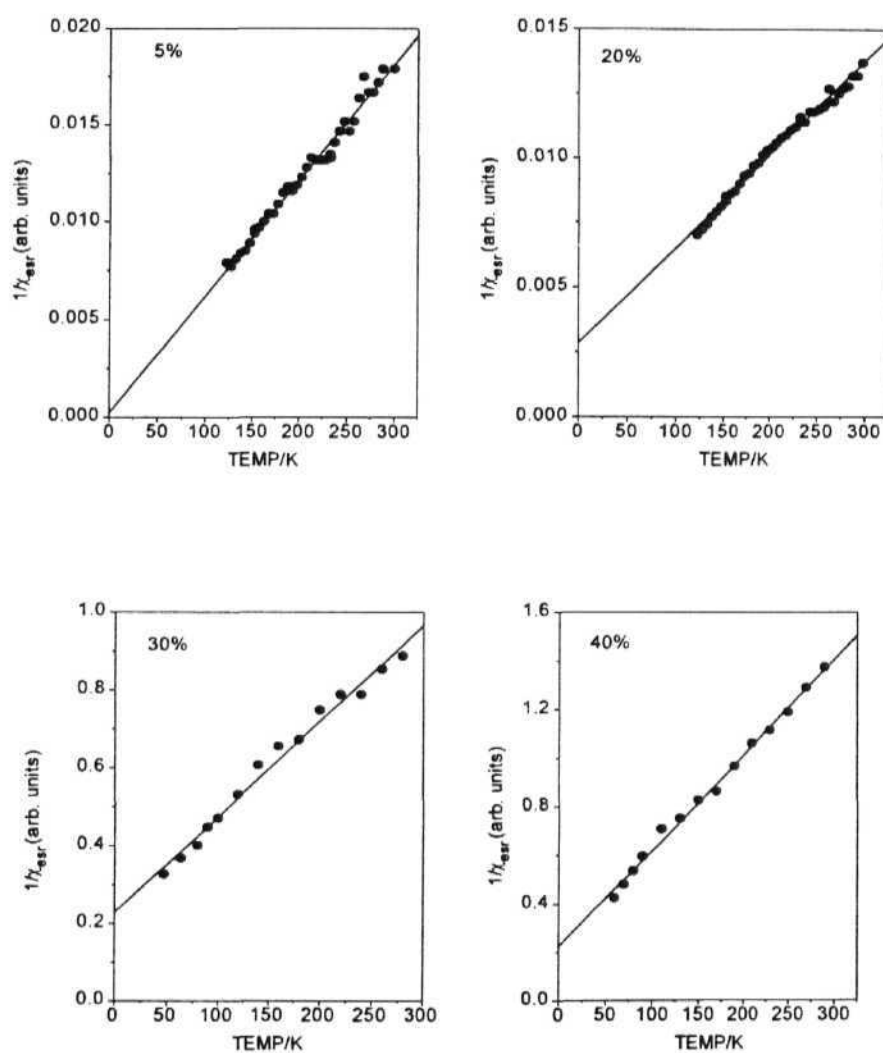| Compound | linewidth (G) | Weiss Constant (°) |
|---|---|---|
| DPPH (solid) | 2.5 | -36.8 |
| 5% | 9.5 | -5.3 |
| 20% | 12.5 | -70.5 |
| 30% | 9 | -92.6 |
| 40% | 6.5 | -50 |

**Figure 4.18:** *1/$\chi_{esr}$ plots of 5%, 20%, 30% and 40% DPPH doped polystyrene films; the lines are the best fits to Curie-Weiss law.*

From the Weiss constants it is clear that the bulk solid, with a very strong exchange coupling, follows a Curie - Weiss law with a moderate antiferromagnetic coupling in accord with earlier reports[41]. The 5%-doped film behaves as perfect Curie paramagnet within experimental error. The 20%, 30%-doped films show moderately strong antiferromagnetic coupling as shown by the high Weiss constants. In the case of the 40%-doped film the magnitude of the antiferromagnetic coupling decreases slightly. The esr linewidths continuously decrease with increasing concentrations of DPPH. From the above observations we come to the following conclusions. DPPH in its pure bulk state behaves like a weak antiferromagnet with a small negative Weiss constant. When very low concentrations of DPPH are included in polystyrene the radicals are isolated in the polymer matrix with no interaction between them and the behaviour is, as expected, that of a perfect Curie paramagnet, within experimental error. When the concentration of DPPH is increased in the film there is antiferromagnetic exchange between the DPPH spins, very different from the interactions in its bulk state; this reaches a maximum at 30% doping levels. As the concentration is further increased the behaviour tends towards the bulk solid again. The variation in esr linewidths is in agreement with the above description. However, the nature and mode of the antiferromagnetic coupling within the polymer at concentrations in the range 20 - 30% is not completely clear since the structure of the DPPH in polystyrene is not understood. It is possible that the method of preparation of these films at the water-benzene interface leads to some local ordering of the DPPH molecules and some new mechanism of spin interaction between DPPH

radicals occurs. A possibility is that the phenyl groups of the polystyrene mediate the spin interactions. At higher concentrations, clusters of DPPH may form that start showing the bulk crystalline effects. Detailed microscopic techniques like scanning tunnelling microscopy or atomic force microscopy may provide some important clues in this direction.

These studies highlight a simple approach to the inclusion of organic radicals in high enough concentration in a host matrix that allows novel magnetic interactions to be initiated. We have investigated the DPPH-polystyrene system in some detail. Unusual magnetic interactions which are different from that seen in the pure crystals of DPPH are observed. Structural information on the host-guest systems would greatly help in understanding these magnetic properties. Studies of this kind can be extended to other radicals like the popular p-nitrophenyl nitronylnitroxide (NPNN). We have made preliminary attempts in this direction; however, technical problems like finding appropriate solvents and liquid interfaces have to be overcome. We believe that systems with strongly alternating spin densities would be very important candidates to investigate, since novel packing arrangements would create interesting magnetic materials.

## 4.5 CONCLUSIONS

In this chapter we described our experimental investigations on novel methodologies for designing new molecule-based magnetic materials

based on host-guest systems. It was shown that graphite with its possible role in mediating the exchange interactions between the intercalated paramagnetic organic ion radicals, is a unique host lattice compared to the other inorganic lamellar hosts. TCNE could be intercalated into CgK and $C_{24}K$. While TCNE intercalation into CgK leads to inhomogeneous products, it gives homogeneous GIC's when intercalated in $C_{24}K$. These materials show interesting magnetic properties with ferromagnetic spin coupling for $C_8K(TCNE)_{\sim 0.4}$o and $C_{24}K(TCNE)_{0.42}$ in restricted temperature regimes. This result is very interesting and warrants further research, in this area.

We have attempted the synthesis of ternary systems based on several organic acceptors other than TCNE as well. We note in particular, our efforts to intercalate $C_{60}$ into $C_{24}K$. We believe that the intercalation does occur, however, the products are highly reactive and no characterisation or magnetic studies could be carried out. It is interesting to note that while these studies were in progress, we came across theoretical[42] and experimental[43] studies on K-graphite-$C_{60}$ system. The latter involved a solution phase synthesis and suggested possible superconducting transition at about 20 K.

We also presented results of our investigations on DPPH doped in noninteracting media such as silica gels and polystyrene. DPPH spins seem to be getting destroyed due to covalent bond formation with the free Si-O bonds during the silica gel formation; however, DPPH can be included in

polystyrene up to high concentrations using a novel preparation technique. Strong anti ferromagnetic interactions between these stable organic radicals can be induced at appropriate concentrations in these polymer materials. This preliminary approach brings forth possibilities of new designs for organic magnetic materials.

## REFERENCES

1.  (a) G. Wannier, *Solid State Theory*, Cambridge University Press, Cambridge, 1959, p. 104. (b) F. Palacio, *Magnetic Molecular Materials*, D. Gatteschi, O. Kahn, J. S. Miller and F. Palacio (eds.), NATO ASI Series, **198,** Kluwer Academy Press, Dordrecht, 1991, p. 1. (c) R. Peierls, *Proc. Camb. Phil. Soc,* 32, 477 (1936).

2.  E. Hernandez, M. Mas, E. Molins, C. Rovira and J. Veciana, *Angew. Chem. Int. Edn. Engl.,* 32, 882 (1993). (b) J. Cirujeda, M. Mas, E. Molins, F. L. de Panthou, J. Laugier, J. G. Park, C. Paulsen, P. Rey, C. Rovira and J. Veciana, *J. Chem. Soc, Chem. Commn.,* 709(1995).

3.  N. Nakamura, K. Inoue, H. Iwamura and T. Fujioka and Y. Sawaki, *J. Am. Chem. Soc,* **114,** 1484(1992).

4.  (a) M. S. Dresselhaus and G. Dresselhaus, *Adv. Phys.,* 30, 139 (1982). (b) H. Selig and L. B. Ebert, *Adv. Inorg. Chem. and Radio Chem.,* 23, 281 (1988). (c) R. Schlögl in *Progress in Intercalation Research,* W. M. Warmuth and R Schöllhorn (eds.), Kluwer Academy Publishers, 1994, p. 83.

5.  N. Daumas and A. Hérold, *C R. Acad. Sci. C,* 286, 373 (1969).

6.  M. B. Dowell and D. S. Badorrek, *Carbon,* 16, 241 (1978).

7.  J. Thomas, G. R. Millword, R. F. Schlögl and H. P. Boehm, *Mat. Res. Bull.,* 15,671 (1980).

8.  J. E. Fischer and T. E. Thompson, *Phys. Today,* 31, 36 (1978).

9.  Y. Koike, S. Tanuma, H. Suematsu and K. Higuchi, *J. Phys. Chem. Solids,* 41, 1111 (1980).

10. C. Kittel, *Introduction to Solid State Physics,* John Wiley, Fifth Edition, 1976, p. 555.

11. H. Suematsu, K. Ohmatsu and R. Yoshizaki, *Solid State Commun.,* **38,** 1103 (1981).

12. I. S. Suzuki, F. Khemai, M. Suzuki and C. R. Burr, *Phys. Rev. B,* 45, 4721 (1992) and Ref. 1-5 cited therein.

13. J. V José, L. P. Kadanoff. S. Kirkpatrick and D. R. Nelson, *Phys. Rev. B,* **16,** 1217(1977).

14. M. Yeh, M. Suzuki and C. R. Burr, *Phys. Rev. B,* 40, 1422 (1989).

15. I. S. Suzuki, M. Suzuki, L. F. Tein and C. R. Burr, *Phys. Rev. B,* 43, 6393(1991).

16. (a) J. M. Lalancette, J. M. Roy and J. LaFontaine, *("an. J. Chem.,*54, 2505 (1976). (b) F. Beguin and R. Setton, *J. Chem. Soc, Chem. Commun.,*611 (1976). (e) M. Lissel, J. Kottmann and L). Lenoir. *Chemosphere,* 19, 1499(1989). (d) J. Jegoudez, C. Mazieres and R. Setton, *Synth. Met.,* 7, 85 (1983). (e) F. Beguin, R. Setton, A. Hamwi and P. Touzain, *Mater. Sci. Eng.,* 40, 167 (1979). (1) S. R. Su (GTE) Products Corpn., US Patent No.4 608 192 (1986). S. R. Su, *Chem. Ahstr.,* **106,** P59 869a (1987).

17. Y. Nakamura and T. Watanabe, *Anal. Sci.,* 7,431 (1991).

18. (a) P. G.Lacroix, R. Clément, K. Nakatani, J. Zyss, I. Ledoux, *Science,* **263,** 658 (1994). (b) L. Lomas, P. G. Lacroix, J. P. Audière and R. Clément,./. *Mater. Chem,* 1, 475 (1991). (c) A. Léaustic, J. P. Audière, P. G. Lacroix, R. Clément, L. Lomas, A. Michalowicz, W. R. Dunham and A. H. Francis *Chem Mater.,* 7, 1103 (1995).

19. W. Fujita and K. Awaga, *Mol. Cryst. Liq. Cryst.*, **271,** 123 (1995). (b) W. Fujita and K Awaga,./. *Chem. Soc. Chem., Commun.,* 739 (1995).

20. (a) T. Yamashita, V. Z. Mordkovich, Y. Murakami, H. Suematsu and T. Enoki,./. *Phys. Chem. Solids,* 57, 765 (1996). (b) V. Z. Mordkvich, Y. Ohki, S. Yoshimura, S. Hino, T. Yamashita and T. Enoki, *Synth. Met.,* 68, 79 (1994). (c) V. Z. Mordkovich, M. Baxendale, Y. Ohki, S. Yoshimura, T. Yamashita and T. Enoki,./. *Phys. Chem. Solids,* 57, 821 (1996). (d) T. Yamashita, Ph. D. Thesis, Tokyo Institute of Technology, 1997.

21. A. Hérold, *Bull. Soc. Chim. Fr.,* 999 (1955).

22. D. E. Nixon and G. S. Parry, *J. Phys. D: Appl. Phys. Ser. 2,* 1, 291 (1968).

23. P. Laugine, H. Estrade, J. Conard, D. Guérard, P. Lagrange and M. E. Markini, *Physica,* **99B,** 514 (1980).

24. J. G. Vcgter, T. Hibma and J. Kommandeur, *Chem. Phys. Lett.,* 3, 427 (1969).

25. J. C. Moore, D. Smith, Y. Youhne and J. P. Devlin, *J. Phys. Chem.,* 75, 325(1971).

26. J. Stanley, D. Smith, B. Latimer and J. P. Devlin, *J. Phys. Chem.,* 70, 2011 (1966).

27. S. Y. Leung, C. Underhill, G. Dresselhaus, T. Krapchev, R. Ogilvie and M. S. Dresselhaus, *Solid State Commun.,* 32, 635 (1979).

28. T. Enoki, M. Sano and H. Inokuchi,./. *Chem. Phys.,* 78, 2017 (1983).

29. K. A. Müller and R. Kleiner, *Phys. Lett.,* 1, 98 (1962).

30. M. Matsuura, *Ann. Phys. Colloque. No. 2 Supplement,* **11,** 117 (1986). (b) H. Suematsu, R. Nishitani, R. Yoshizaki, M. Suzuki and H. Ikeda, *J. Phys. Soc. Jpn.,* 52, 3874 (1983). (c) M. Suzuki, I. S. Suzuki, W. Zhang, F. Khemai and C. R. Burr, *Phys. Rev. B,* 46, 5311 (1992).

31. Always a slight excess (about 10%) of $C_{24}K$ was taken.

32. N. -C. Yeh, K. Sugihara, M. S. Dressselhaus and G. Dresselhaus, *Phys. Rev. B,*38, 12 615(1988).

33. P. W. Anderson in *Solid State Physics,* F. Setz and D. Turnbull, (eds.), Vol. **14,** Academic Press, New York, 1963, p. 99.

34. (a) C. S. Bahn, W. J. Lauderdale and R. T. Carlin, *Int. J. Qua. Chem.,* 29, 533 (1995). (b) D..). Hankinson and J. Almlöf, *J. Mol. Str. (THEOC 'HEM),*388, 245 (1996).

35. S. Kalyani, Masters Thesis, University of Hyderabad, 1997.

36. M. J. Bottomley, G. S. Parry. A. R. Ubbelohde and D. A. Young,./. *Chem. Soc. B,* 5674 (1963).

37. F. L. Vogel and W. C. Foreman. US Patent No. 4 461 719. *Chem. Abstr.,* **101,** P182 I 82v (1984).

38. R. A. Roy and R. Roy, *Mater. Res. Bull..* 19, 169 (1984). (b) A. Chatterjee and D. Chakravorthy, *J. Phys. D,* 23, 1097 (1990).

39. N. Gracia, P. Crespo, A. Hernando, C. Bovier, J. Serughetti and E. Duval, *Phys. Rev. B,* **47,** 570 (1993).

40. N. D. Yordanov, *Appl. Magn. Reson.,* 10, 339 (1996).

41. (a) W. Duffy Jr. and D. L. Strandburg, *J. Chem. Phys.,* 46, 456 (1967). (b) D. A. Fedders and J. Kommandeur, *J. Chem. Phys.,* 52, 2014 (1970).

(c) T. Fujito, T. Enoki, H. Ohya-Nishiguchi and Y. Deguchi, *Chem. Lett.,* 557 (1972).

42. (a) S. Saito and A. Oshiyama, *Phys. Rev. B,* 49, 17 413 (1994). (b) J. Song and R. L. Capelletti, *Phys. Rev. B,* 50, 14 678 (1994).

43. M. S. Fuhrer, J. G. Hou, X. -D. Xiang and A. Zettl, *Solid State Commun.,* 90, 357(1994).

# CHAPTER 5

---

# OVERVIEW OF THE PRESENT WORK
# AND FUTURE PROSPECTS

---

We have described in this thesis our computational as well as experimental studies in the area of molecule-based magnetic materials. The focus of the work is on organic molecular spin systems, though some experiments relate to metal ion (Cu(II)) spins as well.

On the computational side we have used predominantly the semiempirical AM1/CI calculations, to obtain insight into the mode of spin coupling in organic conjugated (usually non-Kekulé structures) as well as nonconjugated di and multiradicals. Open shell RHF AM1/CI procedure is found to be an optimal and efficient procedure to predict the ground state spin of organic conjugated radicals. We have shown that the spin densities calculated using this procedure can be used to compute the ZFS splitting parameters of $\pi$-conjugated organic diradicals accurately and to quantify their singlet-triplet energy gaps using an empirical approach. The latter exercise also provided a graphic illustration of the spin polarisation invoked to explain ground state spin of organic diradicals. We have also shown that if sufficient CI is included, the AM1 method can mimic high level *ab initio* calculations in the controversial case of the prediction of the ground state spin of tetramethyleneethane. Our computational studies provide various suggestions for the design of new organic molecular magnetic materials based on polyradical systems. Compared to the extensive literature available on conjugated radicals, the studies on nonconjugated organic di and multiradicals are very few. In view of the several interesting experimental as well as theoretical reports that have been appearing recently on the mode of spin coupling in organic nonconjugated radicals we have

taken up a systematic investigation of this problem.  Using high level *ab initio* calculations on some prototypical systems as benchmarks we first confirmed the efficiency of the semiempirical methods in calculations involving nonconjugated radicals.  A detailed analysis of the nature of spin coupling in nonconjugated systems revealed that the spin coupling in these systems not only depends on the topology of the molecule, but also on the relative orientation of the spin bearing orbitals.  Application of these calculations to the ferrocarbon model proposed by Ovchinnikov, shows that it may not be possible to achieve ferromagnetic interaction of spins in this hypothetical three dimensional lattice of carbon.

Cyclohexane skeleton provides an appropriate framework to test the mode of spin coupling we have discussed for nonconjugated radicals.  Our computational results on the cyclohexane-1,3,5-triyl showed that the ground state is a quartet and that there is a barrier *of ca* 8 kcal/mol to go over to the doublet state with 1-3 bonding.  Hence if the triradical can be generated it may be possible to test these computational results.  We have initiated some experiments in this direction.  We have formulated a synthetic route (Scheme 1) to generate radicals at 1,3,5 positions in the cyclohexane moiety.  The precursors 1 and 2 were prepared.  Though low temperatures are essential to generate and detect any radicals that can be produced, we have carried out some preliminary experiments as shown in the scheme. Transient and highly reactive radicals do appear on photolysis.  Low temperature experiments to monitor these radicals and elucidate their

ground state spin will prove to be of great value in providing a basic insight into the spin interactions in nonconjugated radical systems.

**Scheme 1**
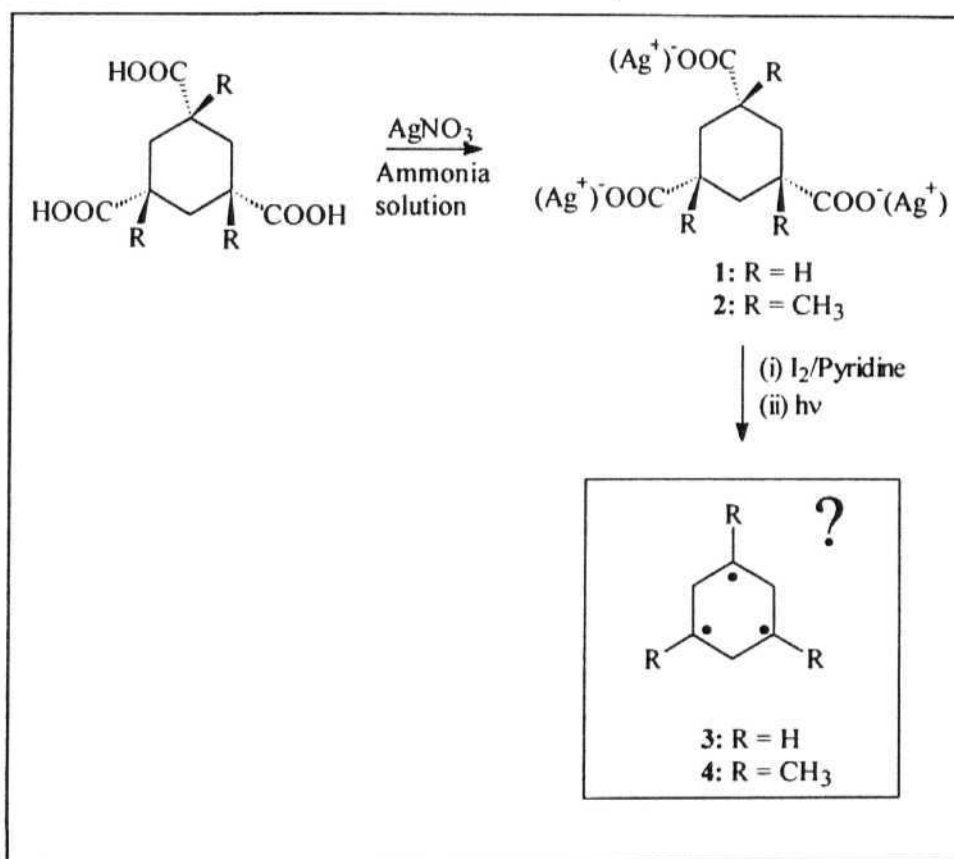


**In** chapter three we presented our experimental investigations of two approaches to molecule-based magnetic materials. We have synthesised

organic charge transfer complexes to test on a new proposal for organic ferromagnets, combining aspects of charge transfer complexes and the idea of intermolecular spin polarisation. While the complexes TPC-HCTMCP and TPC-DDQ were anti ferromagnetic as expected, NMP-DDQ showed a completely different and complex magnetic behaviour. Some insight into the magnetism of the latter complex can be gained through our model calculations based on the proposed intermolecular spin polarisation. Lack of structural information is a major hurdle in obtaining a clearer picture of the magnetic properties of these materials. Growth of single crystals in inert atmosphere will have to be attempted in future work.

In an effort to realise the topological model for spin coupling in a metal coordination polymer, we attempted the synthesis of Cu(II) complexes with 4,5-dicyanoimidazole as a bridging ligand which could provide an odd $\pi$-electron path between the metal ions coordinated through the N atoms. By modifying reaction conditions, we were able to produce novel complexes where DCI$^-$ is coordinated to Cu(II). One of the complexes we prepared appears to have a polymeric structure and shows strong anti ferromagnetic behaviour. It would be interesting to substitute the bipy ligand we have used in these complexes, by other ligands which may promote polymeric systems based on the Cu-DCI unit. Molecules such as tetracyanobiimidazole and tetrabromobiimidazole which also can provide a 3 $\pi$-electron pathway between the metal ions coordinated at the N atoms could also be tried in place of DCI. Some efforts in this direction are already under way in our laboratory.

Chapter four presents some novel designs to achieve ferromagnetic interactions in host-guest systems. One-dimensional or quasi one-dimensional materials have been the major focus of research in the filed of molecule-based magnetism, especially in purely organic materials. Keeping in view, the necessity for 2-D and 3-D spin interactions to achieve long range magnetic order, we envisaged that if organic free/ion radicals could be included as guests in host lattices like graphite interesting magnetic materials may be produced. Graphite with its possible role of mediating the magnetic interactions through its conducting electrons will be a unique host lattice in these cases. Our experimental studies showed that the strong organic acceptor molecule TCNE could be intercalated into first stage or second stage potassium graphite binary intercalation compounds. Esr and magnetic susceptibility studies revealed interesting features in these materials such as ferromagnetic interaction in restricted temperature regimes. This result appears to be very interesting and could lead to the development of a new area in molecule-based magnetic materials research. Of particular interest for more detailed future investigations are the ternary GIC's $C_{24}K(TCNE)_{0.42}$ and $C_8K(TCNE)_{0.40}$. In the latter case, the problem of inhomogeneous intercalation of TCNE may be overcome with careful monitoring of the intercalation procedure. *In situ* powder diffraction studies over extended periods of time will provide insight into the TCNE intercalation process and may suggest ways to achieve intercalation of a full equivalent of TCNE into $C_{24}K$ leading to the formation of $K^+TCNE^{-\cdot}$ inside graphite. Fabrication of other ternary systems with a variety of alkali

metals and organic acceptors would be necessary to delineate trends and provide further understanding of the magnetism in these materials. Intercalation of a Lewis acid, followed by an organic donor would be a parallel approach to the method described above. We have developed a mild electrochemical procedure to prepare second stage-GIC's of inorganic counterions. Intercalation of donors like TMPD (N,N,N'N'-tetramethyl-phenylenediamine) and TTF (tetrathiafulvalene) into these second stage-GIC's will also be interesting.

We also discussed in the last chapter, magnetic properties of organic free radicals like DPPH incorporated in polymers like polystyrene. Here the motivation was to look for novel arrangement of organic radicals in host matrices, that would result in novel magnetic interactions among the radicals. It was found that conventional film forming techniques do not allow high concentrations of dopant to be included in polymers which is essential for exchange interactions to be initiated between the doped radicals. We have developed a simple technique for forming films on water surface which enabled us to include high concentrations of DPPH (up to 50% by weight) in polystyrene. Antiferromagnetic interactions very different from that of pure crystalline DPPH were observed with moderate concentrations and a slow progression to bulk behaviour with increasing concentration of the radical could be demonstrated. The structural details of these materials are not known. Detailed studies using reflection spectroscopy or microscopic techniques may provide some important clues in this direction. Other film forming polymers like PMMA

(polymethylmethacrylate) could be used in place of polystyrene. The radical part also could be substituted with a large variety of free radicals and ion radicals available. Systems with large alternating positive and negative spin densities are of particular interest.

This thesis thus details work directed towards a fundamental understanding of spin interactions in molecular systems as well as the development of new strategies in the search for molecule-based magnetic materials.

Part of the work described in this thesis has appeared as the following publications.

1. "Dependence of Spin Coupling in Non-Kekulé Molecules on the $\pi$ - electron Network". B. I, V. Prasad and T. P. Radhakrishnan,./. *Phys. Chem.*, 96, 9232(1992).

2. "Zero Field Splitting Parameters of Diradicals and the Elusive Case of Tetramethyleneethane", B. L V. Prasad and T. P. Radhakrishnan, *J. Mol. Str. (THEOCHEM)*, **361,**175 (1996).

3. "Potassium-Graphite-Tetracyanoethylene Ternary Intercalation Compounds - Modified Conduction Electron Spin System", B. L. V. Prasad and T. P. Radhakrishnan, *Synth. Metals,* 81, 9 (1996).

4. "Spin Coupling in Nonconjugated Organic Radicals", B. L. V. Prasad and T. P. Radhakrishnan,./. *Phys. Chem.* (in press).